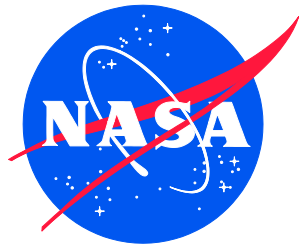


NASA/TM-2015-218781/Volume I
NESC-RP-12-00783



Empirical Model Development for Predicting Shock Response on Composite Materials Subjected to Pyroshock Loading

*Steven J. Gentz/NESC
Langley Research Center, Hampton, Virginia*

*David O. Ordway, David S. Parsons, Craig M. Garrison, C. Steven Rodgers, and Brian W. Collins
Marshall Space Flight Center, Huntsville, Alabama*

NASA STI Program . . . in Profile

Since its founding, NASA has been dedicated to the advancement of aeronautics and space science. The NASA scientific and technical information (STI) program plays a key part in helping NASA maintain this important role.

The NASA STI program operates under the auspices of the Agency Chief Information Officer. It collects, organizes, provides for archiving, and disseminates NASA's STI. The NASA STI program provides access to the NTRS Registered and its public interface, the NASA Technical Reports Server, thus providing one of the largest collections of aeronautical and space science STI in the world. Results are published in both non-NASA channels and by NASA in the NASA STI Report Series, which includes the following report types:

- **TECHNICAL PUBLICATION.** Reports of completed research or a major significant phase of research that present the results of NASA Programs and include extensive data or theoretical analysis. Includes compilations of significant scientific and technical data and information deemed to be of continuing reference value. NASA counter-part of peer-reviewed formal professional papers but has less stringent limitations on manuscript length and extent of graphic presentations.
- **TECHNICAL MEMORANDUM.** Scientific and technical findings that are preliminary or of specialized interest, e.g., quick release reports, working papers, and bibliographies that contain minimal annotation. Does not contain extensive analysis.
- **CONTRACTOR REPORT.** Scientific and technical findings by NASA-sponsored contractors and grantees.

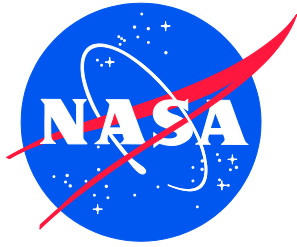
- **CONFERENCE PUBLICATION.** Collected papers from scientific and technical conferences, symposia, seminars, or other meetings sponsored or co-sponsored by NASA.
- **SPECIAL PUBLICATION.** Scientific, technical, or historical information from NASA programs, projects, and missions, often concerned with subjects having substantial public interest.
- **TECHNICAL TRANSLATION.** English-language translations of foreign scientific and technical material pertinent to NASA's mission.

Specialized services also include organizing and publishing research results, distributing specialized research announcements and feeds, providing information desk and personal search support, and enabling data exchange services.

For more information about the NASA STI program, see the following:

- Access the NASA STI program home page at <http://www.sti.nasa.gov>
- E-mail your question to help@sti.nasa.gov
- Phone the NASA STI Information Desk at 757-864-9658
- Write to:
NASA STI Information Desk
Mail Stop 148
NASA Langley Research Center
Hampton, VA 23681-2199

NASA/TM-2015-218781/Volume I
NESC-RP-12-00783



Empirical Model Development for Predicting Shock Response on Composite Materials Subjected to Pyroshock Loading

*Steven J. Gentz/NESC
Langley Research Center, Hampton, Virginia*

*David O. Ordway, David S. Parsons, Craig M. Garrison, C. Steven Rodgers, and Brian W. Collins
Marshall Space Flight Center, Huntsville, Alabama*

National Aeronautics and
Space Administration

Langley Research Center
Hampton, Virginia 23681-2199

July 2015

Acknowledgments

The team would like to acknowledge the following for providing their expertise:

Dr. Curt Larsen/Johnson Space Center (JSC), of the NESC, for championing the Pyroshock Characterization of Composites task.

Mr. Ken Johnson/MSFC for his tireless support statistically analyzing the post-processed acceleration data.

Mr. Lee Allen/MSFC for supporting Ken Johnson in statistically analyzing the post-processed data


Ms. Barbara Breithaupt/MSFC for post-processing the pseudo-velocity data.

Mr. Justin Jackson/MSFC for providing his expertise in composite test panel fabrication.

The use of trademarks or names of manufacturers in the report is for accurate reporting and does not constitute an official endorsement, either expressed or implied, of such products or manufacturers by the National Aeronautics and Space Administration.


Available from:

NASA STI Program / Mail Stop 148
NASA Langley Research Center
Hampton, VA 23681-2199
Fax: 757-864-6500

	NASA Engineering and Safety Center Technical Assessment Report	Document #: NESC-RP- 12-00783	Version: 1.0
Title: Empirical Model Development for Predicting Shock Response on Composite Materials Subjected to Pyroshock Loading		Page #: 1 of 123	

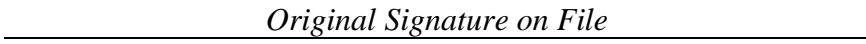
**Empirical Model Development for Predicting Shock Response on Composite
 Materials Subjected to Pyroshock Loading**

April 16, 2015

	NASA Engineering and Safety Center Technical Assessment Report	Document #: NESC-RP-12-00783	Version: 1.0
Title: Empirical Model Development for Predicting Shock Response on Composite Materials Subjected to Pyroshock Loading			Page #: 2 of 123

Report Approval and Revision History

NOTE: This document was approved at the April 16, 2015, NRB. This document was submitted to the NESC Director on May 4, 2015, for configuration control.

Approved:	 <i>Original Signature on File</i>	<u>5/5/15</u> Date
	NESC Director	

Version	Description of Revision	Office of Primary Responsibility	Effective Date
1.0	Initial Release	Mr. Steve J. Gentz, NESC Chief Engineer's Office, MSFC	4/16/15



	NASA Engineering and Safety Center Technical Assessment Report	Document #: NESC-RP-12-00783	Version: 1.0
Title: Empirical Model Development for Predicting Shock Response on Composite Materials Subjected to Pyroshock Loading		Page #: 3 of 123	

Table of Contents

Technical Assessment Report

1.0	Notification and Authorization	8
2.0	Signature Page	9
3.0	Team List	10
3.1	Acknowledgements.....	10
4.0	Executive Summary	11
5.0	Assessment Plan	14
6.0	Problem Description	14
7.0	Composite Panel Fabrication, Pyroshock Test Conduct, and Data Analysis	15
7.1	Composite Panel Fabrication and NDE.....	15
7.2	Pyroshock Test Conduct.....	18
7.2.1	Test Planning.....	18
7.2.2	Test Articles.....	25
7.2.3	Test Setup.....	28
7.2.4	Instrumentation and Data Acquisition.....	31
7.2.5	Procedures.....	37
7.2.6	Post-Test Operations.....	39
7.2.7	Data Requirements.....	39
7.2.8	Evaluation Criteria.....	39
7.3	Post-Test Data Processing and Data Evaluation.....	40
7.3.1	Post-Test Data Processing.....	40
7.3.2	Post-Test Data Evaluation.....	45
7.3.3	Algorithm Response Spectra Development.....	49
7.3.4	PV Spectra.....	59
7.3.5	Energy Spectral Density.....	59
7.3.6	SRS Evaluation.....	59
7.3.7	PV Evaluation.....	88
7.3.8	ESD Evaluation.....	97
7.3.9	Time History, Velocity, and Displacement.....	102
7.3.10	Temporal Moments.....	106
7.3.11	MEFE Prediction Example.....	107
7.3.12	MAF Qualitative Pyroshock Assessment.....	114
8.0	Findings, Observations, and NESC Recommendations	118
8.1	Findings.....	118
8.2	Observations.....	120
8.3	NESC Recommendations.....	120

	NASA Engineering and Safety Center Technical Assessment Report	Document #: NESC-RP-12-00783	Version: 1.0
Title: Empirical Model Development for Predicting Shock Response on Composite Materials Subjected to Pyroshock Loading		Page #: 4 of 123	

9.0	Alternate Viewpoint.....	120
10.0	Other Deliverables	121
11.0	Lessons Learned.....	121
12.0	Recommendations for NASA Standards and Specifications.....	121
13.0	Definition of Terms.....	121
14.0	Acronyms List	122
15.0	References.....	123

List of Figures

Figure 4.0-1.	Pyroshock of Composites Task Flow Diagram.....	13
Figure 7.1-1.	IR Thermography Indications not present using PAUT.....	16
Figure 7.1-2.	CT Scan of ROHACELL® Foam with known Flaw.....	17
Figure 7.2.2-1.	LSC Severance Plate to Test Panel Mounting.....	25
Figure 7.2.2-2.	Solid Composite Test Panel	26
Figure 7.2.2-3.	Al Pathfinder Panel	26
Figure 7.2.2-4.	LSC Mounted to Shims on LSC Plate.....	26
Figure 7.2.2-5.	Composite Solid Panel Test Setup	27
Figure 7.2.2-6.	Composite Sandwich Panel Test Setup.....	27
Figure 7.2.2-7.	Composite Sandwich Panel Test Setup, LSC Plate Mounting	28
Figure 7.2.2-8.	Composite Sandwich Panel with MAF	28
Figure 7.2.3-1.	Panel Attachment to Test Facility	29
Figure 7.2.3-2.	Calculated Severance Al Sheath LSC with Al Target.....	30
Figure 7.2.3-3.	Optimum Standoff Al Sheath LSC.....	30
Figure 7.2.4.1-1.	PCB 350C02 and PCB 350D02 Accelerometer Comparisons	31
Figure 7.2.4.1-2.	Location of Accelerometers, PCB 350C02 versus PCB 350D02.....	32
Figure 7.2.4.1-3.	Monolithic Composite Panel Pyroshock Test Setup (Typical)	33
Figure 7.2.4.1-4.	Composite Sandwich Panel Pyroshock Test Setup (Typical)	34
Figure 7.2.4.1-5.	Composite Sandwich Panel Pyroshock Test Setup with Composite LSC Panel (Typical).....	35
Figure 7.2.4.1-6.	Composite Panel with Melamine Foam Pyroshock Test Setup (Typical).....	36
Figure 7.2.5.2-1.	Estimated Source Shock, 10-gpf LSC.....	38
Figure 7.2.5.2-2.	Estimated Source Shock, 22-gpf LSC.....	38
Figure 7.3.1.2-1.	Comparison of Raw Time History Signal (Top) to Post-Processed Signal (Bottom)	41
Figure 7.3.1.2-2.	Acceleration Time History Signal Post-Processing Procedure	42
Figure 7.3.1.2-3.	MATLAB® Code for Retrieving the First 20 msec of a Shock Pulse from a Time History Signal.....	43
Figure 7.3.1.2-4.	MATLAB® Code for Shifting a Time Signal to Begin at 0 sec	44
Figure 7.3.1.2-5.	Reference MATLAB® Code for Mean Removal	44
Figure 7.3.2-1.	Data Output from SRS Enveloping Algorithm	47
Figure 7.3.2-2.	Data Output from SRS Enveloping Algorithm – Double Plateau.....	48


	NASA Engineering and Safety Center Technical Assessment Report	Document #: NESC-RP-12-00783	Version: 1.0
Title: Empirical Model Development for Predicting Shock Response on Composite Materials Subjected to Pyroshock Loading		Page #: 5 of 123	

Figure 7.3.2-3.	PVRS (4CP)	49
Figure 7.3.3.1-1.	SRS Enveloping Procedure	50
Figure 7.3.3.1-2.	MATLAB® Code for Performing SRS Enveloping Procedure	51
Figure 7.3.3.1-3.	(a) Enveloping SRS Algorithm	52
Figure 7.3.3.1-3.	(b) Enveloping SRS Algorithm	53
Figure 7.3.3.1-3.	(c) Enveloping SRS Algorithm	54
Figure 7.3.3.1-3.	(d) Enveloping SRS Algorithm	55
Figure 7.3.3.1-3.	(e) Enveloping SRS Algorithm	56
Figure 7.3.3.1-3.	(f) Enveloping SRS Algorithm.....	57
Figure 7.3.3.1-4.	Sample of the SRS Enveloping Algorithm.....	58
Figure 7.3.4-1.	Reference Code for Calculating Max PV and Frequency	59
Figure 7.3.6.1-1.	SRS Predicted Slope from Statistical Analysis (untransformed)	62
Figure 7.3.6.1-2.	SRS Predicted Slope from Statistical Analysis (log-transformed).....	63
Figure 7.3.6.1-3.	SRS Predicted Slope from Statistical Analysis (Percentile).....	64
Figure 7.3.6.1-4.	Monolithic Composite Average SRS Slope	65
Figure 7.3.6.1-5.	Composite Sandwich Panel Slope Change versus Distance.....	66
Figure 7.3.6.2-1.	Predicted Frequency Breakpoint versus Distance by Panel Type	68
Figure 7.3.6.2-2.	SRS Frequency Breakpoint – Ply Type Evaluation	69
Figure 7.3.6.2-3.	SRS Frequency Breakpoint Composite Sandwich Fill Evaluation (all data)	70
Figure 7.3.6.2-4.	SRS Frequency Breakpoint Composite Sandwich Fill Evaluation (less 69-inch data and composite LSC plate data)	70
Figure 7.3.6.3-1.	Predicted SRS Peak Acceleration versus Distance by Panel Type	74
Figure 7.3.6.3-2.	Monolithic Composite Panel Peak Acceleration with Distance Comparison	77
Figure 7.3.6.3-3.	Peak Acceleration versus Distance, Group I Re-Test 2	78
Figure 7.3.6.3-4.	Monolithic Composite Group I, Re-Test 2, Percent Median Peak Acceleration versus Distance.....	79
Figure 7.3.6.3-5.	Peak Acceleration – Tape versus Fabric Ply	80
Figure 7.3.6.3-6.	Comparison of Ply Layup Direction –Peak Acceleration and PV.....	81
Figure 7.3.6.3-7.	Comparison of Monolithic Composite Panel Thickness – Peak Acceleration and PV	82
Figure 7.3.6.3-8.	Comparison of Monolithic Composite Panel and Sandwich Composite Panel – Peak Acceleration versus Distance.....	83
Figure 7.3.6.3-9.	Percentile of Shock Remaining – All Panel Types	84
Figure 7.3.6.3-10.	Percentile of Shock Remaining - Monolithic Composite Panel.....	85
Figure 7.3.6.3-11.	Percentile of Shock Remaining – Al Honeycomb Composite Sandwich Panel.....	86
Figure 7.3.6.3-12.	Percentile of Shock Remaining – ROHACELL® Foam Composite Sandwich Panel	87
Figure 7.3.6.3-13.	Percentile of Shock Remaining- Comparison of Martin Marietta Data with Al Honeycomb Sandwich Panel Data	88
Figure 7.3.7-1.	Mean PV versus Distance, 0.2-inch-thick Monolithic Composite Panel	89
Figure 7.3.7-2.	Percentile of PV Remaining versus Distance, 0.2-inch-thick Monolithic Composite Panel.....	90




	NASA Engineering and Safety Center Technical Assessment Report	Document #: NESC-RP-12-00783	Version: 1.0
Title: Empirical Model Development for Predicting Shock Response on Composite Materials Subjected to Pyroshock Loading		Page #: 6 of 123	

Figure 7.3.7-3.	Mean PV versus Distance, 0.3-inch-thick Monolithic Composite Panel	91
Figure 7.3.7-4.	Percentile of PV Remaining versus Distance, 0.3-inch-thick Monolithic Composite Panel.....	92
Figure 7.3.7-5.	Mean PV versus Distance, Al Honeycomb Composite Sandwich Panel	93
Figure 7.3.7-6.	Percentile of PV Remaining versus Distance, Al Honeycomb Composite Sandwich Panel	94
Figure 7.3.7-7.	Mean PV versus Distance, ROHACELL® Foam Composite Sandwich Panel	95
Figure 7.3.7-8.	Percentile of PV Remaining versus Distance, ROHACELL® Foam Composite Sandwich Panel	96
Figure 7.3.8-1.	ESD Plot – 0.2-inch Monolithic Panel, 10-gpf LSC	98
Figure 7.3.8-2.	ESD Plot – Al Honeycomb Composite Sandwich Panel, 10-gpf LSC.....	99
Figure 7.3.8-3.	ESD Plot – ROHACELL® Foam Composite Sandwich Panel, 10-gpf LSC.....	100
Figure 7.3.8-4.	Maximum Predicted ESD – LSC Plate Type and LSC Explosive Core Load	102
Figure 7.3.9-1.	Time Histories for Group I, Test 2, Monolithic Composite Panel – Accelerometers 2 and 8	103
Figure 7.3.9-2.	Time Histories for Group II, Test 11, Al Honeycomb Sandwich Composite Panel – Accelerometers 2 and 8	104
Figure 7.3.9-3.	Time Histories for Group II, Test 13, ROHACELL® Foam Sandwich Composite Panel – Accelerometers 2 and 8	105
Figure 7.3.10-1.	Monolithic Composite Temporal Energy Sensitivities	107
Figure 7.3.11-1.	Predictive MEFE, Monolithic Composite	108
Figure 7.3.11-2.	Predicted MEFE Example at 48 inches, Monolithic Composite	110
Figure 7.3.11-3.	Predicted MEFE, Al Honeycomb.....	111
Figure 7.3.11-4.	Predicted MEFE at 48-inch Distance, Al Honeycomb.....	112
Figure 7.3.11-5.	Predicted MEFE, ROHACELL® Foam.....	113
Figure 7.3.11-6.	Predicted MEFE at a Distance of 48-inches, ROHACELL® Foam	114
Figure 7.3.12-1.	MAF Evaluation, SRS Slope.....	115
Figure 7.3.12-2.	MAF Evaluation, SRS Frequency Breakpoint	116
Figure 7.3.12-3.	MAF Evaluation, SRS Peak Acceleration.....	117

	NASA Engineering and Safety Center Technical Assessment Report	Document #: NESC-RP-12-00783	Version: 1.0
Title: Empirical Model Development for Predicting Shock Response on Composite Materials Subjected to Pyroshock Loading		Page #: 7 of 123	

List of Tables

Table 7.2.1-1.	Pyroshock Composite Material Characterization Test Matrix (Pathfinder Tests).....	18
Table 7.2.1-2.	Modified Pyroshock Composite Material Characterization Test Matrix	20
Table 7.2.1-3.	Modified Pyroshock Composite Material Characterization Test Matrix	21
Table 7.2.1-4.	Modified Pyroshock Composite Material Characterization Test Matrix	22
Table 7.2.1-5.	Pyroshock Composite LSC Plate Ply Layup	23
Table 7.2.1-6.	Pyroshock Composite Group II Re-Tests.....	24
Table 7.2.1-7.	Melamine Foam Damped Test Series	24
Table 7.3.6.1-1.	Predictive Slope versus Distance (regardless of panel type).....	61
Table 7.3.6.2-1.	Predicted Frequency Breakpoint with Distance (by panel type)	67
Table 7.3.6.3-1.	Predicted Peak Acceleration Values by Panel Material Type	75
Table 7.3.8-1.	Predicted Maximum ESD.....	101
Table 7.3.11-1.	Predictive 8,000 g Shock, Monolithic Composite.....	109
Table 7.3.11-2.	Predictive 8,000-g Shock Attenuated for 48-inch Distance, Monolithic Composite.....	110

	NASA Engineering and Safety Center Technical Assessment Report	Document #: NESC-RP-12-00783	Version: 1.0
Title: Empirical Model Development for Predicting Shock Response on Composite Materials Subjected to Pyroshock Loading		Page #: 8 of 123	

Technical Assessment Report

1.0 Notification and Authorization

The NASA Engineering and Safety Center (NESC) received a request to develop an analysis model based on both frequency response and wave propagation analyses for predicting shock response spectrum (SRS) on composite materials subjected to pyroshock loading. The model would account for near-field environment (~9 inches from the source) dominated by direct wave propagation, mid-field environment (~2 feet from the source) characterized by wave propagation and structural resonances, and far-field environment dominated by lower frequency bending waves in the structure.

Mr. Steve Gentz, NESC Chief Engineer at Marshall Space Flight Center (MSFC), was selected to lead this assessment. Mr. David Ordway (MSFC) was selected as the Technical Lead.

The key stakeholders for this assessment include:

Space Launch System (SLS) Program

- Todd May (SLS Program Manager)
- Gary Lyles (SLS Chief Engineer)
- Mindy Nettles (SLS Advanced Development Program Manager)
- Chris Crumbly (SLS Spacecraft and Payload Integration Manager)

Technical Discipline


- Dynamic Environment Analysts

Other NASA Programs

- Atlas V
- Delta IV
- SpaceX

Other Government Agencies

- Department of Defense

	NASA Engineering and Safety Center Technical Assessment Report	Document #:	Version:
		NESC-RP-12-00783	1.0
Title:		Page #:	
Empirical Model Development for Predicting Shock Response on Composite Materials Subjected to Pyroshock Loading		10 of 123	


3.0 Team List

Name	Discipline	Organization
Core Team		
Steve Gentz	NESC Lead	MSFC
David Ordway	Technical Lead	MSFC
Brian Collins	Structural Materials, Composite	MSFC
Craig Garrison	Pyroshock Test, Structural Dynamics	MSFC
Steve Rodgers	Pyroshock, Structural Dynamics	MSFC
Karen Oliver	Pyroshock Analysis	MSFC
Patricia Pahlavani	MTSO Program Analyst	LaRC
David Parsons	Pyroshock Analysis	MSFC
Ken Johnson	NESC Systems Engineering Office/ Statistics and Trending	MSFC
Lee Allen	Nonmetallic Materials	MSFC
Stephen Richardson	Flight Systems	MSFC
Stanley Smeltzer	Composite Materials	LaRC
Jackie Thomas	CAD Support	MSFC
Administrative Support		
Linda Burgess	Project Coordinator	LaRC/AMA
Tina Dunn-Pittman	Planning and Control Analyst	LaRC/AMA
Erin Moran	Technical Writer	LaRC/AMA

3.1 Acknowledgements

The team would like to acknowledge the following for providing their expertise:

- Dr. Curt Larsen/Johnson Space Center (JSC), of the NESC, for championing the Pyroshock Characterization of Composites task.
- Mr. Ken Johnson/MSFC for his tireless support statistically analyzing the post-processed acceleration data.
- Mr. Lee Allen/MSFC for supporting Ken Johnson in statistically analyzing the post-processed data
- Ms. Barbara Breithaupt/MSFC for post-processing the pseudo-velocity data.
- Mr. Justin Jackson/MSFC for providing his expertise in composite test panel fabrication.

	NASA Engineering and Safety Center Technical Assessment Report	Document #: NESC-RP-12-00783	Version: 1.0
Title: Empirical Model Development for Predicting Shock Response on Composite Materials Subjected to Pyroshock Loading		Page #: 11 of 123	

4.0 Executive Summary


Historically, the aerospace industry has used the shock response spectrum for defining a maximum expected flight environment (MEFE) at any one location, or zone, for a spacecraft or launch vehicle. The data used for defining the MEFE is usually based on the collective data compiled by Martin Marietta in NASA CR-114606, *Pyrotechnic Shock Design Guidelines Manual*, which was compiled about 45 years ago. The compilation of data in NASA CR-114606 is primarily for metallic structures. The pyroshock data and the data evaluation process documented within this report are to expand upon the data compilation contained in NASA CR-114606 for composite structures.

The objective of this assessment was to develop an analytical tool to be used for accurate prediction of the MEFE for pyroshock induced into a composite material. Pyroshock tests were conducted to capture the acceleration time history of the shock wave as it transverses across the composite panel at various locations (commonly referred to as near field, mid-field, and far field) on the panel. These data provided the necessary information for the generation of attenuation curves for each of the types of composite materials resulting in an empirical analytical model for prediction of the shock MEFE. The composite material variables that were evaluated in this assessment included the thickness of the composite (monolithic) material, direction of the ply orientation (unidirectional versus quasi-isotropic plies), tape versus fabric plies, monolithic versus filled composite, and the type of fill used in the composite sandwich. The explosive load of the pyroshock source induced into the composite panel was also evaluated.

Composite materials offer a number of advantages with respect to isotropic materials due to their low density and the possibility of optimizing their strength and stiffness by properly determining the fiber or tape orientation of every layer in the laminate. As a result, the analysis of their static and dynamic behavior is important, especially in the aerospace engineering field where the minimization of the structural mass is one of the first objectives of the design.

A composite test panel configuration of 3 feet in height and 6 feet in length was selected for the pyroshock testing. The test panel thickness was one of the variables for evaluation, which is governed by the type and number of plies used for panel fabrication. The test panel fabrication processes and nondestructive evaluation (NDE) of the composite material is summarized in Appendix A.

Transient shock, which is induced by explosives, occurs in all three orthogonal axes. It was decided to measure the acceleration in only the out-of-plane axis since these data would be the most useful for comparison of the variables being evaluated. The number of tests performed exceeded the baseline test matrix originally proposed for the Pyroshock Characterization of Composites task. The additional tests include performing five pathfinder tests validating the test setup, repeating four Group I monolithic composite panel tests, and performing pyroshock tests with acoustic dampening melamine foam bonded to the composite panels (or Al panel) for a total of 47 tests. The test results for each of the pyroshock tests performed are documented in Appendix B.

	NASA Engineering and Safety Center Technical Assessment Report	Document #: NESC-RP-12-00783	Version: 1.0
Title: Empirical Model Development for Predicting Shock Response on Composite Materials Subjected to Pyroshock Loading		Page #: 12 of 123	

The acceleration data acquired from the pyroshock test were evaluated for suitability (or quality) prior to post-test processing. Post-test data processing was performed by input of the data into MATLAB[®] algorithms for generation of data sets that could efficiently evaluate each of the variables independent of the other variable effects. Any changes made to the test matrices were analyzed using STATGRAPHICS[®] and Design-Expert[®] software for test design efficiency evaluation prior to incorporation into the test planning and procedural documentation.

Once the acceleration data were acquired, they were post-processed and MATLAB[®] algorithms were developed to provide a data set of factors to be further analyzed statistically to determine whether the factor was significant to the shock response. An outline of the steps involved for post-processing the data, the MATLAB[®] algorithms, and a summary of the statistical software utilized in these analyses is documented in Section 7.3.


A summary of the tasks for conducting the pyroshock tests and data processing is shown in Figure 4.0-1.

The single value inputs (SVI) used for evaluation of the shock response were centric for shock response spectrum (SRS) since it is the shock data processing methodology of choice for the aerospace industry (including NASA). Evaluation of the SVIs for the SRS included the SRS slope, frequency breakpoint, and the peak acceleration.

The composite sandwich panels attenuated the shock (with distance) much better than the monolithic composite panels with the ROHACELL[®] foam sandwich-filled panels having the greatest shock attenuation characteristics. The SRS slope showed little change from 20 inches up to 60 inches from the shock source whereas the SRS frequency breakpoint decreased with distance from the shock source.

Other composite materials factors evaluated, such as ply orientation and type of ply, were not significant factors for the shock response. The thickness of the monolithic composite panels did show different levels of shock attenuation (a lower level for the 0.2-inch-thick versus the 0.3-inch-thick) but the rate at which the shock was attenuated was equivalent.

Evaluation of the pseudo-velocity response spectrum (PVRs) was also performed to supplement the SRS since the PVRs provides an indication on the severity of the shock, which cannot be directly discerned from the SRS. The shock induced into the composite panels is classified as a moderate to severe shock and post-test NDE (phased array ultrasound) showed no indications of damage to the composites after being subjected to pyroshock loading. The attenuation of the mean (rather than maximum) pseudo-velocity (PV) with distance from the shock source was in alignment SRS peak acceleration attenuation. The determination of the mean PV was performed manually since a MATLAB[®] algorithm for determining the mean PV was not developed.

	NASA Engineering and Safety Center Technical Assessment Report	Document #:	Version:
		NESC-RP-12-00783	1.0
Title:		Page #:	
Empirical Model Development for Predicting Shock Response on Composite Materials Subjected to Pyroshock Loading		13 of 123	

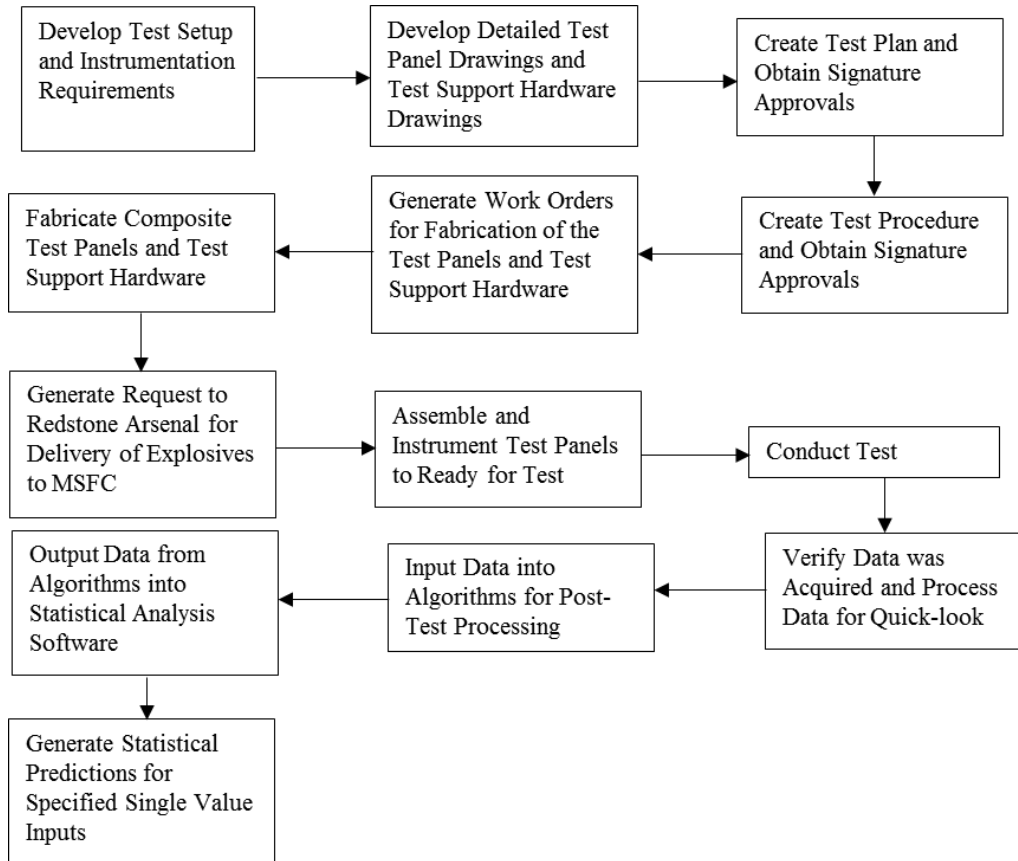



Figure 4.0-1. Pyroshock of Composites Task Flow Diagram

The addition of melamine foam for acoustic dampening did not affect the SRS peak acceleration, SRS slope, or the attenuation of the shock with distance (peak acceleration). The acoustic melamine foam did decrease the SRS frequency breakpoint approximately 30 to 40 percent as compared to the composite material without the acoustic foam.

To make most efficient use of NASA or other provider resources, the project should consider using the results from this testing in planning future testing, including test article design, test article quality assurance, sensor placement, expected magnitude of effect and variability around the effect, and analysis method.

The pyroshock characterization of composites project was successful in establishing a methodology for evaluating the quality of the acceleration time history data, developing algorithms for post-processing the data, and for establishing a database, which may be used for future higher-fidelity pyroshock testing of composites (e.g., large cylindrical structures). It is recommended further tests be performed to increase the composite shock database for the Space Launch System (SLS) Composite Exploration Upper Stage (EUS) technology and development project to more accurately predict pyroshock loading for the EUS.

	NASA Engineering and Safety Center Technical Assessment Report	Document #: NESC-RP-12-00783	Version: 1.0
Title: Empirical Model Development for Predicting Shock Response on Composite Materials Subjected to Pyroshock Loading		Page #: 14 of 123	

5.0 Assessment Plan

A series of pyroshock tests were conducted on various types of composite panels and the shock response obtained from the tests were used to develop an analytical tool to predict a MEFE shock environment based on the explosive loading of the separation system and the type of composite material into which the shock was induced. Initially, 28 pyroshock tests were planned for this assessment to evaluate each of the variables described above.


This assessment required the test specimens (i.e., the different types of composite panels) to be fabricated and detail design drawings developed. MSFC pyrotechnic test facility personnel conducted testing and quick-look data reduction. There was sufficient linear-shaped charge (LSC) of various core loads available at MSFC for conducting these tests without the need to procure new LSC. Loads and dynamics personnel developed the analytical model based on the reduced data from the test results.

The activities required to complete this assessment included:

- Test planning and composite panel fabrication
 - Test plan development
 - Composite panel computer aided design drawings
 - Composite panel fabrication and Insert Installation
 - Pyroshock test setup
- Pyroshock testing and data reduction
 - Perform pyroshock tests
 - Reduce data and generate SRS plots
- Analytical model and accompanying handbook development and final report
 - Assist in test planning and development
 - Research development of distance attenuation curves and shock propagation prediction methods
 - Research pyroshock analytical modeling methods
 - Correlate pyroshock test data with analytical model
 - Develop analytical model to predict shock MEFE
 - Develop handbook for analytical model usage
 - Generate final report

6.0 Problem Description

The primary purpose of this test series was to capture the acceleration time history of the shock wave as it transverses across various types of composite panels at various locations (commonly referred to as near field, mid-field, and far field) on the panel. These tests were performed to provide the necessary information for the generation of attenuation curves for each of the types of composite materials resulting in an empirical analytical model for prediction of the shock MEFE.

	NASA Engineering and Safety Center Technical Assessment Report	Document #: NESC-RP-12-00783	Version: 1.0
Title: Empirical Model Development for Predicting Shock Response on Composite Materials Subjected to Pyroshock Loading		Page #: 15 of 123	

This test series did not determine the cumulative effects of vibro-acoustic exposure of the composite material prior to being subjected to the induced pyroshock event. The test series was limited to flat panel testing only, which did not allow evaluation of the composite material response to pyroshock with regard to ring frequency. Ring frequency corresponds to the mode in which all points move radially outward together and then radially inward together. This is the first extension mode of a cylindrical structure and is analogous to a longitudinal mode in a rod. Evaluation of the ring frequency of a composite material cylindrical structure would greatly enhance analytical prediction of the shock MEFÉ for flight structures.


7.0 Composite Panel Fabrication, Pyroshock Test Conduct, and Data Analysis

7.1 Composite Panel Fabrication and NDE

All of the composite panels used for the pyroshock tests were fabricated at MSFC by the Nonmetallic Materials and Manufacturing Branch (EM42) personnel. The panels were fabricated per steps listed in MSFC work orders approved by EM42 Engineering and the task assessment technical lead. The baseline task assessment composite panels were fabricated from IM7/TC350 composite material manufactured by TenCate Advanced Composites. This material is a 350°F toughened epoxy resin system used for structural advanced composite applications, which include space structures. The composite material in both tape and fabric prepreg formats was used for this assessment. The composite material was chosen in place of IM7/977-3 composite material, which is more commonly used for aviation and aerospace applications, primarily due to the long lead-time for procurement (29 weeks) of the IM7/977-3 material. Additionally, the material properties for the IM7/TC350 and the IM7/977-3 are comparable.

A second composite material was also used for the pyroshock characterization, which was IM7-R913. This material was originally procured by Redstone Arsenal for fabrication of helicopter blades and later given to MSFC since its age life had expired. Prior to usage, some of the material was removed from the freezer, thawed, and evaluated to determine if it was suitable for usage. The material was determined to be acceptable and three 38-ply tape panels were fabricated for usage in the five test pathfinder test series.

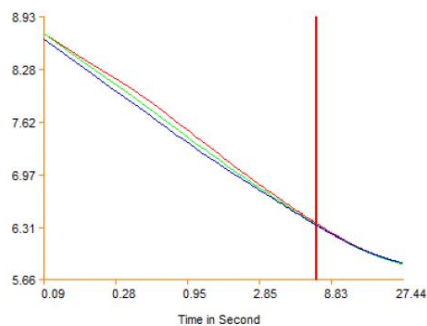
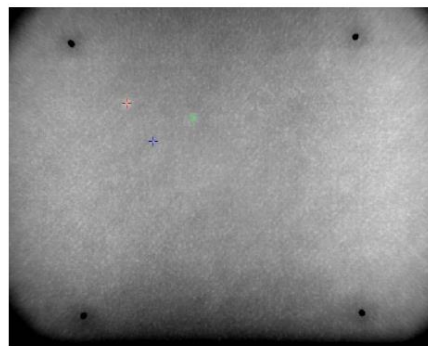
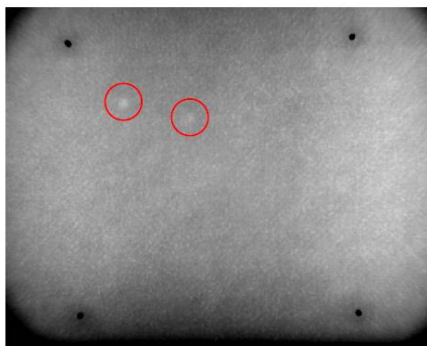
In addition to the composite prepreg material, two other primary materials were required for the composite sandwich panel configurations, which was the filler materials. The two-filler materials chosen were Al honeycomb and ROHACELL® foam, both of which are used for aerospace applications. The Al honeycomb fill material used was procured from Texas Almet part number 3.1 1/8 .0007P 5052 (3.1 pounds per cubic feet (pcf), 1/8-inch hexagonal cell size, 0.0007-inch foil gauge, P = perforated, and 5052 was the Al alloy). The ROHACELL® foam used was ROHACELL® 200 WF, which is a closed-cell rigid polymethacrylimade foam and was procured from Evonik Industries. The thickness of the filler materials was 1 inch; whether Al honeycomb or ROHACELL® foam, and 8-ply face sheets of IM7/TC350 (tape or fabric plies) were used to make up the composite sandwich panel.

	NASA Engineering and Safety Center Technical Assessment Report	Document #:	Version:
		NESC-RP-12-00783	1.0
Title:		Page #:	
Empirical Model Development for Predicting Shock Response on Composite Materials Subjected to Pyroshock Loading		16 of 123	

The type of ply material, ply orientation, number of plies used, fill material type (as applicable), along with dimensional requirements were documented on drawings generated by EV32 Engineering (reference Appendix A for drawing details).

Following fabrication of the composite test panels, the panels were subjected to NDE for flaws (voids, delamination, etc.) and the location of the flaws, if they existed, for correlation to accelerometer location time history data to aid in understanding whether the flaw influenced the shock response. Initially, two NDE methods were used, infrared (IR) thermography and phased array ultrasonic testing (PAUT). It was determined from the initial NDE of the composite panels the IR thermography method produced false indications for the monolithic composite panels, which were 0.2 inches or 0.3 inches in thickness. The conclusion was IR thermography was not the NDE methodology of choice for composites materials of the thicknesses used in this testing and only PAUT was used thereafter. Figure 7.1.1 illustrates an indication from IR thermography inspection, which was not present using PAUT and as considered to be a surface condition.

Indication: D3




Two indications, approximately 0.25" by 0.25", were found in inspection location D3 and denoted by the red circles. Time-temperature cursors, shown in red and green, were placed on each indication and measured the average intensity value of the local 3 by 3 pixel area. A blue reference time-temperature cursor was placed over a nominal area for comparison. Plotting the data from the two indications and the reference point shows that both indications deviate from the behavior of nominal areas of the panel.

In addition to infrared thermography, phased array ultrasound (PAUT) was used to inspect the panel. PAUT did not detect any anomalies at grid location D3, and as a result, it is believed the indications present in the thermographic data are the result of a surface condition.

Figure 7.1-1. IR Thermography Indications not present using PAUT

Fabrication of the composite sandwich panels generated new challenges of NDE methodology for evaluation of the filler material. PAUT generated acceptable results for evaluation of the face sheets and the bond line between the face sheets and the filler, but was unable to detect flaws in the filler material. It was concluded PAUT is not a suitable NDE method for evaluating flaws in the foam filler core material. A study was undertaken to evaluate an acceptable NDE

	NASA Engineering and Safety Center Technical Assessment Report	Document #: NESC-RP-12-00783	Version: 1.0
Title: Empirical Model Development for Predicting Shock Response on Composite Materials Subjected to Pyroshock Loading		Page #: 17 of 123	

methodology for resolving a flaw (crack) in the ROHACELL[®] foam. Two methods were evaluated; digital radiography (DR) and computed tomography (CT). The results of the study are documented in Appendix A, reference Figure A35, which show only the CT method was able to detect flaws in the foam filler material. Figure 7.1-2 illustrates the CT results for detecting a known flaw (crack) in the ROHACELL[®] foam.

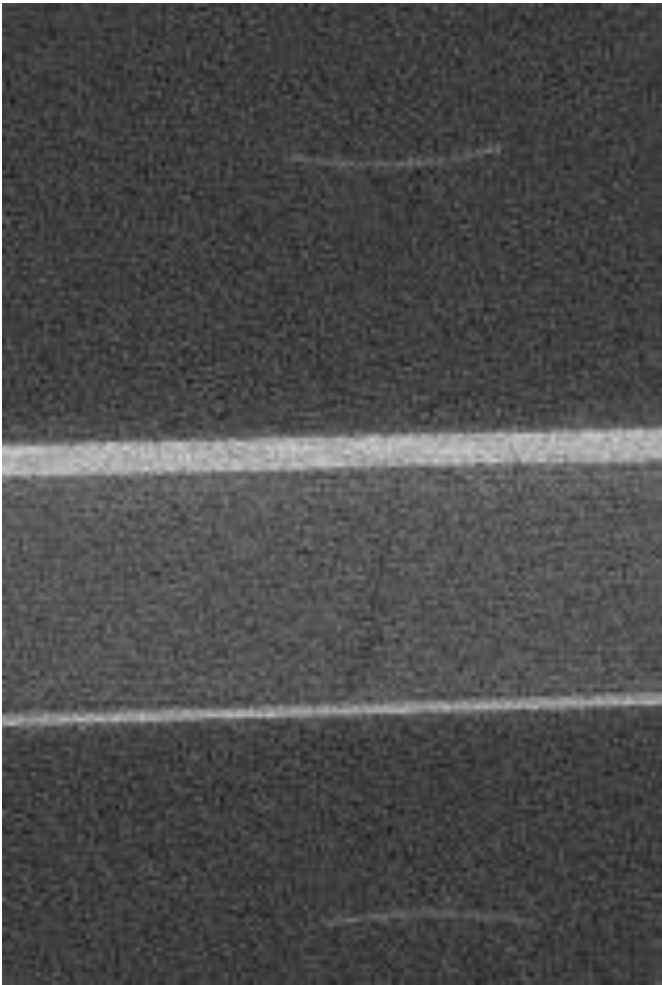
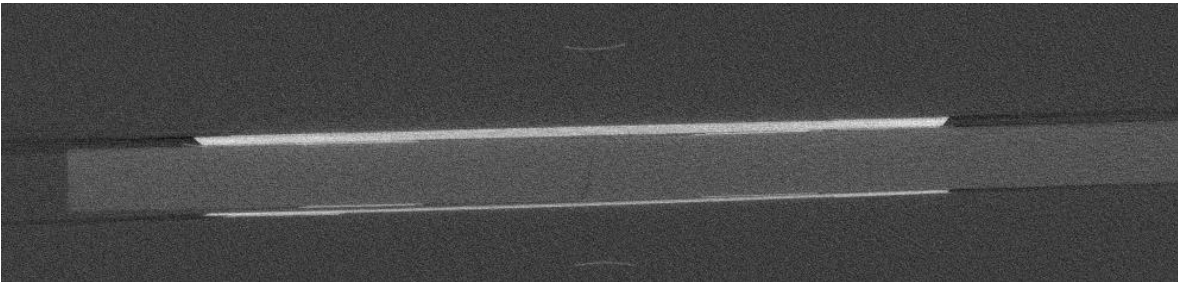



Figure 7.1-2. CT Scan of ROHACELL[®] Foam with known Flaw

	NASA Engineering and Safety Center Technical Assessment Report	Document #:	Version:
		NESC-RP-12-00783	1.0
Title:		Page #:	
Empirical Model Development for Predicting Shock Response on Composite Materials Subjected to Pyroshock Loading		18 of 123	

7.2 Pyroshock Test Conduct

7.2.1 Test Planning

A Pyroshock Characterization of Composites Test Plan was generated by the assessment technical lead to document the specifics for the test panel configurations, test order, test setup, and instrumentation for data acquisition. The approved baseline test plan was dated July 2, 2012, and during the course of this estimate, the test plan was revised four times, ultimately ending in revision D, to accommodate changes to the test matrices and scope of the testing performed.


Initially, 28 tests (initial baseline task assessment plan) were planned for this test series utilizing the composite panel configurations.

Prior to conducting the tests, using composite panels fabricated from IM7/TC350 material, it was decided to conduct a series of five pathfinder tests to evaluate the test setup and data acquisition system (DAS). The configuration for the pathfinder panel tests are tabulated in Table 7.2.1-1. The IM7/913 composite panels were inspected using pulse echo ultrasound prior to subjection to the pyroshock test. The baseline panels used for this testing, fabricated from IM7/TC350, were initially inspected using both flash thermography and pulse echo ultrasound (PAUT), but only pulse echo ultrasound was ultimately used, prior to test for the reasons documented in Section 7.1.

Table 7.2.1-1. Pyroshock Composite Material Characterization Test Matrix (Pathfinder Tests)

Test Number	Material	Panel Thickness	Ply	Orientation	Type	LSC Core Load
1	Al (Al), 5052 alloy	0.187	N/A	N/A	Homogenous	10 gpf
2	Al, 5052 alloy	0.187	N/A	N/A	Homogenous	22 gpf
3	Composite, IM7/R913	0.200	Tape 38 plies	((+45°/-45° (2X), 0° (2x), +45°/-45° (2X), 90° (2x)) (X 3.2)	Solid	10 gpf
4	Composite, IM7/R913	0.200	Tape 38 plies	All plies 0°	Solid	10 gpf
5	Composite, IM7/R913	0.200	Tape 38 plies	All plies 90°	Solid	10 gpf

Following completion of the pathfinder tests and determination the test setup and instrumentation was satisfactory for progressing with the baseline composite panel tests. Initially, the tests were divided into three groups: Group I representing the monolithic composite panels, Group II being the first eight sandwich panels, and Group III was the last ten sandwich panels. Of note, a change in the scope of the testing included repeating four of the Group I monolithic composite panels to help better understand within panel variability and also to evaluate the panel for damage utilizing PAUT as the NDE method after subjection to pyroshock. (Note: Since new

	NASA Engineering and Safety Center Technical Assessment Report	Document #: NESC-RP-12-00783	Version: 1.0
Title: Empirical Model Development for Predicting Shock Response on Composite Materials Subjected to Pyroshock Loading		Page #: 19 of 123	

indications were not noted, it was concluded the damage tolerance of the composite material was above the shock levels induced into the composite). The increased scope of the task also included the addition of the tests with and without melamine acoustic foam (MAF), identified as Group IV, utilizing panels previously subjected to shock in either the pathfinder test series (A1 panel), Group I (monolithic composite panel), or Group II (composite sandwich panel). Randomness in testing of the panels, whether they were from Groups I, II, III, or IV, was introduced for determination of which parameters have the greatest sensitivity to shock response. Each test matrix was planned so the effects of each input factor (i.e., core load, monolithic panel thickness, presence of foam dampening, etc.) could be efficiently calculated and separated from the effects of the other input factors per the goals of this task. Standard efficient test matrix design methods (design of experiments (DOE)) were used. The test matrices were planned and the efficiency of changes recommended by subject matter experts (SME) were analyzed using STATGRAPHICS[®] and Design-Expert[®] software before implementation of the changes into the test plan.

The initial tests, identified in the test planning as Group I, are tabulated in Table 7.2.1-2. These tests evaluated the following parameters:

- Composite thickness
- Type of ply and ply orientation
- Source shock induced into the panel

Following completion of the Group I tests, the results from these tests were evaluated and, based on the evaluation, the test matrix in Table 7.2.1-3 was adjusted to focus the follow-on tests (tests 10-18) for focus on evaluating the data processing SVI in comparison with the Group I test results, which have the greatest sensitivity to the induced shock. The SVIs evaluated were:

- Acceleration time history
- Velocity time history
- Displacement time history
- SRS peak g's, frequency breakpoint, and slope


	NASA Engineering and Safety Center Technical Assessment Report	Document #:	Version:
		NESC-RP-12-00783	1.0
Title:		Page #:	
Empirical Model Development for Predicting Shock Response on Composite Materials Subjected to Pyroshock Loading		20 of 123	

Table 7.2.1-2. Modified Pyroshock Composite Material Characterization Test Matrix

Group I – Solid Composite Panels						
Test Number	Material	Panel Thickness	Ply	Orientation	Type	LSC Core Load
1	Composite, IM7/TC350	0.200	Fabric	0-Deg, 18 ply	Solid	10
2	Composite, IM7/TC350	0.200	Fabric	+45°/-45°, 0° (2x), +45°/-45°, 90° (2x), 18 ply	Solid	10
3	Composite, IM7/TC350	0.300	Tape	+45°/-45°, 0° (2x), +45°/-45°, 90° (2x), 54 ply	Solid	10
4	Composite, IM7/TC350	0.300	Fabric	+45°/-45°, 0° (2x), +45°/-45°, 90° (2x), 27 ply	Solid	22
5	Composite, IM7/TC350	0.200	Tape	+45°/-45°, 0° (2x), +45°/-45°, 90° (2x), 38 ply	Solid	22
Analyzed results from Tests 1-5 to incorporate any re-planning for tests 6 through 10 was deemed necessary. (Note: No re-planning was required.)						
6	Composite, IM7/TC350	0.200	Fabric	0-Deg, 18 ply	Solid	22
7	Composite, IM7/TC350	0.200	Fabric	+45°/-45°, 0° (2x), +45°/-45°, 90°, 18 ply	Solid	22
8	Composite, IM7/TC350	0.300	Fabric	+45°/-45°, 0° (2x), +45°/-45°, 90° (2x), 27 ply	Solid	10
9	Composite, IM7/TC350	0.300	Tape	+45°/-45°, 0° (2x), +45°/-45°, 90° (2x), 54 ply	Solid	22
10	Composite, IM7/TC350	0.200	Tape	+45°/-45°, 0° (2x), +45°/-45°, 90° (2x), 38 ply	Solid	10


	NASA Engineering and Safety Center Technical Assessment Report	Document #:	Version:
		NESC-RP-12-00783	1.0
Title:		Page #:	
Empirical Model Development for Predicting Shock Response on Composite Materials Subjected to Pyroshock Loading		21 of 123	

Table 7.2.1-3. Modified Pyroshock Composite Material Characterization Test Matrix

Group II – Sandwich Composite Panels						
Test Number	Material	Panel Thickness	Fill/Ply	Orientation	Type	LSC Core Load
11	Composite, IM7/TC350	8 Ply/ 1-inch-thick fill	Al Honeycomb & Tape	+45°/-45°, 0° (2x), +45°/-45°, 90° (2X), 8 ply both faces	Sandwich	10
12	Composite, IM7/TC350	8 Ply/ 1-inch-thick fill	Al Honeycomb & Tape	+45°/-45°, 0° (2x), +45°/-45°, 90° (2X), 8 ply both faces	Sandwich	22
13	Composite, IM7/TC350	8 Ply/ 1-inch-thick fill	ROHACELL® Foam & Tape	+45°/-45°, 0° (2x), +45°/-45°, 90° (2X), 8 ply both faces	Sandwich	10
14	Composite, IM7/TC350	8 Ply/ 1-inch-thick fill	ROHACELL® Foam & Tape	+45°/-45°, 0° (2x), +45°/-45°, 90° (2X), 8 ply both faces	Sandwich	22
15	Composite, IM7/TC350	8 Ply/ 1-inch-thick fill	Al Honeycomb & Tape	+45°/-45°, 0° (2x), +45°/-45°, 90° (2X), 8 ply both faces	Sandwich	10
16	Composite, IM7/TC350	8 Ply/ 1-inch-thick fill	Al Honeycomb & Tape	+45°/-45°, 0° (2x), +45°/-45°, 90° (2X), 8 ply both faces	Sandwich	22
17	Composite, IM7/TC350	8 Ply/ 1-inch-thick fill	ROHACELL® Foam & Tape	+45°/-45°, 0° (2x), +45°/-45°, 90° (2X), 8 ply both faces	Sandwich	10
18	Composite, IM7/TC350	8 Ply/ 1-inch-thick fill	ROHACELL® Foam & Tape	+45°/-45°, 0° (2x), +45°/-45°, 90° (2X), 8 ply both faces	Sandwich	22

Upon completion of the tests tabulated in Table 7.2.1-3, the test series continued with the tests shown in Table 7.2.1-4 for the Group III tests (test numbers 19 through 28). One new variable was introduced in the Group III tests, which was using a monolithic composite LSC plate in lieu of the Al panel used in all of the previous testing. The new variable was introduced since in some applications (e.g., a LSC-based stage separation system required to separate at a composite filament wound motor case interface, would have the shock introduced into the composite material from severance of the composite interface). The ply type, number of plies, and their layup for the composite LSC plates are tabulated in Table 7.2.1-5.


	NASA Engineering and Safety Center Technical Assessment Report	Document #:	Version:
		NESC-RP-12-00783	1.0
Title: Empirical Model Development for Predicting Shock Response on Composite Materials Subjected to Pyroshock Loading		Page #: 22 of 123	

Table 7.2.1-4. Modified Pyroshock Composite Material Characterization Test Matrix

Group III – Sandwich Composite Panels							
Panel and Test Number	Material	Panel Thickness	Fill/Ply	Test Panel Ply Orientation	Type	LSC (gpf)	LSC Plate*
19	Composite, IM7/TC350	8 Ply/1-inch-thick fill	Al Honeycomb & Fabric Face Sheets	90°/+45°/-45°/0°/0°/-45°/+45°/90°, 8 ply both faces	Sandwich	10	Fabric Composite, IM7/TC350
20	Composite, IM7/TC350	8 Ply/1-inch-thick fill	ROHACELL® Foam & Fabric Face Sheets	90°/+45°/-45°/0°/0°/-45°/+45°/90°, 8 ply both faces	Sandwich	22	Fabric Composite, IM7/TC350
21	Composite, IM7/TC350	8 Ply/1-inch-thick fill	Al Honeycomb & Tape Face Sheets	90°/+45°/-45°/0°/0°/-45°/+45°/90°, 8 ply both faces	Sandwich	22	Al
22	Composite, IM7/TC350	8 Ply/1-inch-thick fill	ROHACELL® Foam & Fabric Face Sheets	90°/+45°/-45°/0°/0°/-45°/+45°/90°, 8 ply both faces	Sandwich	10	Al
23	Composite, IM7/TC350	8 Ply/1-inch-thick fill	Al Honeycomb & Fabric Face Sheets	90°/+45°/-45°/0°/0°/-45°/+45°/90°, 8 ply both faces	Sandwich	10	Al
24	Composite, IM7/TC350	8 Ply/1-inch-thick fill	Al Honeycomb & Fabric Face Sheets	90°/+45°/-45°/0°/0°/-45°/+45°/90°, 8 ply both faces	Sandwich	22	Al
25	Composite, IM7/TC350	8 Ply/1-inch-thick fill	Al Honeycomb & Fabric Face Sheets	90°/+45°/-45°/0°/0°/-45°/+45°/90°, 8 ply both faces	Sandwich	22	Fabric Composite, IM7/TC350
26	Composite, IM7/TC350	8 Ply/1-inch-thick fill	ROHACELL® Foam & Tape Face Sheets	90°/+45°/-45°/0°/0°/-45°/+45°/90°, 8 ply both faces	Sandwich	22	Tape Composite, IM7/TC350
27	Composite, IM7/TC350	8 Ply/1-inch-thick fill	ROHACELL® Foam & Fabric Face Sheets	90°/+45°/-45°/0°/0°/-45°/+45°/90°, 8 ply both faces	Sandwich	10	Fabric Composite, IM7/TC350
28	Composite, IM7/TC350	8 Ply/1-inch-thick fill	Al Honeycomb & Tape Face Sheets	90°/+45°/-45°/0°/0°/-45°/+45°/90°, 8 ply both faces	Sandwich	10	Tape Composite, IM7/TC350

*See Table 7.2.1-5 for LSC plate ply layout.


	NASA Engineering and Safety Center Technical Assessment Report	Document #: NESC-RP-12-00783	Version: 1.0
Title: Empirical Model Development for Predicting Shock Response on Composite Materials Subjected to Pyroshock Loading			Page #: 23 of 123

Table 7.2.1-5. Pyroshock Composite LSC Plate Ply Layout

Ply Number	Orientation Fabric Ply	Orientation Tape Ply
1	45°	45°
2	-45°	-45°
3	0°	0°
4	0°	0°
5	45°	45°
6	-45°	-45°
7	90°	90°
8	90°	90°
9	-45°	45°
10	45°	-45°
11	90°	0°
12	90°	0°
13	-45°	45°
14	45°	-45°
15	0°	0°
16	0°	90°
17	-45°	90°
18	45°	0°
19		-45°
20		45°
21		0°
22		0°
23		-45°
24		45°
25		90°
26		90°
27		-45°
28		45°
29		0°
30		0°
31		-45°
32		45°

Following evaluation of the Group I tests 1 through 10 test data, it was determined to perform re-tests of selected Group II tests, which were performed as tabulated in Table 7.2.1-6. NDE (pulse echo ultrasound) was performed and an evaluation comparing the initial NDE results and the post-test results for any differences in the panel's integrity was performed prior to conducting the re-tests. As previously stated, no new indications were found in the four composite monolithic panels.


	NASA Engineering and Safety Center Technical Assessment Report	Document #:	Version:
		NESC-RP-12-00783	1.0
Title:		Page #:	
Empirical Model Development for Predicting Shock Response on Composite Materials Subjected to Pyroshock Loading		24 of 123	

Table 7.2.1-6. Pyroshock Composite Group II Re-Tests

Test No.	Group I Previous Test #	LSC Core Load	Panel Thickness (in)	Composite Ply
Rep 1	10	10	0.2	Tape
Rep 2	4	22	0.3	Fabric
Rep 3	2	22	0.2	Fabric
Rep 4	9	22	0.3	Tape


Based on input from the SLS Program, a test series incorporating the use of foam acoustic damping material, which is designed to mitigate acoustics transmitted to components mounted inside a payload fairing to selected test panels, was performed. The objective of this test series was to characterize the damping ability of the material when mounted to either metallic (Al), monolithic composite, or sandwich composite panels with regards to pyroshock. The data from these tests allowed data analysis from dampened panels to be directly compared with the data collected with the panels without the dampening material.

These tests provided a qualitative comparison of pyroshock energy attenuation of Al, monolithic composite with a quasi-isotropic ply layup, and composite sandwich panels (Al honeycomb or ROHACELL[®] foam fill and quasi-isotropic ply face sheets) with and without the acoustic dampening material. Test panels that were previously subjected to the pyroshock test were modified with the addition of the foam acoustic material adhesively bonded to the backside of the panels for this testing. See Table 7.2.1-7 for the test panels used for this testing.

Table 7.2.1-7. Melamine Foam Damped Test Series

Test Order	Panel No	Type	Core Load	Dampening
1	17	ROHACELL [®]	22	0
2	12	Monolithic	22	Damped
3	8	Al	22	0
4	18	ROHACELL [®]	22	Damped
5	11	Al Honeycomb	22	0
6	Pathfinder	Al	22	0
7	Pathfinder	Al	22	Damped
8	17	ROHACELL [®]	22	Damped
9	11	Al Honeycomb	22	Damped
10	8	Monolithic	22	Damped

The replicate tests performed in the Group IV testing used a number of different panels since the panel-to-panel variability was considered more important than the “within-panel” variability (i.e., for a flight application the composite material would only be subjected to pyroshock once within its anticipated lifetime). Note: For tests 27 and 28, severance of the LSC composite plate

	NASA Engineering and Safety Center Technical Assessment Report	Document #:	Version:
		NESC-RP-12-00783	1.0
Title:		Page #:	
Empirical Model Development for Predicting Shock Response on Composite Materials Subjected to Pyroshock Loading		25 of 123	

was not achieved; however, the shock data were acquired and used in the analysis of the shock data, but not in the statistical analysis of the post-processed data.

7.2.2 Test Articles

Figure 7.2.2-1 illustrates the concept for mounting the LSC to an Al severance plate and the mounting of the severance plate to either the Al or composite panel. The LSC was mounted to the Al plate on shims to obtain the optimum standoff for each of the LSCs used.

Figure 7.2.2-2 illustrates the solid composite panel configuration.

Figure 7.2.2-3 illustrates the Al pathfinder panel and Figure 7.2.2-4 illustrates the shimmed LSC mounted onto the LSC plate.

The LSCs were secured to Al standoff shims (mounted to the sacrificial severance LSC plate) with tape. However, for some of the Group IV tests there was insufficient 4-ft lengths of 22-gpf LSC remaining and two 2-ft lengths spliced together were used. For mounting, the two short lengths of LSC splice plates were introduced for securing the LSC to the LSC shims along with tape. (Reference Appendix A, Section A1, Figure A13 for details on the splice plate drawing).

Figures 7.2.2-5 and 7.2.2-6 illustrate the solid and sandwich composite panel configurations, respectively. Figure 7.2.2-7 illustrates the mounting of the LSC to the sandwich panel configuration.

Figure 7.2.2-8 illustrates the melamine foam bonded to the backside of the composite sandwich panel.

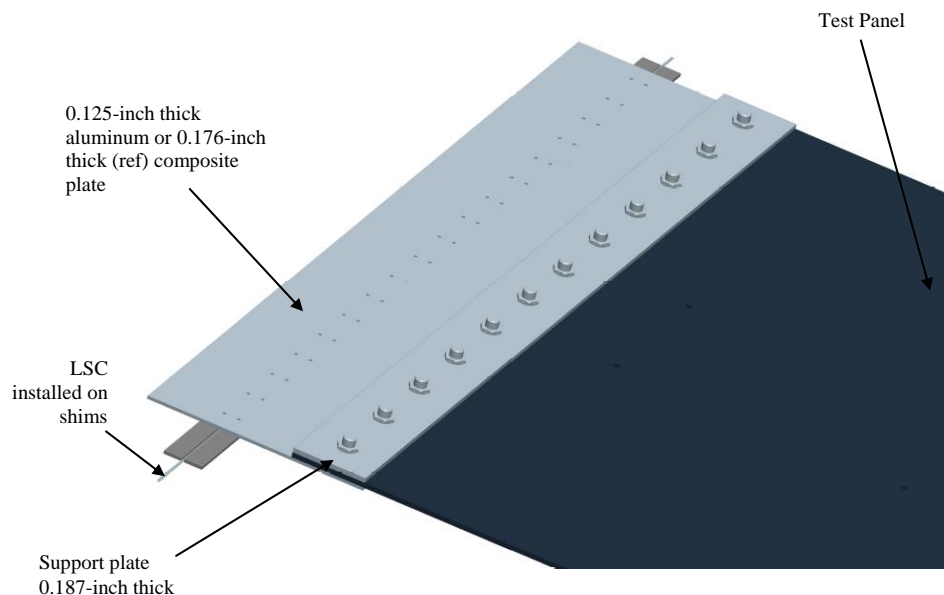



Figure 7.2.2-1. LSC Severance Plate to Test Panel Mounting

	<p align="center">NASA Engineering and Safety Center Technical Assessment Report</p>	<p>Document #: NESC-RP-12-00783</p>	<p>Version: 1.0</p>
<p>Title: Empirical Model Development for Predicting Shock Response on Composite Materials Subjected to Pyroshock Loading</p>		<p>Page #: 26 of 123</p>	

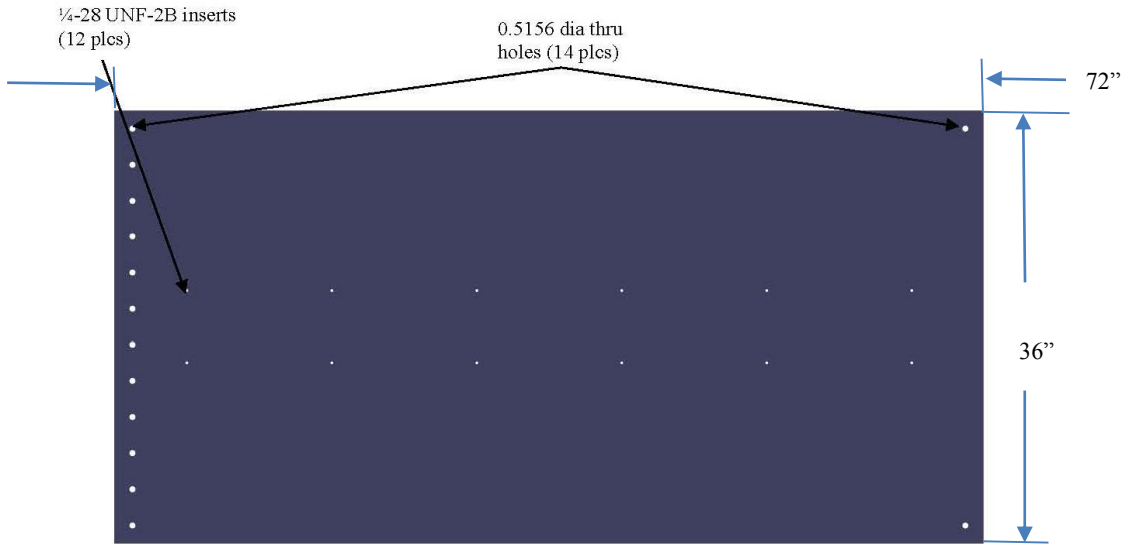


Figure 7.2.2-2. Solid Composite Test Panel



Figure 7.2.2-3. Al Pathfinder Panel

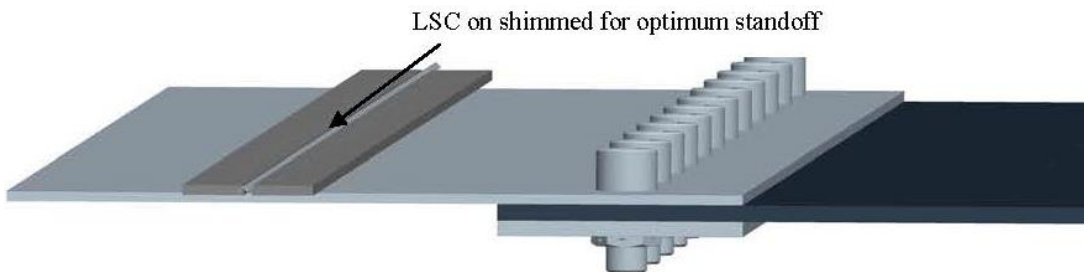



Figure 7.2.2-4. LSC Mounted to Shims on LSC Plate

	NASA Engineering and Safety Center Technical Assessment Report	Document #: NESC-RP-12-00783	Version: 1.0
Title: Empirical Model Development for Predicting Shock Response on Composite Materials Subjected to Pyroshock Loading		Page #: 27 of 123	

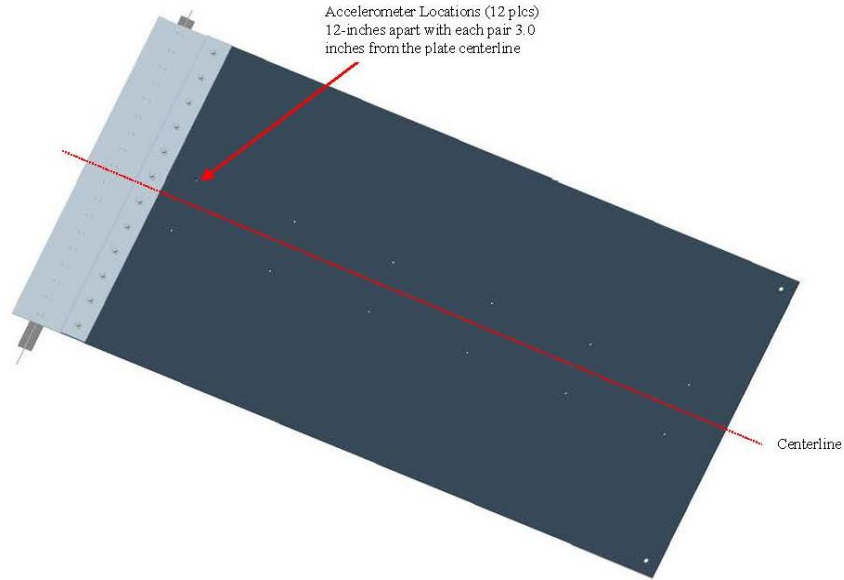


Figure 7.2.2-5. Composite Solid Panel Test Setup

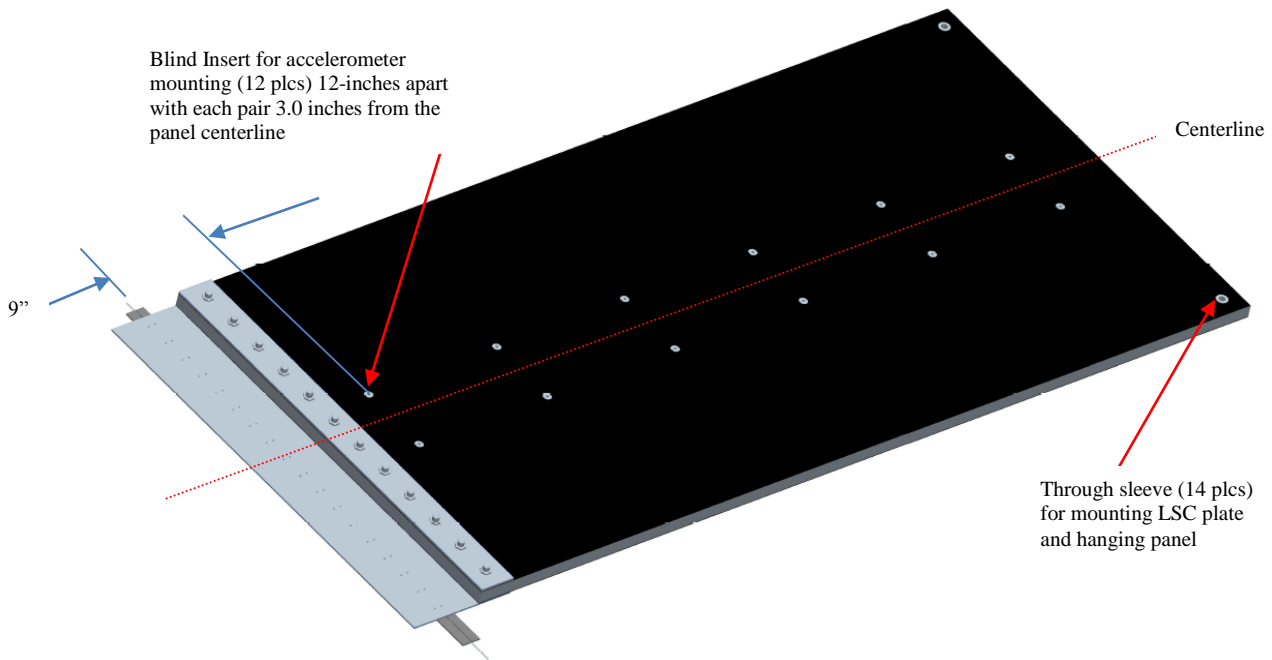

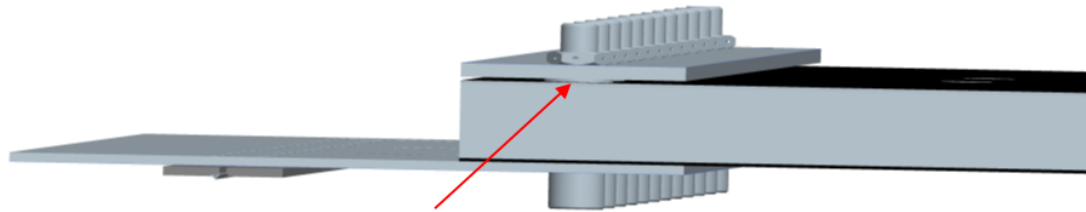


Figure 7.2.2-6. Composite Sandwich Panel Test Setup

	NASA Engineering and Safety Center Technical Assessment Report	Document #:	Version:
		NESC-RP-12-00783	1.0
Title:		Page #:	
Empirical Model Development for Predicting Shock Response on Composite Materials Subjected to Pyroshock Loading		28 of 123	



Through sleeve for mounting LSC installed in sandwich panel for LSC plate and backer plate fastener installation.

Figure 7.2.2-7. Composite Sandwich Panel Test Setup, LSC Plate Mounting

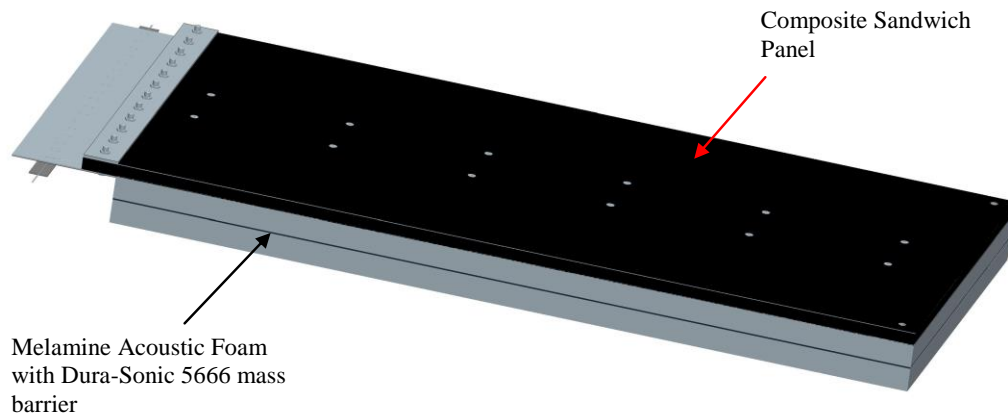


Figure 7.2.2-8. Composite Sandwich Panel with MAF


7.2.3 Test Setup

To achieve the objectives outlined for this task, acquiring “quality” shock time history data is imperative. Acquiring “quality” data begins with careful test planning. IEST-RP-DTE012.1, *Handbook for Dynamic Data Acquisition and Analysis*, provides some recommended guidelines for pyroshock measurement locations listed below.

- For homogeneous structures between the pyrotechnic source and measurement location, never select a measurement location within 6 inches of the source.
- Always select measurement locations that are as far from the pyrotechnic source as feasible to continue to acquire meaningful engineering information.
- When applicable, select measurement locations that are separated from the source by a structural path with discontinuities (e.g., riveted or bolted joints or isolation elements).

The test setup for the pyroshock characterization of composites was purposely designed to acquire the shock data via the accelerometers separated by a bolted joint from the source shock.

Another recommendation from IEST-RP-DTE012.1 to check for possible electromagnetic radiation (EMR) by freely suspending an additional accelerometer adjacent to, but not touching, the structure, and to acquire data from the accelerometer using an identical signal conditioner

	NASA Engineering and Safety Center Technical Assessment Report	Document #: NESC-RP-12-00783	Version: 1.0
Title: Empirical Model Development for Predicting Shock Response on Composite Materials Subjected to Pyroshock Loading		Page #: 29 of 123	

with the same gain setting. Any significant output from the signal conditioner on the freely suspended accelerometer due to the pyroshock event is an indication of an EMR noise interference problem. Per the test reports contained in Appendix B of this report, accelerometer channel 13 used in each test was a freely suspended accelerometer. The data from this accelerometer were analyzed and output from accelerometer channel 13 for any of the pyroshock tests conducted for this task assessment was insignificant.

The tests were conducted at MSFC Building 4619 by Structural Dynamics Test Branch (ET40) personnel. The tests were conducted in accordance with an ET40 test checkout procedure (TCP), which included all explosive safety handling requirements. The panels were suspended at two corners from the facility ceiling using braided steel cables and secured to the facility floor at the opposite corners of the panel with braided steel cable. An LSC was fired, and acceleration data were collected at multiple locations on the panel. Figure 7.2.3-1 illustrates this configuration.

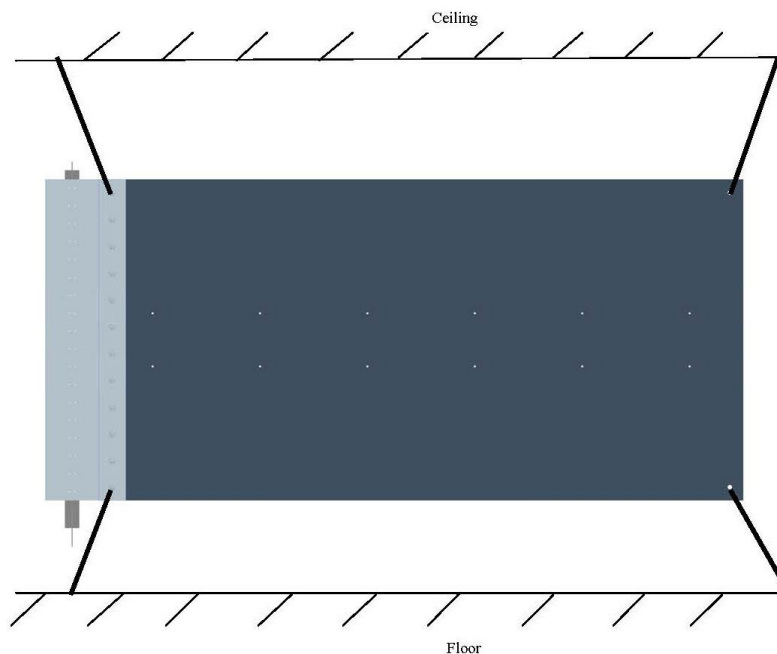


Figure 7.2.3-1. Panel Attachment to Test Facility

ET40 provided D-rings and cables for attaching the panels to the facility ceiling and rope for securing the bottom edge of the panel to the facility floor.

Both 10-gpf and 22-gpf LSC were used to generate the source shock. To determine the Al LSC shim heights for the respective LSC used for this testing and to determine a thickness of the Al LSC severance plate the theoretical severance of the LSC was calculated and is shown in Figure 7.2.3-2. The LSC severance calculations were based upon positioning the LSC at its optimum standoff, which is shown in Figure 7.2.3-3.



Title:

Empirical Model Development for Predicting Shock Response on Composite Materials Subjected to Pyroshock Loading

Page #:
30 of 123

Calculated severance Aluminum sheath (aluminum target)

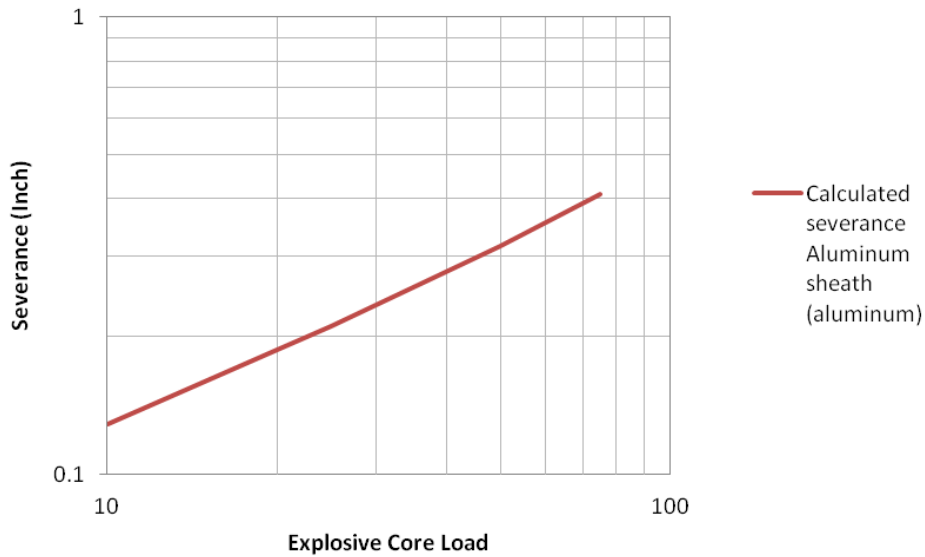


Figure 7.2.3-2. Calculated Severance Al Sheath LSC with Al Target

Standoff (RDX/CH6 Aluminum Sheath LSC)

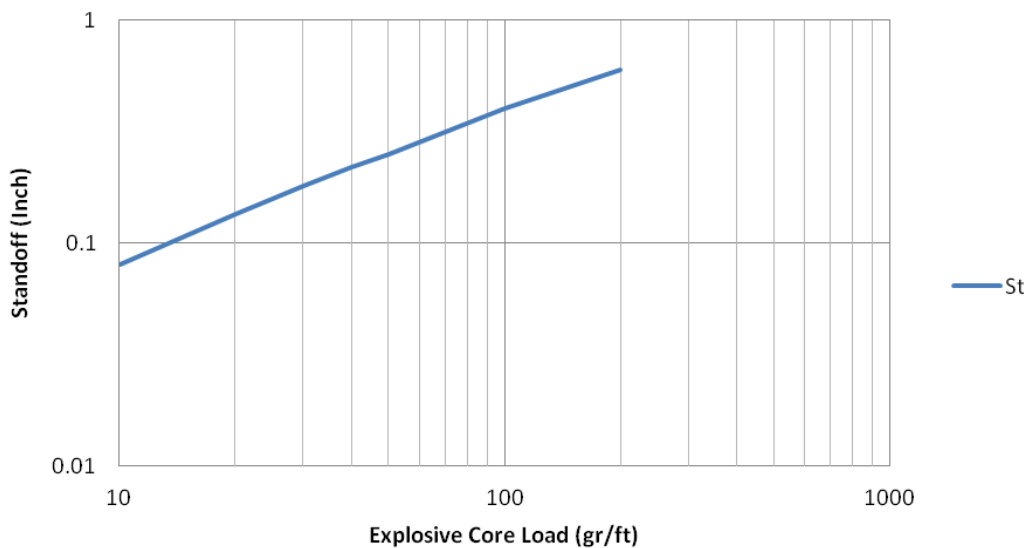



Figure 7.2.3-3. Optimum Standoff Al Sheath LSC

	NASA Engineering and Safety Center Technical Assessment Report	Document #:	Version:
		NESC-RP-12-00783	1.0
Title:		Page #:	
Empirical Model Development for Predicting Shock Response on Composite Materials Subjected to Pyroshock Loading		31 of 123	

7.2.4 Instrumentation and Data Acquisition

7.2.4.1 Instrumentation

Response data of interest for this testing was in the frequency range from 100 Hz to 10,000 Hz. Stud-mount PCB 350C02 and PCB 350D02 accelerometers were used to collect both high and low frequency shock data. The pathfinder tests and the initial Group I test (tests 1 through 5) were all instrumented with the PCB 350C02 accelerometers mounted to the panel for data collection. Starting with Group I, Tests 7 through 10, continuing with the same pattern through the Group II tests, 11 through 18, and the Group III tests, 19 through 28, and Group IV tests, the PCB D02 accelerometers were introduced in a random pattern to evaluate whether a difference exists in the data acquired by the two versions of accelerometers. This evaluation resulted in the conclusion the difference data output between the two versions of accelerometers was indiscernible.

Figure 7.2.4.1-1 shows the attributes of both the PCB 350C02 and PCB 350D02 accelerometers. Figure 7.2.4.1-2 illustrates the pattern for locating for the PCB 350C02 and PCB 350D02 for Group I tests 7 through 10 and the balance of the remaining tests performed (i.e., alternating the PCB 350C02 and PCB 350 D02 from top to bottom on alternating tests).

Performance Characteristic	PCB350C02	PCB350D02
Electrical Filter Corner Frequency	13 kHz	17 kHz
Mechanical Filter Resonant Frequency	23 kHz	45 kHz

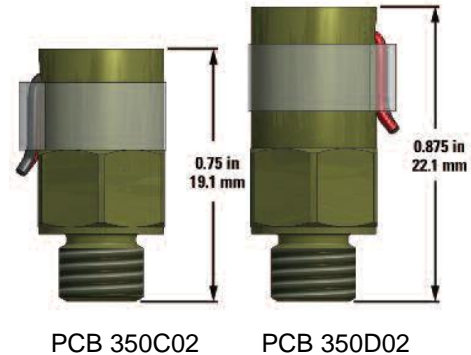



Figure 7.2.4.1-1. PCB 350C02 and PCB 350D02 Accelerometer Comparisons

Accelerometers were mounted every 12 inches along the length of the plate, beginning at 9 inches from the location of the LSC and 3 inches from either side of the panel centerline. (Reference Figures 7.2.2-5 and 7.2.2-6).

	NASA Engineering and Safety Center Technical Assessment Report	Document #:	Version:
		NESC-RP-12-00783	1.0
Title:		Page #:	
Empirical Model Development for Predicting Shock Response on Composite Materials Subjected to Pyroshock Loading		32 of 123	

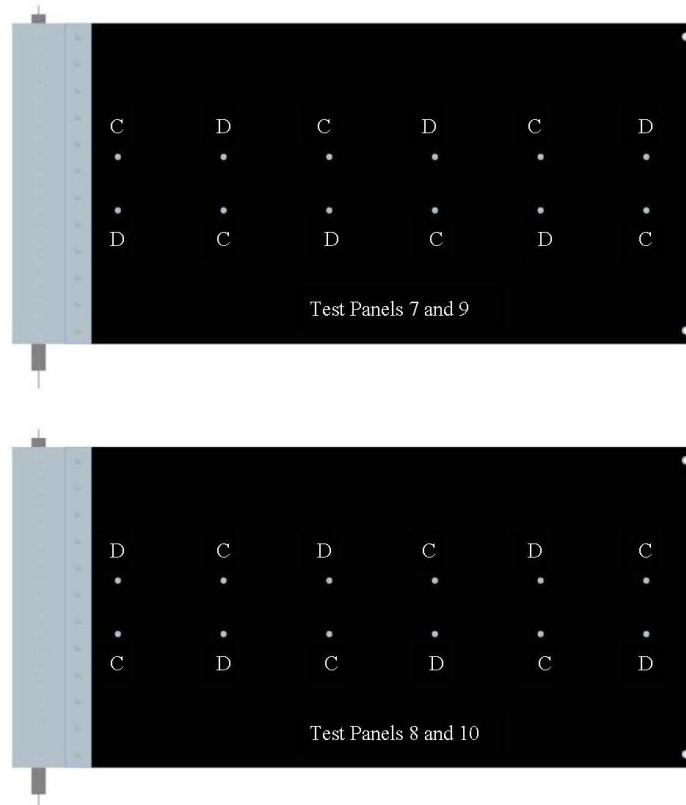


Figure 7.2.4.1-2. Location of Accelerometers, PCB 350C02 versus PCB 350D02

Inserts were installed in each of the panels for accelerometer mounting. The type of insert used for the monolithic composite was a stainless steel threaded insert (7/16-14 outside diameter thread and 1/4-28 internal diameter thread). Prior to installation of the threaded inserts, the monolithic composite panels were tapped with a 7/16-14 tap for insert installation and bonded in place (flush with the composite panel surface) with Hysol[®] EA 9394 adhesive. For the composite sandwich panels, a different type of insert was needed to mount the accelerometers. For the sandwich panels, a clipnut blind insert was used, which had a 1/4-28 internal thread. The blind inserts were installed to a specified depth, such that the top surface of the insert would be flush with the top surface of the composite face sheet, and bonded in place. The location of the inserts are as depicted on the composite panel drawings for mounting the accelerometers (reference Appendix A, Section A1). Appendix A, Section A2.3, provides details on each of the inserts used and mounting of the inserts into the composite test panels.

Typical pyroshock test setups for the monolithic composite panels, sandwich composite panels, and the tests with the MAF added to the composite panel is shown in Figures 7.2.4.1-3 through 7.2.4.1-6.



NASA Engineering and Safety Center Technical Assessment Report

Document #:
**NESC-RP-
12-00783**

Version:
1.0

Title:

**Empirical Model Development for Predicting Shock Response on
Composite Materials Subjected to Pyroshock Loading**

Page #:
33 of 123



Figure 7.2.4.1-3. Monolithic Composite Panel Pyroshock Test Setup (Typical)



NASA Engineering and Safety Center Technical Assessment Report

Document #:
**NESC-RP-
12-00783**

Version:
1.0

Title:

**Empirical Model Development for Predicting Shock Response on
Composite Materials Subjected to Pyroshock Loading**

Page #:
34 of 123

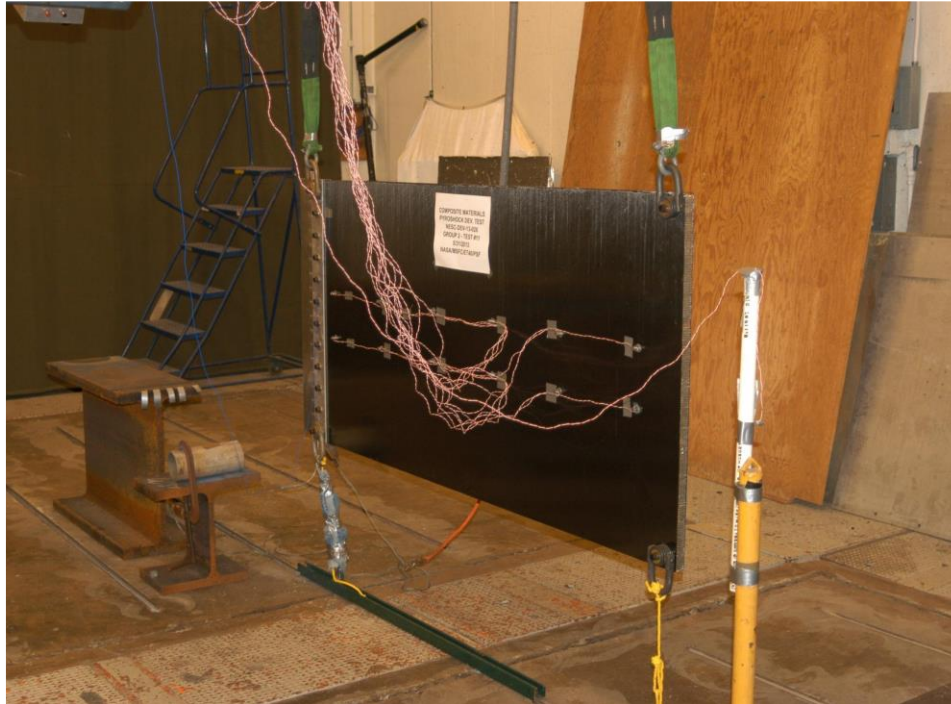



Figure 7.2.4.1-4. Composite Sandwich Panel Pyroshock Test Setup (Typical)

	<p align="center">NASA Engineering and Safety Center Technical Assessment Report</p>	<p>Document #: NESC-RP-12-00783</p>	<p>Version: 1.0</p>
<p>Title: Empirical Model Development for Predicting Shock Response on Composite Materials Subjected to Pyroshock Loading</p>		<p>Page #: 35 of 123</p>	

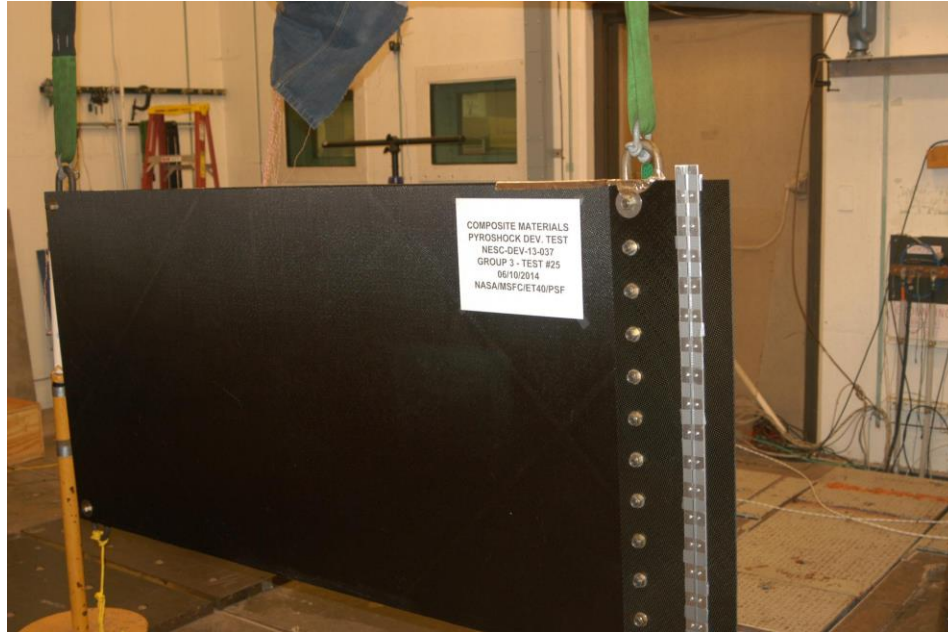



Figure 7.2.4.1-5. Composite Sandwich Panel Pyroshock Test Setup with Composite LSC Panel (Typical)

	NASA Engineering and Safety Center Technical Assessment Report	Document #: NESC-RP-12-00783	Version: 1.0
Title: Empirical Model Development for Predicting Shock Response on Composite Materials Subjected to Pyroshock Loading		Page #: 36 of 123	

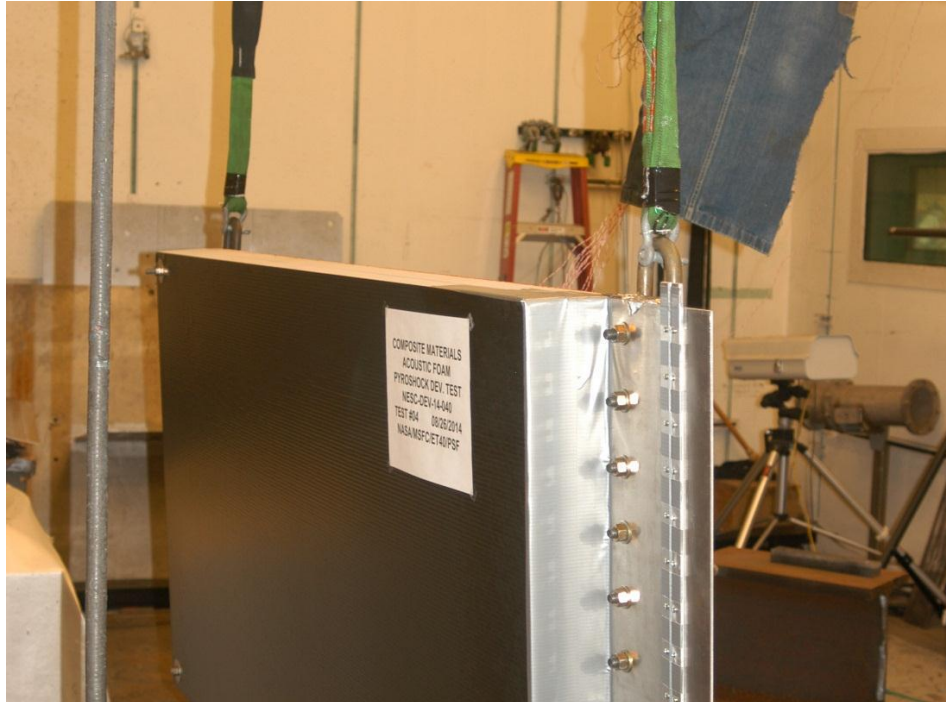



Figure 7.2.4.1-6. Composite Panel with Melamine Foam Pyroshock Test Setup (Typical)

	NASA Engineering and Safety Center Technical Assessment Report	Document #: NESC-RP-12-00783	Version: 1.0
Title: Empirical Model Development for Predicting Shock Response on Composite Materials Subjected to Pyroshock Loading		Page #: 37 of 123	

7.2.4.2 Data Acquisition

The instrumentation DAS was set up for data to be acquired from the response accelerometers at a rate consistent with best lab practice to obtain meaningful data in the frequency range specified which was a sample rate of 1 M samples per second. One of the absolute necessities for acquiring pyroshock acceleration data is to use anti-aliasing filters to prevent the high-frequency shock from “rolling-off” into the low-frequency data content thus artificially elevating the shock response in the low frequencies. Anti-aliasing filters were used for each of the response accelerometers and filtered output response from the accelerometers recorded. The filters used were Bessel infinite-impulse-response (IIR) (Fc@-3 dB) set at 33 kHz for each channel, as shown in the data acquisition setup tables at the end of each test report (reference Appendix B). Nicolet 614CB 4-channel cards were the specific cards chosen to acquire the accelerometer data.

7.2.5 Procedures

7.2.5.1 Roles/Responsibilities

ET40 provided the LSC plate, the backer plate, shims for mounting the LSC, the LSC, and electric blasting caps for initiation of the LSC.

ET40 test engineers installed all accelerometers, cables, and data acquisition equipment and verified the equipment was in proper working order. ET40 test engineers took digital photographs to document the pre-test setup, including locations and orientations of all accelerometers for each test, and the post-test results. ET40 test engineers secured the test panel to the facility ceiling/flooring. EV32 engineer (task assessment technical lead) assisted in installation of the LSC as required.

7.2.5.2 Test Levels

Two core loads of LSC were used for this testing for generation of the source shock. A 10-gpf LSC was used for the source shock and to evaluate the effect the core load had on the shock propagation through the composite material, 22-gpf LSC was used to generate the source shock for comparison with the 10-gpf LSC. To ensure proper data acquisition from the accelerometers, the peak acceleration needs to be estimated to ensure the proper model of accelerometer is used and the DAS is properly ranged. Figures 7.2.5.2-1 and 7.2.5.2-2 illustrate the estimated source shock produced by each of these LSCs. The source shock estimates are based on Martin Marietta Aerospace Systems Pyrotechnic Shock Design Guidelines Manual (NASA-CR-116406, Contract NAS5-15208, March 1970).



NASA Engineering and Safety Center Technical Assessment Report

Document #:
**NESC-RP-
12-00783**

Version:
1.0

Title:

Empirical Model Development for Predicting Shock Response on Composite Materials Subjected to Pyroshock Loading

Page #:
38 of 123

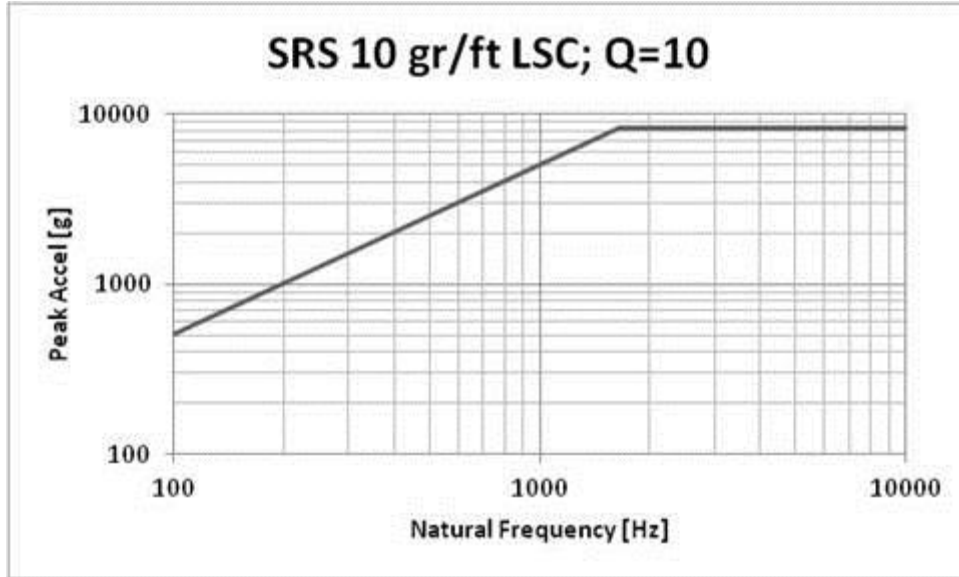


Figure 7.2.5.2-1. Estimated Source Shock, 10-gpf LSC

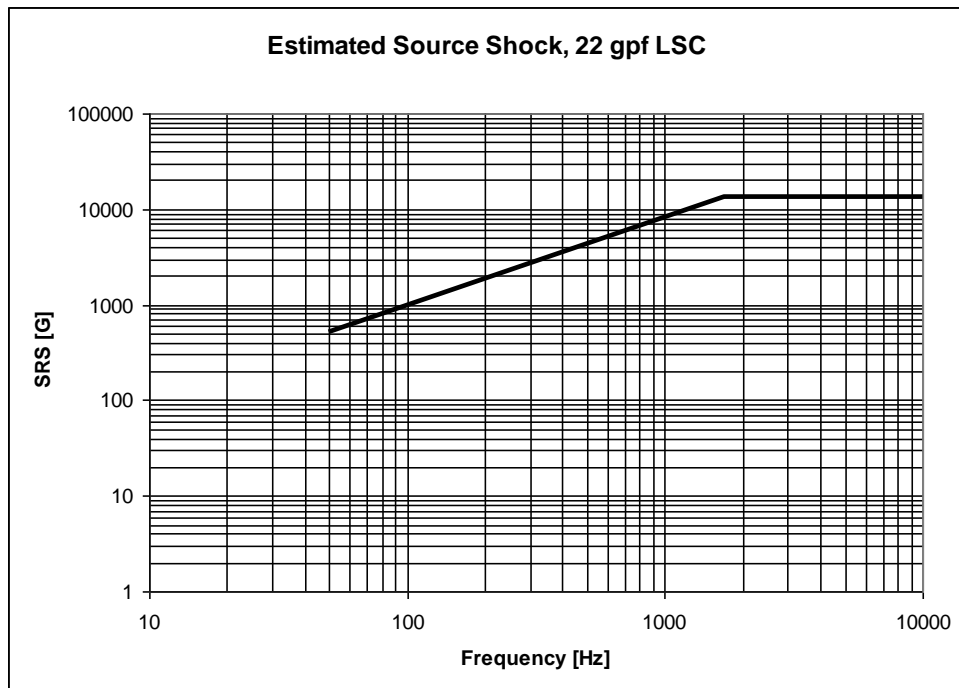



Figure 7.2.5.2-2. Estimated Source Shock, 22-gpf LSC

	NASA Engineering and Safety Center Technical Assessment Report	Document #: NESC-RP-12-00783	Version: 1.0
Title: Empirical Model Development for Predicting Shock Response on Composite Materials Subjected to Pyroshock Loading		Page #: 39 of 123	

7.2.6 Post-Test Operations

Following completion of each LSC firing, the test panel was visually inspected for indications of damage, loosening of accelerometers, and any other off-nominal condition. Post-test digital photographs were taken of each test documenting the test result. Off-nominal conditions, for example failure of the LSC to sever the LSC plate, were photographed and documented. Typical pre-test and post-test photos are documented in the test reports for each test group in Appendix B.

7.2.7 Data Requirements

The ET40 TCP used to perform the testing included data sheets to record the following information:

- Panel material and configuration
- Panel serial number (S/N)
- LSC core load and explosive material
- LSC L/N
- Accelerometer S/N by location
- AI LSC panel severance (yes/no)


The response data from all accelerometers was provided to EV32 and the Mechanical, Thermal and Life Support Analysis Branch (ES22) in electronic format as the acceleration time history (raw data and Fourier transform) and “quick-look” (prior to post-test data processing) shock response spectra. The test reports within Appendix B contain all of the time history and shock response spectra generated by ET40 for each of the accelerometers for each test categorized by test group.

Digital photographs of each test article, along with the corresponding data listed above, were provided to EV32. Photographs were labeled such that panel S/N, LSC core load, and instrumentation locations and orientations were easily discernible.

All test data from this test series will be retained for a minimum of 10 years following completion of the testing.

7.2.8 Evaluation Criteria

There were no pass/fail criteria for this test series; tests were performed for data acquisition only. The test was considered successful if a shock was introduced into the test panel as defined herein and the acceleration response data from the test was considered valid.

	NASA Engineering and Safety Center Technical Assessment Report	Document #: NESC-RP-12-00783	Version: 1.0
Title: Empirical Model Development for Predicting Shock Response on Composite Materials Subjected to Pyroshock Loading		Page #: 40 of 123	

7.3 Post-Test Data Processing and Data Evaluation

7.3.1 Post-Test Data Processing

7.3.1.1 Pyroshock Time History Data Processing Overview

The purpose of this section is to describe the procedures, methodologies, and tools used and developed to post-process the measured pyroshock time history data and characterize the pyroshock environment for developing empirical models describing the behavior of the shock environment as it propagates across a composite panel. The procedures, methodologies, and algorithms are presented are to provide clarity to the processes involved in preparing the data for empirical model development using statistical analysis methods. The purpose is twofold:

- To provide guidance for processing any future data that may be collected to expand upon the empirical models developed in this study.
- To provide the tools developed for use in processing shock data and for possible additional uses (e.g., "spin off" tools).

7.3.1.2 Data Analysis Procedure

Although "best practices" were incorporated into the pyroshock test setup, the acquired data must be evaluated to ensure it is "suitable" for analysis. The first step identified for analyzing the pyroshock accelerometer data is to develop a set of criteria used to define "suitable," or "quality" time history data. The following criteria were used to define "suitable" time history data:

- An adequate length of time was recorded to produce results in the frequency range of interest.
- The acceleration time history and the integral and double integral is illustrated in Figure 7.3.1.2-1 (i.e., velocity and displacement time histories, begin and end at or near zero and have similar characteristics),
- The methods developed from the processed time history signal used to characterize the pyroshock environment show no signs of typical time history errors such as a 0-g shift (typically a flattening of the SRS curve in the lower frequencies).



NASA Engineering and Safety Center Technical Assessment Report

Document #:
**NESC-RP-
12-00783**

Version:
1.0

Title:

Empirical Model Development for Predicting Shock Response on Composite Materials Subjected to Pyroshock Loading

Page #:
41 of 123

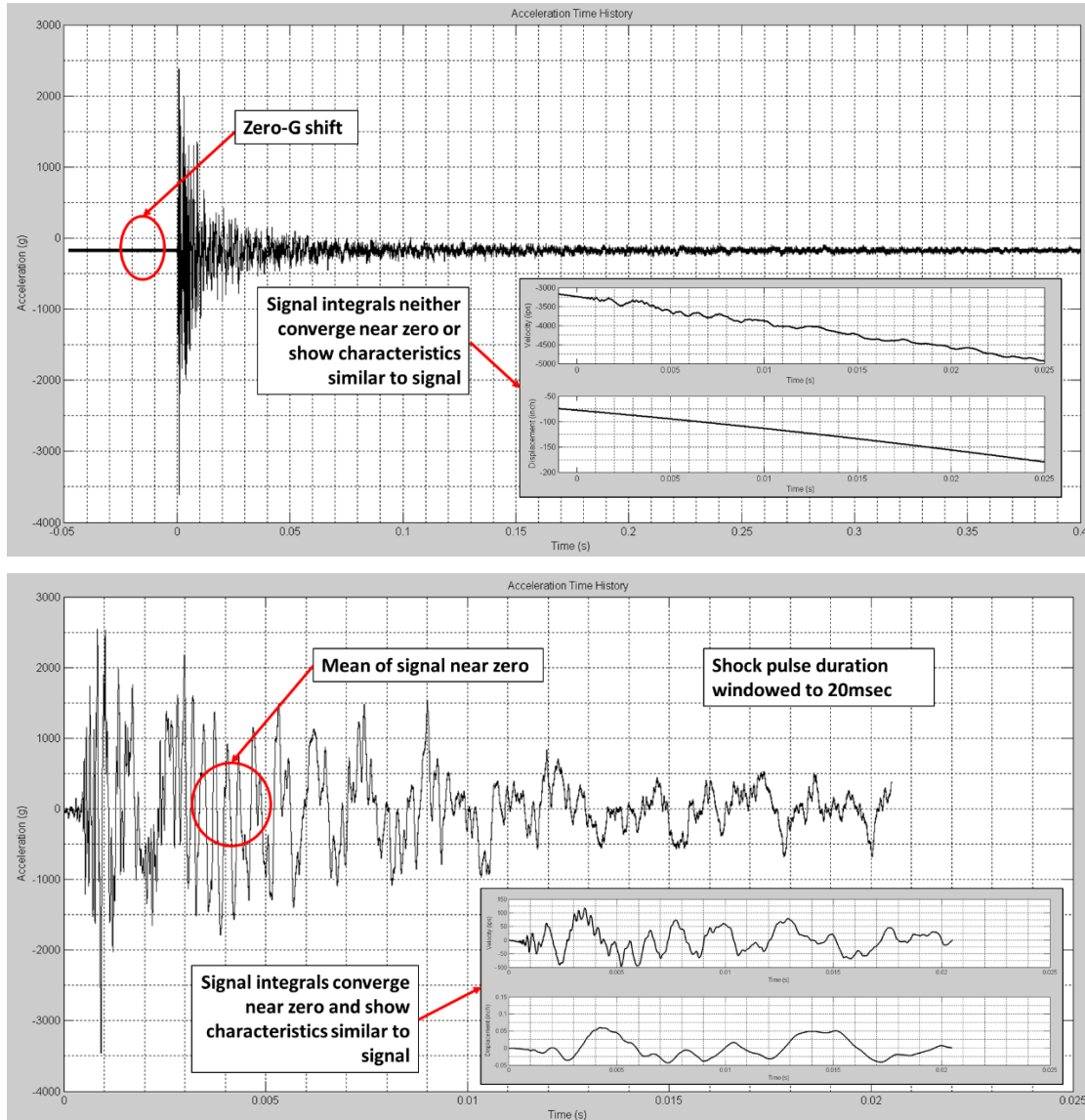



Figure 7.3.1.2-1. Comparison of Raw Time History Signal (Top) to Post-Processed Signal (Bottom)

A primary goal of this assessment was to obtain data that could be used to compare responses across the different test configurations as cleanly and easily as possible given the variations generally seen in this type of data. In addition to the constraints listed above, two additional constraints were applied to the criteria to mitigate the potential for unnecessary variation and uncertainty due to human error and to mitigate human bias:

- All calculations for each test were performed in the same manner.
- Subjective decisions were removed or mitigated. For example, when windowing the time history, simply “eyeballing” a start point for the beginning of the shock pulse would not

	NASA Engineering and Safety Center Technical Assessment Report	Document #: NESC-RP-12-00783	Version: 1.0
Title: Empirical Model Development for Predicting Shock Response on Composite Materials Subjected to Pyroshock Loading		Page #: 42 of 123	

meet the criteria of suitable since this is a subjective decision; therefore, an algorithm was developed for identifying the beginning of the shock pulse. This way, the same criteria for identifying the start of the shock pulse was applied to each data set.

Using the above criteria, the following procedure, reference Figure 7.3.1.2-2, was established for this test program as a process that produces suitable time history data for the characterizing the pyroshock environment.

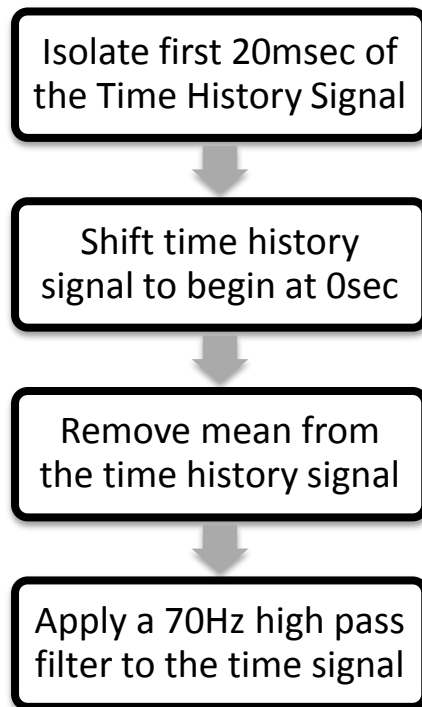



Figure 7.3.1.2-2. Acceleration Time History Signal Post-Processing Procedure

The first step of the procedure, identify first 20 msec of the time history pulse, can be subjective and therefore an algorithm was developed to perform this task to meet the suitability criteria. For reference, Figure 7.3.1.2-3 shows the MATLAB[®] code developed to retrieve the first 20 msec of a shock pulse from the time history data.

	NASA Engineering and Safety Center Technical Assessment Report	Document #: NESC-RP-12-00783	Version: 1.0
Title: Empirical Model Development for Predicting Shock Response on Composite Materials Subjected to Pyroshock Loading		Page #: 43 of 123	


```

1  function [ pulse20ms ] = first20ms( shockpulse )
2  %FIRST20MS Outputs first 20 ms of shock pulse
3  % Function will identify beginning of a shock pulse and output the first
4  % 20ms of the pulse with .5ms of data prior to pulse. Function identifies beginning of shock pulse by
5  % finding the first sign of a pulse that exceeds the value of the bit
6  % errors prior to detonation. Therefore, code assumes some amount of data
7  % has been saved prior to detonation (assumes first 42,500 data points
8  % prior to pulse for a time history recorded for 1 second at 1MHz sample rate).
9  % Input (shockpulse): a two column matrix of time (sec) and acceleration (G).
10 % Output (pulse20ms): two column matrix of just the first 20ms of the shock pulse.
11
12 %Calculate sampling period
13 dt=shockpulse(2,1)-shockpulse(1,1);
14
15 %Check that the time signal is greater than 20ms.
16 if length(shockpulse(:,1))*dt<0.02
17     error('Time signal must contain more than 20ms of data')
18 end
19
20 %Determine the number of sample points needed for 20ms of time data based
21 %on the time between samples. Note that a constant sampling period must be used.
22 ms20=.0205/dt;
23
24 %Determine where the shock pulse first exceeds the value of the bit error.
25 nn=length(shockpulse(:,1));
26 counter=1;
27 for jj=1:nn
28     biterror=max(abs(shockpulse(1:42500,2)));
29     if shockpulse(jj,2)<=biterror
30         counter=counter+1;
31     else
32         break
33     end
34 end
35 %Prevent error by setting a counter value in the event that the bit error is never exceeded.
36 if counter>100000
37     counter=60000;
38 end
39
40 %shift counter to account for addition of 0.5ms of data prior to pulse
41 counter=counter-0.0005/dt;
42 %Output the resulting time history.
43 pulse20ms=[shockpulse(counter:counter+ms20,1),shockpulse(counter:counter+ms20,2)];
44 end

```

Figure 7.3.1.2-3. MATLAB® Code for Retrieving the First 20 msec of a Shock Pulse from a Time History Signal

Note: This algorithm is dependent upon consistent procedures followed by the test laboratory personnel conducting the pyroshock test and should not be considered robust. Engineering judgment must be used when applying this algorithm to other data sets (e.g., the algorithm will not work for a variable sample rate). Therefore, the algorithm may require modifications in order to be suitable for other data sets.

	NASA Engineering and Safety Center Technical Assessment Report	Document #:	Version:
		NESC-RP-12-00783	1.0
Title:		Page #:	
Empirical Model Development for Predicting Shock Response on Composite Materials Subjected to Pyroshock Loading		44 of 123	

The second step of the signal processing procedure (shift time to begin at zero) is intended to remove any negative time values as certain SRS or PVRS codes may have issues dealing with negative values of time. The following MATLAB[®] code for shifting the time signal to begin at 0-sec is provided in Figure 7.3.1.2-4, for reference.

```

1  function [ t2 ] = shift_time( t1 )
2  %shift_time adjust a time series so that ti=0
3  %   Input is a two column vector with column 1 being time and column 2
4  %   being the measured response. The sampling period (dt) must be constant for the
5  %   entire duration.
6
7  t=t1(:,1);
8  N=length(t);
9  dt=t(2)-t(1);
10
11 t2=[(0:N-1)*dt,t1(:,2)];
12
13 end

```

Figure 7.3.1.2-4. MATLAB[®] Code for Shifting a Time Signal to Begin at 0 sec

The third step in the data processing procedure (remove the mean from the signal) is intended to remove any 0-g offsets in the acceleration time history. While there are multiple ways to perform this action, the following MATLAB[®] code, which uses MATLAB[®]'s “de-trend” function, is provided in Figure 7.3.1.2-5, for reference.

```


1  function [ dsig ] = detrend_t( sig, dopt )
2  %detrend_t Detrend the response in a measured time signal
3  %   Input is a measured signal that is a two column vector with the first
4  %   column as time and the second column as the measured signal.
5  %   dopt allows the ability to specify options for the detrend function.
6  %   Detrend options are typically 'constant' or 'linear'
7
8  switch nargin
9  case 1
10     dsig=[sig(:,1),detrend(sig(:,2))];
11     % display('Linear option chosen')
12 case 2
13     dsig=[sig(:,1),detrend(sig(:,2),dopt)];
14     % display('Constant option chosen')
15 end
16 end

```

Figure 7.3.1.2-5. Reference MATLAB[®] Code for Mean Removal

The fourth step in the data processing procedure (apply a high pass filter to the time signal) is a step that in combination with the mean removal produces a cleaner time history signal. For this test program, a 70-Hz high pass sixth-order Butterworth filter was used. The program used to apply this filter was from Tom Irvine’s “vibrationdata” signal analysis package, which can be accessed from the link listed below:

<https://vibrationdata.wordpress.com/2013/05/29/vibrationdata-matlab-signal-analysis-package/>

	NASA Engineering and Safety Center Technical Assessment Report	Document #: NESC-RP-12-00783	Version: 1.0
Title: Empirical Model Development for Predicting Shock Response on Composite Materials Subjected to Pyroshock Loading		Page #: 45 of 123	

Note: The above procedure was established to produce a “suitable” signal for data processing specifically for this task assessment test program. Utilization of other procedures for cleaning up the time history signal may be more suitable for other data sets to accomplish producing a time history signal the meets the “suitable” signal criteria as previously discussed. Engineering judgment should always be used when processing a time history signal for a pyroshock environment.

7.3.2 Post-Test Data Evaluation


The overall goal of post-processing the measured acceleration time history data was to put the data in a form that could be developed into an empirical model that captures the behavior of the shock environment as it propagates across the composite structure. There were two challenges that needed to be overcome:

1. Characterizing the pyroshock environment in a manner that would be suitable to multiple regression and other statistics-based engineering analysis methods. For this test program, that required characterizing the environment using single-value-inputs (SVI), a single number that characterizes some aspect of the environment.
2. Developing a procedure to calculate these SVIs that eliminates or mitigates data noise and the often-subjective decisions made when characterizing a shock environment.

Due to the complex nature of pyroshock acceleration time histories and the difficulties in test labs to recreate these time histories, the acceleration time history has limited practical value in characterizing a pyroshock environment. Therefore, response spectrums are the most common way to capture the nature and severity of a pyroshock environment. The two most common response spectrums for representing a pyroshock environment in the aerospace industry are the SRS and the PVRs. These response spectrums provide the environment as the peak response of a single-degree-of-freedom system to the pyroshock environment across a range of natural frequencies of the single-degree-of-freedom system. Therefore, response spectrums require two values, peak response and frequency, to characterize an environment and therefore are not SVIs. However, these response spectrums are often represented as a simple envelope of the actual spectrums. Therefore, the approach chosen for this test program was to break the spectrums down into SVI inputs that when evaluated together describe the spectrum. One complication is the actual enveloping is often left up to the analyst with little in the way of an industry-established procedure, which introduces an additional source of “human input” to the SVIs used to characterize the shock environment.

To address the first challenge the following methods and the subsequent SVIs used to represent them, for characterizing shock data were calculated for this test series for the purposes of statistical analysis:

- SRS
 - Slope
 - Frequency Break Point

	NASA Engineering and Safety Center Technical Assessment Report	Document #: NESC-RP-12-00783	Version: 1.0
Title: Empirical Model Development for Predicting Shock Response on Composite Materials Subjected to Pyroshock Loading		Page #: 46 of 123	


- Peak SRS Value
- PVRS
 - Mean of the Constant Velocity Line
- Acceleration, Velocity, and Displacement Time History
 - Maximum and minimum value of the acceleration time history
- Energy Spectral Density (ESD)
 - Frequency and amplitude of the peak ESD value
- Temporal Energy (area of the time history squared), which is already an SVI

This report assumes the user has the capabilities to calculate the above shock characterizing methods; however, there are also well-established software codes available online. Several of these codes can be found at <https://vibrationdata.wordpress.com/>. Maxi-max (the maximum value of the combined positive and negative curves), SRS, and PVRS curves were used for this test program.

While each of these methods listed above can provide insight into the nature of a pyroshock environment, based upon the evaluation of the data at the conclusion of this study, the following characteristics were chosen as the most effective for detecting and calculating shock attenuation trends:

- SRS
- Mean PV Value

To address the second challenge, procedures needed to be established for calculating the SVIs of the SRS and PVRS that mitigated noise and subjective decision making that could introduce human error and bias. The maximum PV can be calculated directly from the PV curve and did not need further algorithm processing. To assess the SRS, and divide them into SVIs that may be quantified, an algorithm was required to envelope the SRS and provide the envelope as a set of SVIs that characterize the shock. The SRS was divided into the slope, the maximum peak acceleration plateau, and the intersection of those two lines defined as the frequency break point. The test article parameters were then evaluated in terms on the effect to changes on specific parameters with regard to the slope value (within the sloped portion of the SRS), the break point (defined the beginning of plateau region of the SRS), and the maximum value of the plateau region of the SRS (or peak acceleration). As an example, Figure 7.3.2-1 illustrates the enveloping SRS algorithm calculated slope, plateau, and frequency break point for Group I, Test 2, accelerometer channels 3 and 4 at location 21 inches from the shock source.

	<p align="center">NASA Engineering and Safety Center Technical Assessment Report</p>	<p>Document #: NESC-RP-12-00783</p>	<p>Version: 1.0</p>
<p>Title: Empirical Model Development for Predicting Shock Response on Composite Materials Subjected to Pyroshock Loading</p>		<p>Page #: 47 of 123</p>	

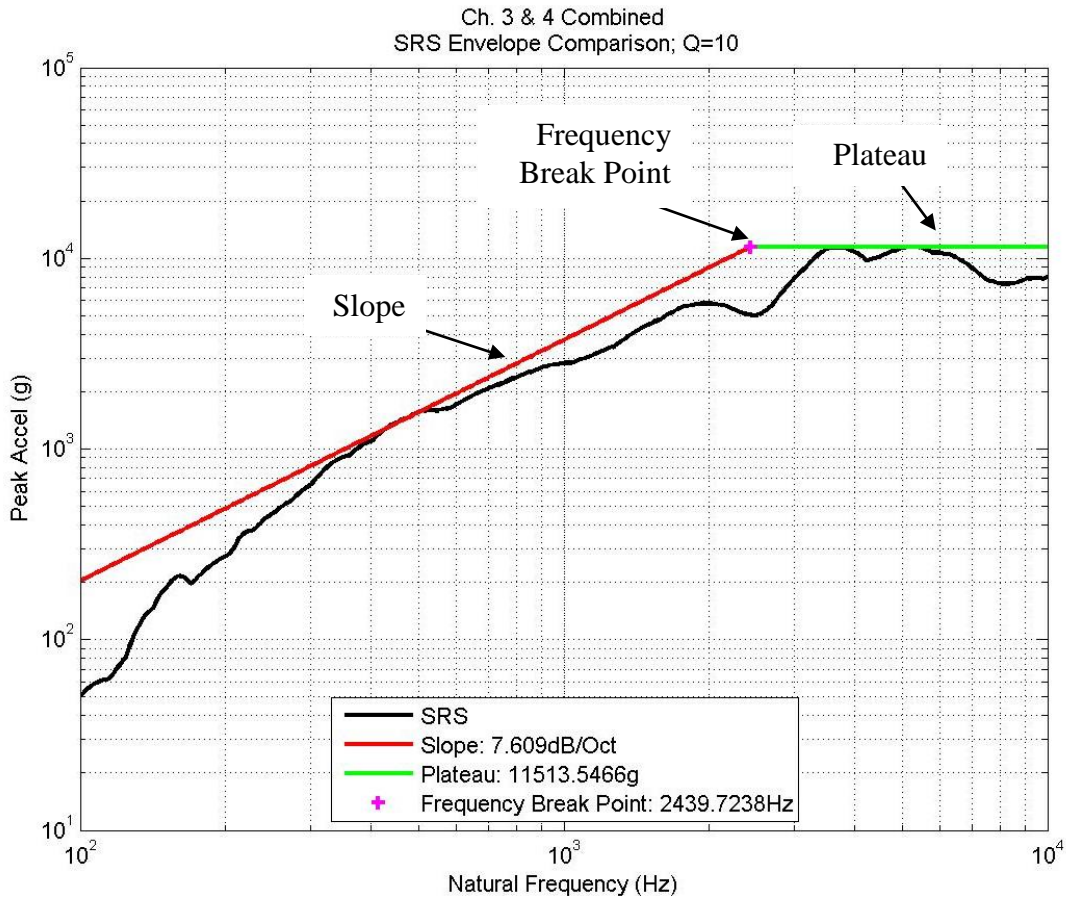


Figure 7.3.2-1. Data Output from SRS Enveloping Algorithm

As the data from the enveloping SRS was being generated it became apparent that certain composite materials produced a double plateau SRS across all locations of the test article. Therefore, the SVI for SRS curves needed to account for this double plateau possibility. The SRS algorithm was modified to account for this result as illustrated in Figure 7.3.2-2 for Group III, Test 25, accelerometer channels 3 and 4 at location 21 inches from the shock source.

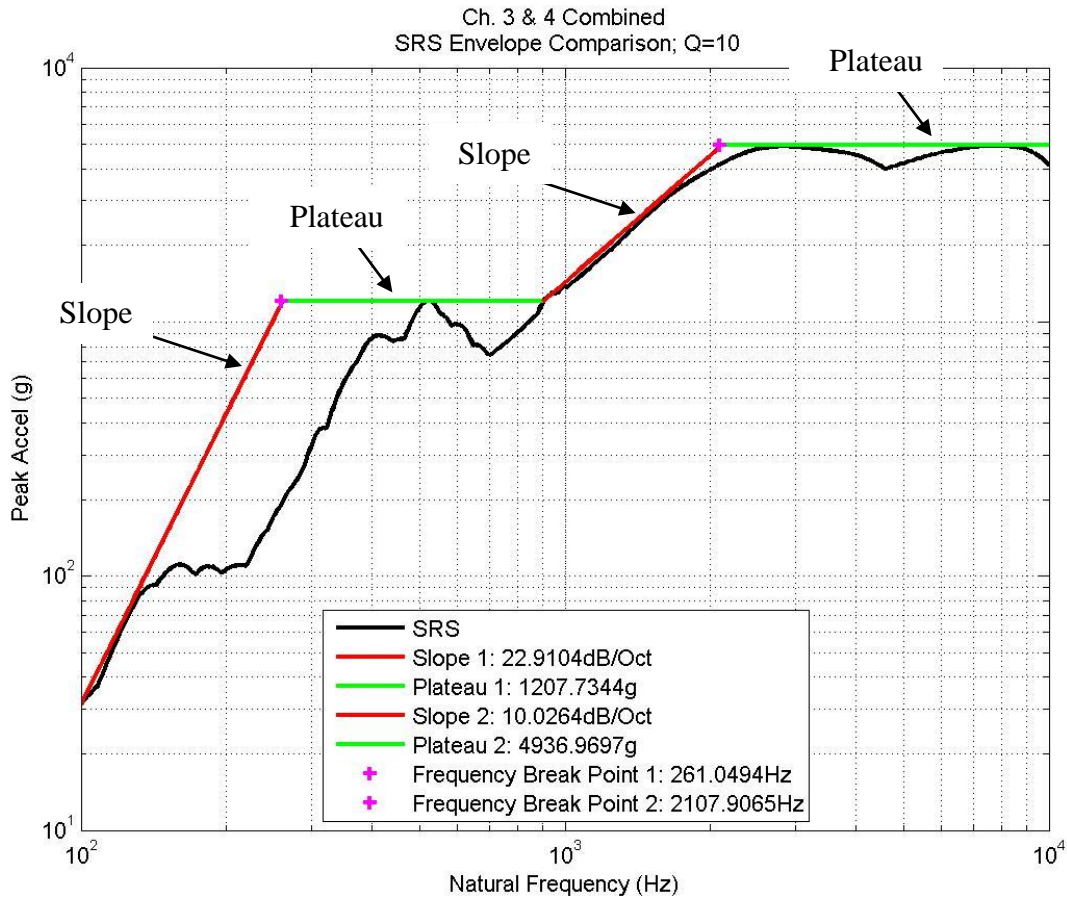


Figure 7.3.2-2. Data Output from SRS Enveloping Algorithm – Double Plateau

The PVRS of a simple shock plotted on four-coordinate paper (4CP) looks like a flattened hill, as shown in Figure 7.3.2-3, for Group I, Test 1, accelerometer channels 5 and 6 at location 33 inches from the shock source. The plateau, or top of the hill, shows the severe frequency range of the shock. The hill slopes down and to the right with an asymptote equal to the maximum acceleration. Maximum acceleration usually defines the high-frequency extent of the plateau. The hill slopes down and to the left with an asymptote equal to the maximum displacement, and maximum displacement defines the low-frequency plateau limit. The height of the plateau of the PVRS on 4CP and its frequency range is the severity of the shock.



Title:

Empirical Model Development for Predicting Shock Response on Composite Materials Subjected to Pyroshock Loading

Page #:
49 of 123

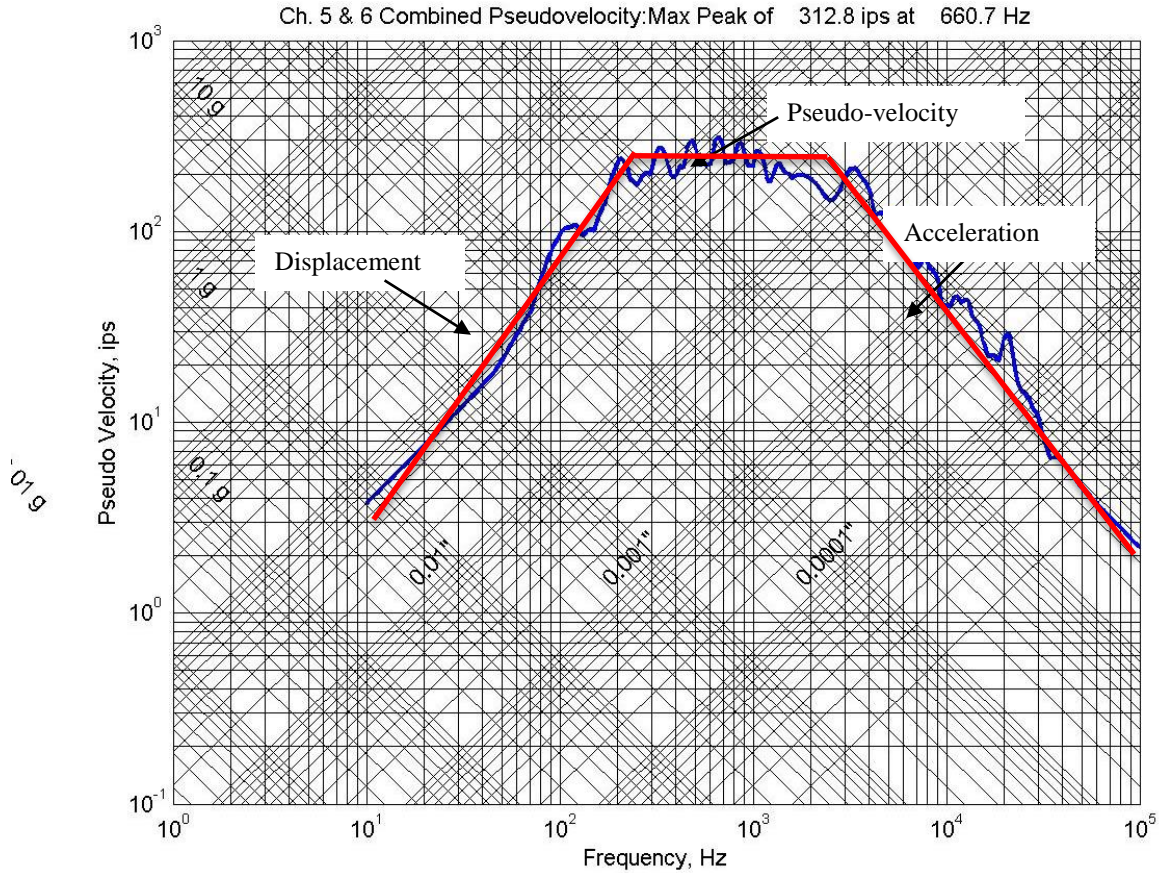



Figure 7.3.2-3. PVRS (4CP)

7.3.3 Algorithm Response Spectra Development

7.3.3.1 Shock Response Spectra

Enveloping an SRS curve can be subjective. Therefore, an algorithm was developed to perform this task to meet the suitability criteria listed in Section 7.3.1. Figure 7.3.3.1-1 illustrates the procedure developed to envelope the SRS curves.

	NASA Engineering and Safety Center Technical Assessment Report	Document #:	Version:
		NESC-RP-12-00783	1.0
Title: Empirical Model Development for Predicting Shock Response on Composite Materials Subjected to Pyroshock Loading		Page #: 50 of 123	

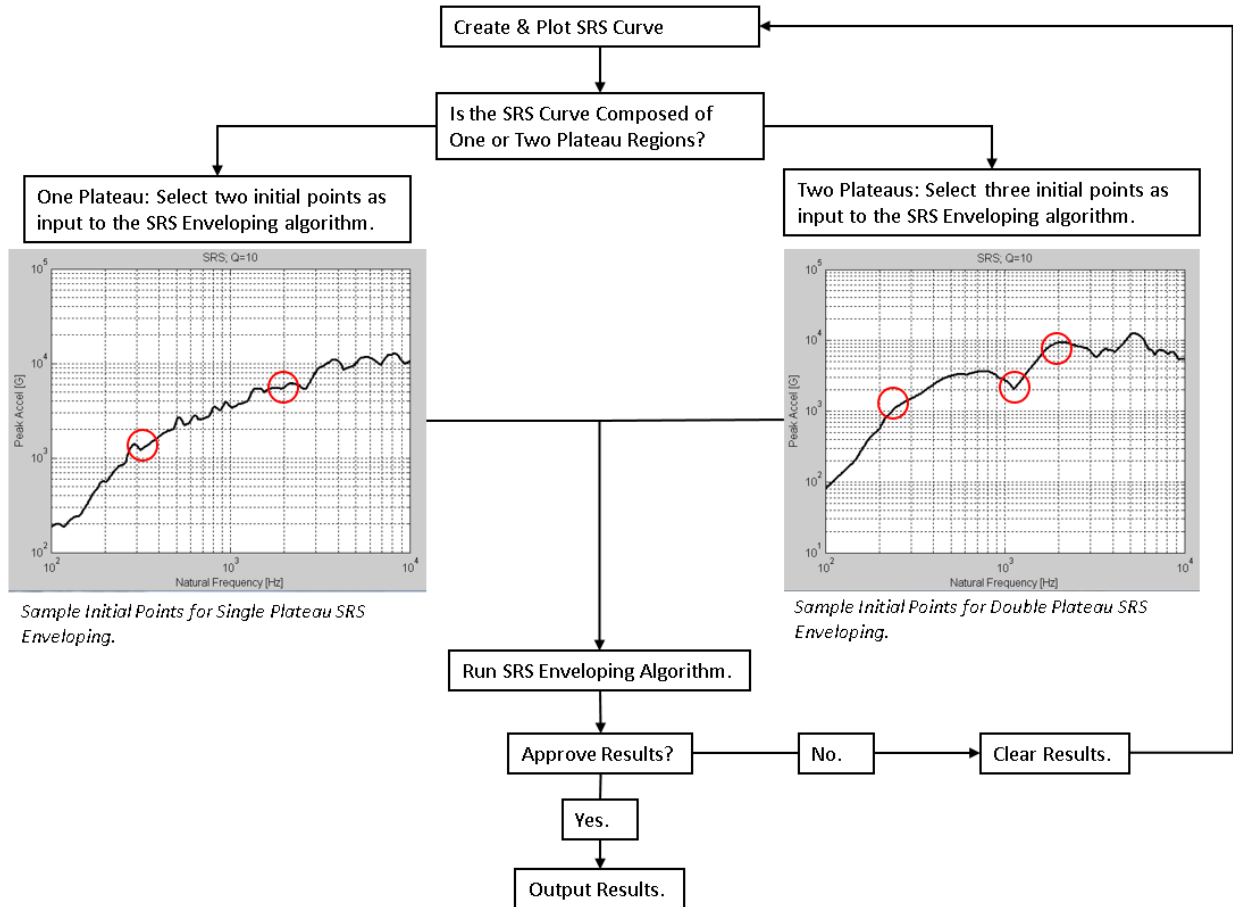



Figure 7.3.3.1-1. SRS Enveloping Procedure

For the tests results acquired for this task assessment, MATLAB[®] was used to perform the procedure, illustrated in Figure 7.3.3.1-1. Figure 7.3.3.1-2 provides the code for enveloping the SRS, for reference. Note: The SRS developed is a combination of the SRS curves produced by the two-paired accelerometers at any one location on the test panel (reference Figure C10, line 124).

	NASA Engineering and Safety Center Technical Assessment Report	Document #: NESC-RP-12-00783	Version: 1.0
Title: Empirical Model Development for Predicting Shock Response on Composite Materials Subjected to Pyroshock Loading		Page #: 51 of 123	

```

122  %% Calculate max SRS envelope of paired accel channels
123  for ff=2:length(test)
124      test(ao(ff)).srscomb=[test(ao(ff)).srs(:,1),max([test(ao(ff-1)).srs(:,2),test(ao(ff)).srs(:,2)).[]],2)];
125      [-,mxind]=max(test(ao(ff)).srscomb(:,2));
126      test(ao(ff)).srsmax=[test(ao(ff)).srscomb(mxind,1),test(ao(ff)).srscomb(mxind,2)];%location of max SRS value
127      clear mxind
128  end
129  clear ff mxind
130  save(test_set,'test');
131
132  %% Perform SRS Enveloping procedure.
133  % Allow user to iterate the enveloping processes until the desired result
134  % is achieved.
135  pause on
136  approve=2;
137  for ff=2:length(test)%just retrieve the channel with the combines values
138      while approve~=1
139          %perform srs enveloping procedure
140          loglog(test(1,ao(ff)).srscomb(:,1),test(1,ao(ff)).srscomb(:,2));
141          %Use data cursor button on figure to select data points
142          %Hold alt key for multiple selections
143          %Choose 2-3 points, then right click to select "Export Cursor Data
144          %to Workspace". Save name as cursor_info (default).
145          %Wait for cursor_info input to be created
146          display('Press any key after plot selections are made. ');
147          pause %press any key when ready to continue
148          clf%clear figure before running enveloping algorithm
149          [test(ao(ff)).srs_env_plot,test(ao(ff)).srs_env_prop]=srs_envelope5(test(1,ao(ff)).srscomb,cursor_info,['C', num2str(ff-1), ' & ', num2str(ff), ' Combined']);
150          approve=input('Approve? (1 for yes, 2 for no): ');
151          if approve~=1
152              clf
153              close
154              clear cursor_info test(ao(ff)).srs_env_plot test(ao(ff)).srs_env_prop
155          end
156      end
157  end
158  set(gcf,'Units','normalized','OuterPosition',[0 0 1 1]);
159  saveas(gcf,[test(1,ao(ff)).name,'_srs_cmbnenvelop',dd],'.jpeg');
160  close
161  approve=2;
162  end

```

Figure 7.3.3.1-2. MATLAB® Code for Performing SRS Enveloping Procedure

Within the MATLAB® code for performing the SRS enveloping procedure is the SRS enveloping algorithm. Provided for reference in Figures 7.3.3.1-3 (a) through 7.3.3.1-3 (f) is the MATLAB® code developed for an enveloping curve of an SRS.



NASA Engineering and Safety Center Technical Assessment Report

Document #:
**NESC-RP-
12-00783**

Version:
1.0

Title:

Empirical Model Development for Predicting Shock Response on Composite Materials Subjected to Pyroshock Loading

Page #:
52 of 123

```
1  function [ pltps,env ] = srs_envelope5( srs,fbi, varargin )
2  %SRS_ENVELOPE5 Captures the slope(s) and max values of the slope(s) and
3  %plateau(s) of an SRS based on user-selected frequency breakpoints.
4
5  %Check that fbi is a structure array
6  if isstruct(fbi)~=1
7      error('Input fbi must be a structure array created from Data Cursor Export');
8  end
9  %Get the number of frequency breakpoints (will be either 2 or 3)
10 nfb=size(fbi,2);
11
12 switch nfb
13     case 2 % One slope and plateau
14         % Two points are chosen on SRS to allow flexibility in slope
15         % selection
16         plto=1;%number of plateaus in SRS curve
17         %retrieve the index for the estimated frequency break point
18         indx=[fbi(1,1).DataIndex,fbi(1,2).DataIndex];
19         fbindx1=min(indx);
20         fbindx2=max(indx);
21         % find line properties from index 1 to index 2
22         mdl=LinearModel.fit(log10(srs(fbindx1:fbindx2,1)),log10(srs(fbindx1:fbindx2,2)));
23         % y=b*x^N
24         N=mdl.Coefficients{2,1}; %slope for exponent
25         b=10^mdl.Coefficients{1,1}; %intercept
26
27         %adjust b such that the slope line is tangent with the largest
28         %offset of the actual srs curve.
29         ytemp=b*srs(1:fbindx2,1).^N;
30         [~,I]=max(srs(1:fbindx2,2)-ytemp);
31         btan=srs(I,2)/srs(I,1)^N;
32
33         % Find max value for the plateau
34         yp=max(srs(fbindx2+1:end,2));
35         % Calculate break point
36         fb=(yp/btan)^(1/N);
37
38         %% Create envelope curve
39         % Determine counter for envelopes
40         ss=1;
41         while srs(ss,1)<fb
42             ss=ss+1;
43             if ss>length(srs(:,1))
44                 break
45             end
46         end
47         ss=ss-1;
```

Figure 7.3.3.1-3. (a) Enveloping SRS Algorithm



NASA Engineering and Safety Center Technical Assessment Report

Document #:
**NESC-RP-
12-00783**

Version:
1.0

Title:

Empirical Model Development for Predicting Shock Response on Composite Materials Subjected to Pyroshock Loading

Page #:
53 of 123

```
49 % Sloped part of line
50 fslope=zeros(ss,1);
51 yslope=zeros(ss,1);
52 for gg=1:ss;
53     fslope(gg)=srs(gg,1);
54     yslope(gg)=btan*srs(gg,1)^N;
55 end
56 % Remove excess zeros
57 fslope(fslope==0)=[];
58 yslope(yslope==0)=[];
59 % Calculate the slope in dB/Oct
60 dbOct=20*log10(2)*N;
61 % Plateau
62 cc=1;
63 fplateau=zeros(length(srs(:,1))-ss,1);
64 yplateau=zeros(length(srs(:,1))-ss,1);
65 for hh=ss:length(srs(:,1))
66     fplateau(cc)=srs(hh,1);
67     yplateau(cc)=yp;
68     cc=cc+1;
69 end
70 % Remove excess zeros
71 fplateau(fplateau==0)=[];
72 yplateau(yplateau==0)=[];
73
74 %% Plot results
75 loglog(srs(:,1),srs(:,2),'k','LineWidth',2)
76 hold on
77 xlim([100 10^4])
78 loglog(fslope,yslope,'r','LineWidth',2)
79 loglog(fplateau,yplateau,'g','LineWidth',2)
80 loglog(fplateau(1),yplateau(1),'m+','LineWidth',2)%Frequency Break Point
81 grid on
82 title([varargin,' SRS Envelope Comparison: Q=10']);
83 legend('SRS',[ 'Slope: ',num2str(dbOct),'dB/Oct'],...
84        [ 'Plateau: ',num2str(yp),'g'],[ 'Frequency Break Point: ',num2str(fb),'Hz'],'Location','South');
85 xlabel('Natural Frequency (Hz)')
86 ylabel('Peak Accel (g)')
87 hold off
88
89 %set non-used values (for double slope curves) to zero as place holders
90 fb2=0;
91 fb3=0;
92 yp1=0;
93 yp2=0;
94 dbOct2=0;
95
96 % Output envelope properties
97 pltps=[fslope(1),fb,fb2,fb3,fplateau(end),yslope(1),yp,yp1,yp2,yp];
98 env=[fb,dbOct,yp,fb3,dbOct2,yp2,plto];
```

Figure 7.3.3-1-3. (b) Enveloping SRS Algorithm



NASA Engineering and Safety Center Technical Assessment Report

Document #:
**NESC-RP-
12-00783**

Version:
1.0

Title:

**Empirical Model Development for Predicting Shock Response on
Composite Materials Subjected to Pyroshock Loading**

Page #:
54 of 123

```
100 case 3 %Two slopes and two plateaus
101     plto=2;%number of plateaus in SRS curve
102     %retrieve the index for the estimated frequency break point
103     indx=[fbi(1,1).DataIndex,fbi(1,2).DataIndex,fbi(1,3).DataIndex];
104     fbindx1=min(indx);
105     fbindx2=median(indx);
106     fbindx3=max(indx);
107     % find line properties of the first slope
108     % y=b*x^N
109     mdl1=LinearModel.fit(log10(srs(1:fbindx1,1)),log10(srs(1:fbindx1,2)));
110     N1=mdl1.Coefficients{2,1}; %slope for exponent
111     b1=10^mdl1.Coefficients{1,1}; %intercept
112
113     %adjust b such that the slope line is tangent with the largest
114     %offset of the actual srs curve.
115     ytempl=b1*srs(1:fbindx1,1).^N1;
116     [~,I1]=max(srs(1:fbindx1,2)-ytempl);
117     b1tan=srs(I1,2)/srs(I1,1)^N1;
118
119     % Find max value for the first plateau
120     yp1=max(srs(fbindx1+1:fbindx2,2));
121     % Calculate the first break point
122     fb1=(yp1/b1tan)^(1/N1);
123     % find line properties of second slope
124     mdl2=LinearModel.fit(log10(srs(fbindx2:fbindx3,1)),log10(srs(fbindx2:fbindx3,2)));
125     N2=mdl2.Coefficients{2,1}; %slope for exponent
126     b2=10^mdl2.Coefficients{1,1}; %intercept
127
128     %adjust b such that the slope line is tangent with the largest
129     %offset of the actual srs curve.
130     ytemp2=b2*srs(fbindx2:fbindx3,1).^N2;
131     [~,I2]=max(srs(fbindx2:fbindx3,2)-ytemp2);
132     b2tan=srs(fbindx2+I2,2)/srs(fbindx2+I2,1)^N2;
133
134     % Find the max value for the second plateau
135     yp2=max(srs(fbindx3+1:end,2));
136     % Calculate the second break point
137     fb2=(yp1/b2tan)^(1/N2);
138     % Calculate the third break point
139     fb3=(yp2/b2tan)^(1/N2);
140
141     %% Create envelope curve
142     % Determine counter for envelopes
143     ssl=1;
144     while srs(ssl,1)<fb1
145         ssl=ssl+1;
146         if ssl>length(srs(:,1))
147             break
148         end
149     end
150     ssl=ssl-1;
```

Figure 7.3.3.1-3. (c) Enveloping SRS Algorithm



NASA Engineering and Safety Center Technical Assessment Report

Document #:
**NESC-RP-
12-00783**

Version:
1.0

Title:

Empirical Model Development for Predicting Shock Response on Composite Materials Subjected to Pyroshock Loading

Page #:
55 of 123

```
152     ss2=1;
153     while srs(ss2,1)<fb2
154         ss2=ss2+1;
155         if ss2>length(srs(:,1))
156             break
157         end
158     end
159     ss2=ss2-1;
160     %
161     ss3=1;
162     while srs(ss3,1)<fb3
163         ss3=ss3+1;
164         if ss3>length(srs(:,1))
165             break
166         end
167     end
168     ss3=ss3-1;
169
170     %Development of first sloped line
171     fslopel=zeros(ss1,1);
172     yslopel=zeros(ss1,1);
173     for ggl=1:ss1;
174         fslopel(ggl)=srs(ggl,1);
175         yslopel(ggl)=bltan*srs(ggl,1)^N1;
176     end
177     % Remove excess zeros
178     fslopel(fslopel==0)=[];
179     yslopel(yslopel==0)=[];
180     % Calculate the slope in dB/Oct
181     dbOct1=20*log10(2)*N1;
182
183     % Development of first plateau
184     ccl=1;
185     fplateaul=zeros(ss2-ss1,1);
186     yplateaul=zeros(ss2-ss1,1);
187     for hhl=ss1:ss2
188         fplateaul(ccl)=srs(hhl,1);
189         yplateaul(ccl)=ypl;
190         ccl=ccl+1;
191     end
192     % Remove excess zeros
193     fplateaul(fplateaul==0)=[];
194     yplateaul(yplateaul==0)=[];
```

Figure 7.3.3.1-3. (d) Enveloping SRS Algorithm



NASA Engineering and Safety Center Technical Assessment Report

Document #:
**NESC-RP-
12-00783**

Version:
1.0


Title:

Empirical Model Development for Predicting Shock Response on Composite Materials Subjected to Pyroshock Loading

Page #:
56 of 123

```
196 %Development of second sloped line
197 cc2=1;
198 fslope2=zeros(ss3-ss2,1);
199 yslope2=zeros(ss3-ss2,1);
200 for gg2=ss2:ss3;
201     fslope2(cc2)=srs(gg2,1);
202     yslope2(cc2)=b2tan*srs(gg2,1)^N2;
203     cc2=cc2+1;
204 end
205 % Remove excess zeros
206 fslope2(fslope2==0)=[];
207 yslope2(yslope2==0)=[];
208 % Calculate the slope in dB/Oct
209 db0ct2=20*log10(2)*N2;
210
211 %Development of second plateau
212 cc3=1;
213 fplateau2=zeros(length(srs(:,1))-ss3,1);
214 yplateau2=zeros(length(srs(:,1))-ss3,1);
215 for hh2=ss3:length(srs(:,1))
216     fplateau2(cc3)=srs(hh2,1);
217     yplateau2(cc3)=yp2;
218     cc3=cc3+1;
219 end
220 % Remove excess zeros
221 fplateau2(fplateau2==0)=[];
222 yplateau2(yplateau2==0)=[];
223
224 %% Plot results
225 loglog(srs(:,1),srs(:,2),'k','LineWidth',2)
226 hold on
227 xlim([100 10^4])
228 loglog(fslope1,yslope1,'r','LineWidth',2)% first slope
229 loglog(fplateau1,yplateau1,'g','LineWidth',2)% first plateau
230 loglog(fslope2,yslope2,'r','LineWidth',2)% second slope
231 loglog(fplateau2,yplateau2,'g','LineWidth',2)% second plateau
232 loglog(fplateau1(1),yplateau1(1),'m+', 'LineWidth',2)%1st Frequency Break Point
233 loglog(fplateau2(1),yplateau2(1),'m+', 'LineWidth',2)%2nd Frequency Break Point
234 grid on
235 title([varargin,' SRS Envelope Comparison; Q=10']):
236 legend('SRS',[ '$lope 1: ',num2str(db0ct1),'dB/Oct'],['Plateau 1: ',num2str(yp1),'g'],...
237     ['$lope 2: ',num2str(db0ct2),'dB/Oct'],['Plateau 2: ',num2str(yp2),'g'],...
238     ['Frequency Break Point 1: ',num2str(fb1),'Hz'],['Frequency Break Point 2: ',num2str(fb3),'Hz'],...
239     'Location','South');
240 xlabel('Natural Frequency (Hz)')
241 ylabel('Peak Accel (g)')
242 hold off
```

Figure 7.3.3.1-3. (e) Enveloping SRS Algorithm

	NASA Engineering and Safety Center Technical Assessment Report	Document #:	Version:
		NESC-RP-12-00783	1.0
Title:		Page #:	
Empirical Model Development for Predicting Shock Response on Composite Materials Subjected to Pyroshock Loading		57 of 123	

```

244      % Output envelope properties
245      pltps=[fslope1(1),fb1,fb2,fb3,fplateau2(end),yslope1(1),yp1,yp2,yp2];
246      env=[fb1,db0ct1,yp1,fb3,db0ct2,yp2,plt0];
247      %
248           env=[b1tan,fb1,db0ct1,yp1,b2tan,fb3,db0ct2,yp2,plt0];
249
250      otherwise
251          error('Incorrect inputs')
252      end
253  end

```


Figure 7.3.3.1-3. (f) Enveloping SRS Algorithm

Using a single plateau SRS as an example, the primary features of the SRS enveloping algorithm are:

1. The properties of the sloped region of the SRS are calculated from the Linear Least Squares fit of the base 10-log transpose of the SRS sloped region selected by the user as an input to the algorithm. This operation (LinearModel.fit function in MATLAB®) calculates the coefficients b and N of the equation, $SRS_{slope} = b * f^N$ (Figure 7.3.3.1-3 (a), lines 18-25).
2. The Linear Least Squares line is then adjusted to envelope the peak value of the sloped region of the SRS. This is performed by adjusting the coefficient b using the equation: $b_{max} = \frac{SRS(f_i)}{f_i^N}$, where f_i is the natural frequency value at the maximum value of SRS-SRSslope (Figure 7.3.3.1-3 (a), lines 29-31).
3. The equation of the max envelope of the sloped portion of the SRS curve is then $SRS_{slope_envelope} = b_{max} * f^N$.
4. The maximum value of the SRS curve is used as the value of the plateau region, i.e., $SRS_{plateau_envelope} = SRS_{max}$ (Figure 7.3.3.1-3 (a), line 34).
5. Therefore, the max envelope of the SRS curve is the combination of the two curves SRSslope_envelope and SRSplateau_envelope (Figure 7.3.3.1-3 (a) and 7.3.3.1-3 (b), lines 38-72). The SVIs are then the slope (in dB/oct), N, of the SRSslope_envelope curve (Figure 7.3.3.1-3 (b), line 60), the peak SRS value from the SRSplateau_envelope curve (Figure 7.3.3.1-3 (a), line 34), and the frequency break point is the natural frequency value, fb, at the intersection of the two curves (Figure 7.3.3.1-3 (a), line 36).

For example,

- Figure 7.3.3.1-4 shows the initial Linear Least Squares fit of the slope portion of the SRS curve as the line SRSslope (red dashed line) defined by equation $SRS_{slope} = b * f^N$, where $b = 5.1439$ g and $N = 5.8131$ dB/Oct (or 0.9655 g/Hz) as calculated by the Linear Least Squares curve fit.
- To adjust the line SRSslope such that it envelopes the curve, find the frequency where SRS-SRSslope is greatest, for Figure 7.3.3.1-4 this occurs at $f_i = 518.8$ Hz where 2704 g - 2151 g = 553 g, then modify the value b using the equation $b_{max} = \frac{SRS(f_i)}{f_i^N}$.

	NASA Engineering and Safety Center Technical Assessment Report	Document #: NESC-RP-12-00783	Version: 1.0
Title: Empirical Model Development for Predicting Shock Response on Composite Materials Subjected to Pyroshock Loading		Page #: 58 of 123	

Therefore, $b_{max} = \frac{2704}{518.8^{0.9655}} = 6.4664$ and the enveloping equation of the sloped portion of the SRS curve becomes $SRS_{slope_envelope} = b_{max} * f^N = 6.4664 * f^{0.9655}$ (solid red line).

- Next, the plateau region of the SRS envelope curve is simply the max value of the SRS curve (i.e., $SRS_{plateau_envelope} = \max(SRS) = 12,754g$).
- The full SRS envelope curve is then developed by combining the $SRS_{slope_envelope}$ and $SRS_{plateau_envelope}$ curves with the intersection frequency (i.e., the frequency break point, calculated with the equation $f_b = \left(\frac{SRS_{plateau_envelope}}{b_{max}}\right)^{\frac{1}{N}} = \left(\frac{12,754}{6.4664}\right)^{\frac{1}{0.9655}} = 2,587Hz$.)

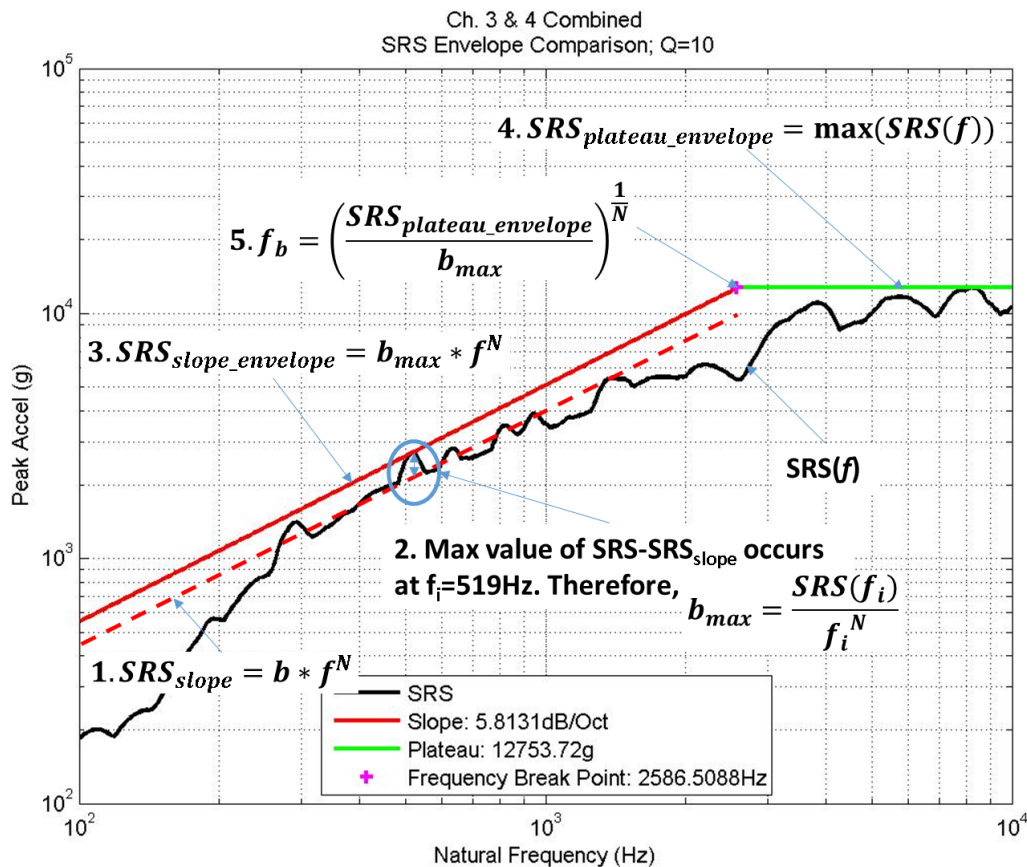



Figure 7.3.3.1-4. Sample of the SRS Enveloping Algorithm

The same procedure is followed for enveloping double plateau SRS curves with the primary difference being that an additional initial value input is needed from the user to separate the regions of the SRS curve, reference Figures 7.3.3.1-3 (c) through 7.3.3.1-3 (f).

The algorithm for enveloping SRS curves does require input from the user for determination of the initial evaluation points. Since the user input can be categorized as a subjective decision, the

	NASA Engineering and Safety Center Technical Assessment Report	Document #: NESC-RP-12-00783	Version: 1.0
Title: Empirical Model Development for Predicting Shock Response on Composite Materials Subjected to Pyroshock Loading		Page #: 59 of 123	

algorithm does not truly meet the criteria for suitability listed in Section 7.3.1. Prior to the development of the SRS enveloping algorithm published in this report, there were two other pattern recognition algorithms developed that did not require input from the user; a MSFC developed algorithm and an algorithm that utilized a k-means cluster analysis algorithm.

The advantage of these initial algorithms was user input was eliminated, thus mitigating user bias. However, there were multiple issues, which ultimately led to these algorithms not being used.

- Neither algorithm could effectively envelope SRS curves with multiple plateau regions.
- The least-squares method used for calculating slope was too sensitive to the sudden roll-off of the slope commonly seen below 200 Hz, therefore, two input values were needed to calculate the slope: the starting and ending frequency of the sloped region, reference Figure C9.
- The k-means cluster analysis method appeared to have a random component as it could provide different results with different runs.

7.3.4 PV Spectra

The maximum PV value and corresponding frequency were calculated from the PVRs using the built-in MATLAB® function, max. Figure 7.3.4-1 provides the code for reference. Note: The PVRs developed is a combination of the PVRs curves produced by the two-paired accelerometers at any one location on the test panel (reference Figure 7.3.4-1, line 47).

```

38 %Combined Channels will be stored with the even numbered channel
39 ao=[1,5,6,7,8,9,10,11,12,2,3,4];%define order such that paired channels are evaluated together
40
41 %% Calculate PV
42 for ff=1:length(test)
43     test(ff).pv=pvssmax(test(1,ff).data,10,100000);%calculate PV curve
44 end
45 %Combine PV and find max values
46 for ff=2:2:length(test)
47     test(ao(ff)).pvcmbn=[test(ao(ff)).pv(:,1),max([test(ao(ff-1)).pv(:,2),test(ao(ff)).pv(:,2)],[],2)];
48     [~,mxind]=max(test(ao(ff)).pvcmbn(:,2));
49     test(ao(ff)).pvcmbnmax=[test(ao(ff)).pvcmbn(mxind,1),test(ao(ff)).pvcmbn(mxind,2)];%location of max PV value
50     clear mxind
51 end

```


Figure 7.3.4-1. Reference Code for Calculating Max PV and Frequency

7.3.5 Energy Spectral Density

The maximum ESD value and corresponding frequency were calculated from the ESD using the built-in MATLAB® function, “max.”

7.3.6 SRS Evaluation

A multiple linear regression analysis was performed for each of the SVIs listed in Section 7.3.3. For example, SRS slope, SRS frequency break point, and SRS plateau (peak acceleration) for panel type (monolithic versus sandwich panel), thickness of monolithic panels, fill type for

	NASA Engineering and Safety Center Technical Assessment Report	Document #: NESC-RP-12-00783	Version: 1.0
Title: Empirical Model Development for Predicting Shock Response on Composite Materials Subjected to Pyroshock Loading		Page #: 60 of 123	

sandwich panels, composite ply type (tape versus fabric), source shock induced (10-gpf LSC versus 22-gpf LSC), and ply orientation (unidirectional versus quasi-isotropic).

Analysis was performed using STATGRAPHICS® Centurion™ XVI Version 16.1.8, StatPoint Technologies, Inc., Warrenton, VA, © 1982 – 2012, and JMP® Version 11.1.1, SAS Institute, Inc., Cary, NC, © 1989 - 2013. Appropriate analysis files are available on request.


The test matrix was designed to be analyzed as a split-plot experiment (seminal source: Fisher, R. A., (1925). *Statistical Methods for Research Workers*. Edinburgh: Oliver and Boyd). For instance, some panels were tested more than once. There is no panel-to-panel variation associated with tests using a single panel. Therefore, even though there were 48 individual tests performed, only 32 panels were used. It would be incorrect to assume there were 48 independent estimates of the effect of panel thickness when panel thickness only changed it 32 times. The engineering effect is a better handle on which effects significantly affected each response, less bias in the model parameter estimates, and presumably better estimates of variance components (see below).

In nearly all cases, the response was transformed before analysis. The logarithm of each response was characterized. This let the analyst use the important assumption of constant variance in regression analysis. The engineering importance is that the prediction's bias is reduced and the tests for significant effects are more trustworthy (Box, G. E. P. and Cox, D. R. (1964). *An analysis of transformations*, *Journal of the Royal Statistical Society, Series B*, 26, 211-252). Note that SRS plots are already scaled logarithmically, so there is an existing justification for using this transformation.

Transformation slightly increases complexity of the prediction model. It greatly increases interpretation of the estimates of variability: the standard deviations calculated only make sense for the log of the response. Thus the uncertainty bounds around a predicted response value will be wider in the “+” direction than on the low side.

The bulk of the final analyses were performed in JMP® using standard least squares regression. The restricted maximum likelihood (REML) estimation method was used because of its capability to estimate variance components and other strengths. Variance components, for a design engineer, would give estimates of standard deviation of the variability in response for any single firing event (within-test variation), the variability added through manufacturing (panel-to-panel variation), and the variability due to differences between firings that isn't due to manufacturing differences (test-to-test variation).

This was partially successful, but panel-to-panel and test-to-test variability were inadvertently confounded during analysis. The result is that the values reported here as panel-to-panel and test-to-test variability are not individually inaccurate. Panel-to-panel variability should usually be higher, and test-to-test lower (within-test variability is believed accurate.) If these values are important to a user, it is believed that a workaround has been identified. It was not exercised for

	NASA Engineering and Safety Center Technical Assessment Report	Document #:	Version:
		NESC-RP-12-00783	1.0
Title:		Page #:	
Empirical Model Development for Predicting Shock Response on Composite Materials Subjected to Pyroshock Loading		61 of 123	

this report, but a statistics-savvy analyst may be able to obtain better variance component estimates for most or maybe all responses.

Only a single Al panel was tested. This means that panel-to-panel variation for Al panels is not available for either analysis or conclusions. This created some complexity for analysis, though the effects are estimated to be negligible for engineering use. Nevertheless, had at least three different Al panels been used, some analysis complexities could have been reduced, including issues with variance components estimation mentioned above.

7.3.6.1 SRS Slope

The data used in the statistical analysis of the slope were generated from the SRS algorithm discussed in Section 7.3.3. If the SRS had a single slope, only initial slope was used in the analysis. If the enveloping SRS generated two slopes (predominate with the sandwich panel tests), only the second slope was used in the statistical analysis. It was found the first slope, in a multiple-slope case, appeared to be due to a different phenomenon than the slope in a single-slope case, whereas the second slope acted like a single slope. No model was found, which adequately characterized the first slope in a multiple-slope case.

The results from the statistical analysis indicated the significant factors to be:

- Distance
- Distance²
- Distance³
- Severance of the LSC panel times distance.

Note: Although the shock data from the tests where the LSC failed to sever the LSC plate (sever = 0 as shown in the plots) were used in the analysis of the shock data, they are not a parameter used for predictive MEFE. Failure of a LSC to sever the target material in flight would likely be a catastrophic occurrence, and therefore is not used in the slope predictive equation.


Slope predictive equation:

$$= \text{Exp} (2.39316377208557 + -0.185201911061676 * ((\text{Distance from LSC} - 39) / 30) + (0.133271932004697) + ((\text{Distance from LSC} - 39) / 30) * (0.106188564068464) + ((\text{Distance from LSC} - 39) / 30) * (((\text{Distance from LSC} - 39) / 30) * (0.195326659484799) + ((\text{Distance from LSC} - 39) / 30) * (((\text{Distance from LSC} - 39) / 30) * (((\text{Distance from LSC} - 39) / 30) * 0.352644069684689)))$$

The empirical model prediction for the SRS slope by distance is tabulated in Table 7.3.6.1-1.

Table 7.3.6.1-1. Predictive Slope versus Distance (regardless of panel type)

Factor	Predicted Slope by Distance from LSC					
Distance	9	21	33	45	57	69
Slope	8.9	10.0	9.8	9.5	10.6	15.3

	NASA Engineering and Safety Center Technical Assessment Report	Document #: NESC-RP-12-00783	Version: 1.0
Title: Empirical Model Development for Predicting Shock Response on Composite Materials Subjected to Pyroshock Loading		Page #: 62 of 123	

A couple of conclusions may be drawn from the slope empirical model prediction:

- The variance in the slope is fairly flat from 9 inches to 57 inches
- The predicted slope at the 69-inch location is elevated likely due to the reflective shock wave from the boundary condition the end of the panel represents.

Figure 7.3.6.1-1 illustrates graphs of the SRS slope data (top graph) and the predicted slope using the untransformed response (linear). For reference, the green dashed line represents a slope of 10 dB/oct.

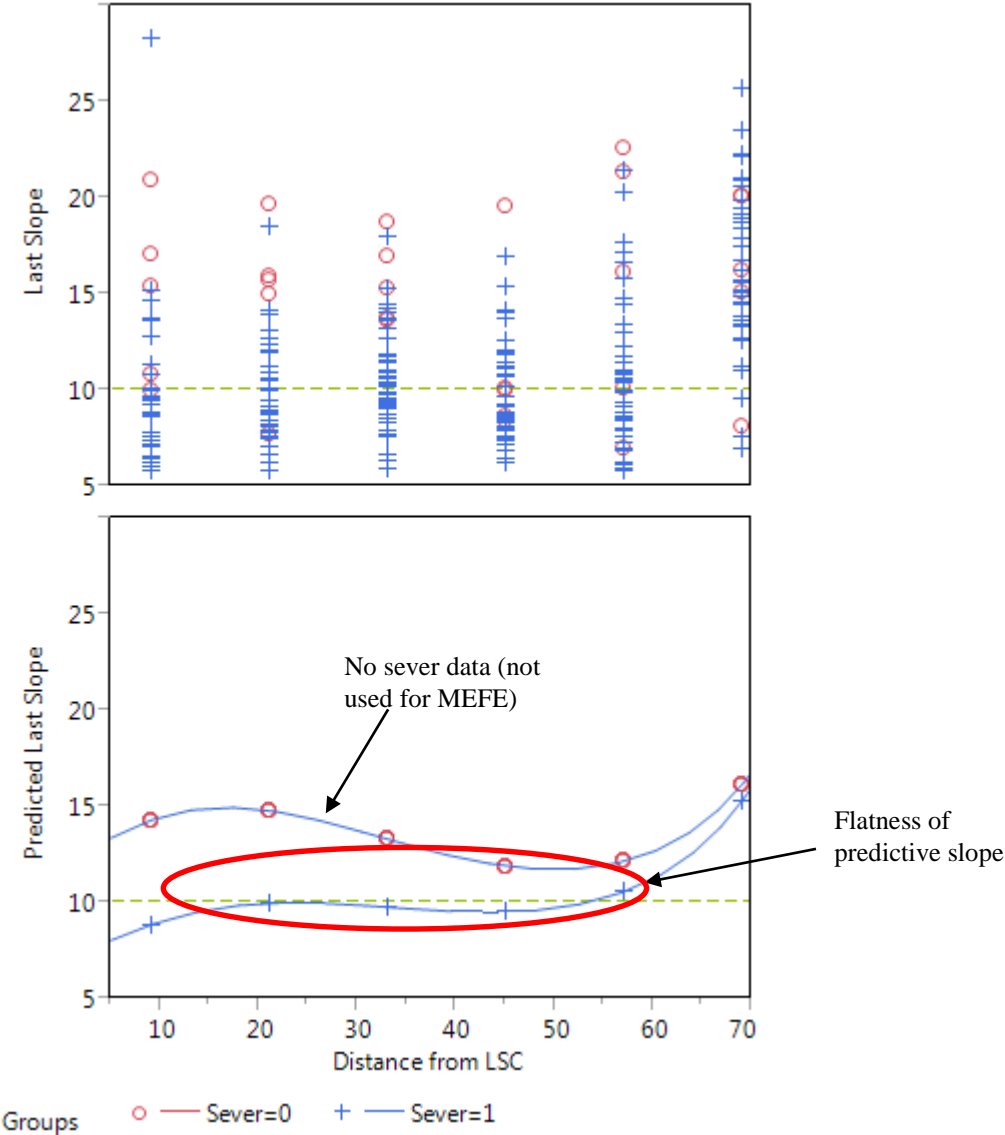


Figure 7.3.6.1-1. SRS Predicted Slope from Statistical Analysis (untransformed)


	NASA Engineering and Safety Center Technical Assessment Report	Document #: NESC-RP-12-00783	Version: 1.0
Title: Empirical Model Development for Predicting Shock Response on Composite Materials Subjected to Pyroshock Loading		Page #: 63 of 123	

Figure 7.3.6.1-2 illustrates graphs of the SRS slope data (top graph) and the predicted slope using a log-transformed response. Again, for reference, the green dashed line represents a slope of 10 dB/oct.

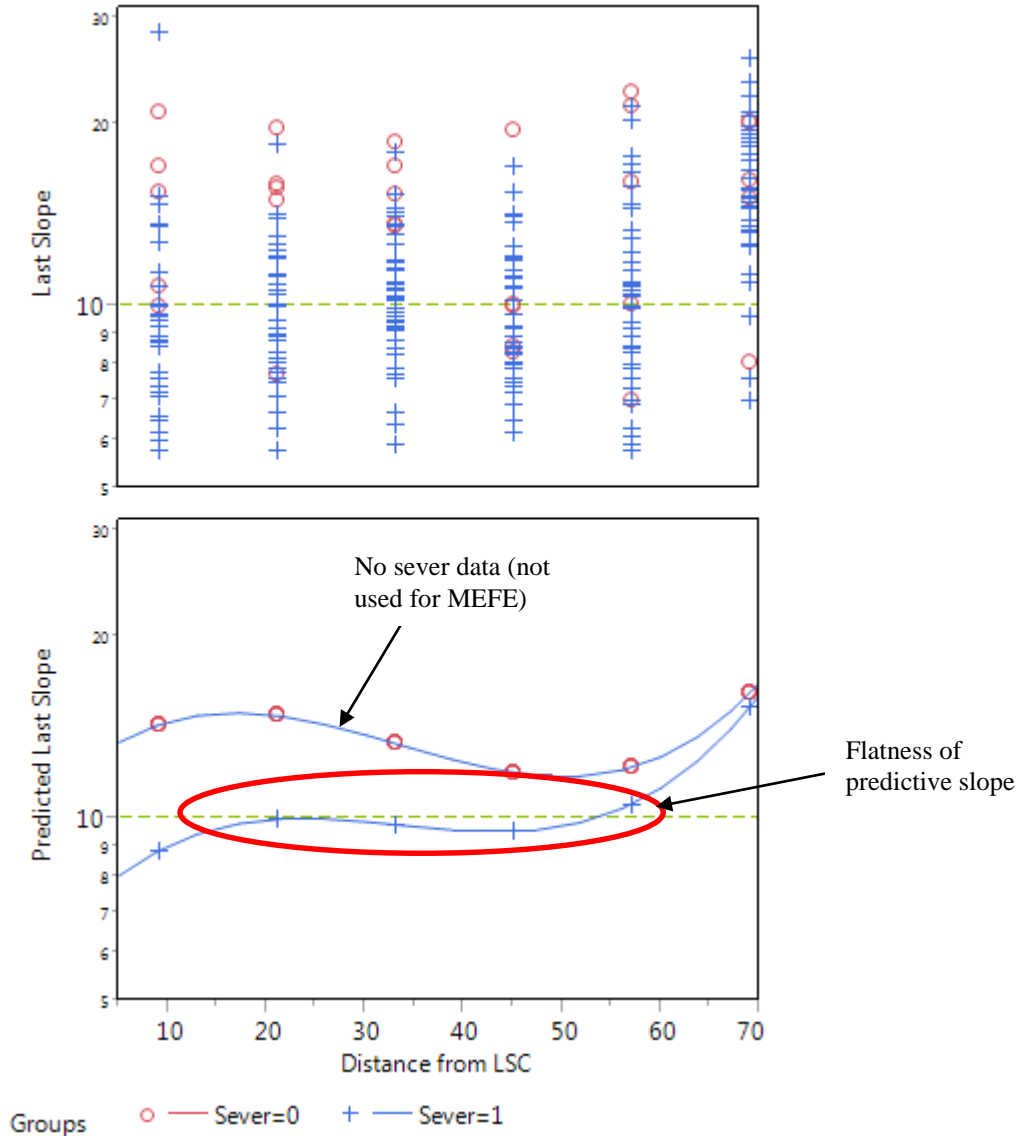


Figure 7.3.6.1-2. SRS Predicted Slope from Statistical Analysis (log-transformed)


	NASA Engineering and Safety Center Technical Assessment Report	Document #: NESC-RP-12-00783	Version: 1.0
Title: Empirical Model Development for Predicting Shock Response on Composite Materials Subjected to Pyroshock Loading		Page #: 64 of 123	

Figure 7.3.6.1-3 illustrates the statistical analysis using the prediction equation with the data normalized at 10 inches and plotted as a percentile. As shown from these data, there is little change to the slope out to approximately 60 inches and may be held as a constant value for MEFÉ estimation purposes.

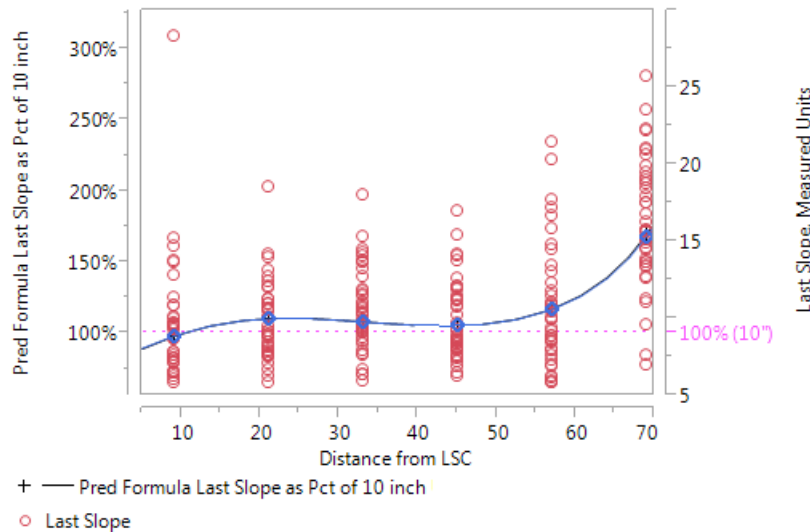



Figure 7.3.6.1-3. SRS Predicted Slope from Statistical Analysis (Percentile)

Using the guidelines outlined in NASA-HDBK-7005, *Dynamic Environmental Criteria*, Figure 5.7 (*Shock Response Spectrum versus Distance from the Pyroshock Source*), the spectrum peak and spectrum ramp both decay, at different rates, with distance from the shock source. The greater the distance the less the percentage of source shock value remains. However, based on the prediction equation for the SRS predicted slope derived from the flat panel test data, as shown in Figures 7.3.6.1-2 and 7.3.6.1-3, the slope can be held constant for the calculation of the MEFÉ, out to a distance of 20 to 60 inches from the source shock, without introducing a large error (i.e., the slope of an SRS curve stays constant with distance. This is consistent with current practices).

Characterization of the composite monolithic panel SRS slope is shown in Figure 7.3.6.1-4. Although mean slope range varies from 10.6 dB/oct to 6.2 dB/oct, the average SRS ramp-up, or slope, was consistent whether the 10-gpf LSC was used or the 22-gpf LSC was used (8.6 dB/oct and 8.4 dB/oct, respectively).

	NASA Engineering and Safety Center Technical Assessment Report	Document #:	Version:
		NESC-RP-12-00783	1.0
Title:		Page #:	
Empirical Model Development for Predicting Shock Response on Composite Materials Subjected to Pyroshock Loading		65 of 123	

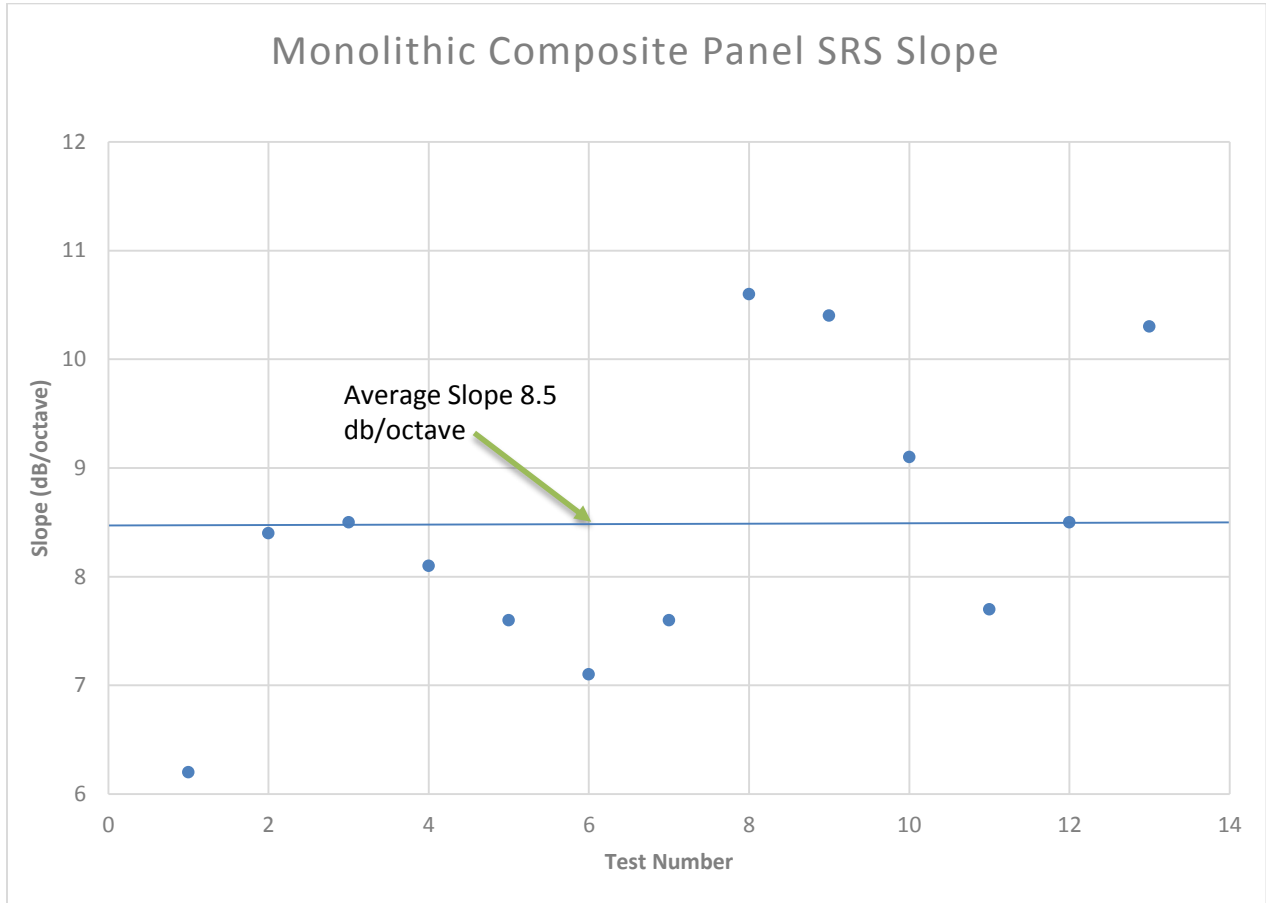


Figure 7.3.6.1-4. Monolithic Composite Average SRS Slope

The sandwich panels were evaluated separately from the monolithic panels due to the predominance of the dual plateau enveloping SRS as computed by the SRS algorithm. Each of the slopes (low frequency first slope 100 Hz to ~350 Hz and mid-frequency slope ~950 Hz to ~2500 Hz) were evaluated. The evaluation showed the first slope of the SRS to be relatively high (average slope of 15 dB/oct) and the second slope to be also relatively high (13 dB/oct), which is not atypical of a far-field pyroshock maxi-max SRS (reference NASA-STD-7003, Figure 1). The average first slope (low-frequency slope) and the second (or mid-frequency slope) plotted versus distance from the shock source is graphically shown in Figure 7.3.6.1-5. Similarly, as shown in Figure 7.3.6.1-4, the delta change for the second slope over distance is minimal. The reasoning for statistically evaluating only the second slope is it can be directly compared to the AI and monolithic composite panels, with a single plateau and typically have a frequency break point between 2000 and 3000 Hz.

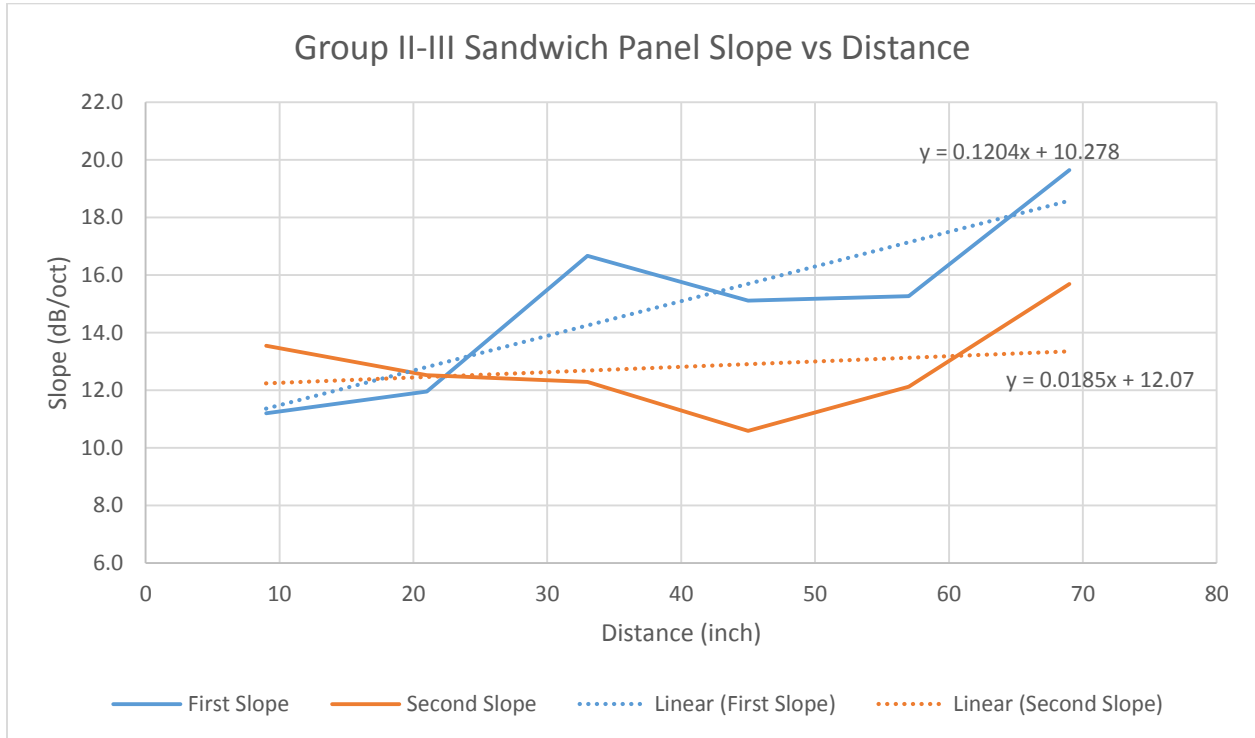


Figure 7.3.6.1-5. Composite Sandwich Panel Slope Change versus Distance

7.3.6.2 SRS Frequency Breakpoint Evaluation


The frequency breakpoint on a SRS is the intersection between the plateau frequency range (peak acceleration) and the slope of the acceleration. Typically, the frequency breakpoint is a resultant point on the SRS based upon how the SRS is enveloped with regard to both the plateau and the slope. For this task, the SRS frequency breakpoint was determined by the enveloping SRS MATLAB[®] algorithm (reference Section 7.3.3).

The results from the algorithm were statistically evaluated for sensitivities. There are two significant factors associated with determination of the frequency breakpoint.

- Distance from the shock source
- The presence of acoustic damping

Factors that were determined to be less significant include type of panel (sandwich versus monolithic versus Al) with distance and composite ply (tape versus fabric).

From the statistical analysis the predictive equation for SRS frequency breakpoint was developed for each type of material type (i.e., Al and composite (monolithic and sandwich)). The predictive equation is listed below and the predictive results for each material type are tabulated in Table 7.3.6.2-1.


	NASA Engineering and Safety Center Technical Assessment Report	Document #:	Version:
		NESC-RP-12-00783	1.0
Title:		Page #:	
Empirical Model Development for Predicting Shock Response on Composite Materials Subjected to Pyroshock Loading		67 of 123	

Frequency breakpoint predictive equation:

$$\begin{aligned}
 &= \text{Exp} (7.47667461668358 + 0.256726082283925 * ((\text{Distance from LSC} - 39) / 30) \\
 &+ (\text{Type} - \text{Thick}: \\
 &\text{If "Monolithic - 0.2", } -0.071171881273597, \\
 &\text{If "Monolithic - 0.3", } -0.132292944311272, \\
 &\text{If "Al Honey - 1", } 0.0876199515198583, \\
 &\text{If "Rohacell - 1", } -0.0130949295614228, \\
 &\text{If "Aluminum - 0.187", } 0.128939803626434) \\
 &+ (\text{Acoustic Damped}: \\
 &\text{If "0", } 0.208717894264659, \\
 &\text{If "1", } -0.208717894264659) \\
 &+ (((\text{Distance from LSC} - 39) / 30) * (\text{Acoustic Damped}: \\
 &\text{If "0", } -0.102207869493011, \\
 &\text{If "1", } 0.102207869493011)) \\
 &+ (((((\text{Distance from LSC} - 39) / 30) * (\text{Distance from LSC} - 39)) / 30) * 0.0279313603300628 \\
 &+ ((\text{Distance from LSC} - 39) / 30) * (\text{Type} - \text{Thick}: \\
 &\text{If "Monolithic - 0.2", } 0.0761703094306936, \\
 &\text{If "Monolithic - 0.3", } 0.0659903940637854, \\
 &\text{If "Al Honey - 1", } -0.0510118941049901, \\
 &\text{If "Rohacell - 1", } -0.105802245822947, \\
 &\text{If "Aluminum - 0.187", } 0.0146534364334584) \\
 &+ ((((((\text{Distance from LSC} - 39) / 30) * (\text{Distance from LSC} - 39)) / 30) * (\text{Distance from LSC} - 39)) / 30) * -0.284608051208915
 \end{aligned}$$

Table 7.3.6.2-1. Predicted Frequency Breakpoint with Distance (by panel type)

Factors			Predicted Frequency Breakpoint by Distance from LSC, inches					
Type	Panel Thickness (inch)	Acoustic Damped (Yes/No)	9	21	33	45	57	69
Al Honey	1	No	2927.9	2398.1	2334.9	2422.5	2401.1	2038.2
Al Honey	1	Yes	1572.1	1397.4	1476.4	1662.4	1788.1	1647.2
Homogeneous	0.187	No	2857.5	2402.7	2401.6	2558.1	2603.0	2268.4
Homogeneous	0.187	Yes	1534.3	1400.1	1518.6	1755.4	1938.4	1833.2
Monolithic	0.2	No	2199.7	1895.7	1942.0	2120.1	2211.0	1974.8
Monolithic	0.3	No	2090.4	1794.2	1830.6	1990.3	2067.3	1838.9
Monolithic	0.3	Yes	1122.5	1045.5	1157.6	1365.8	1539.5	1486.1
ROHACELL®	1	No	2796.5	2240.8	2134.4	2166.5	2100.9	1744.7
ROHACELL®	1	Yes	1501.6	1305.7	1349.7	1486.7	1564.5	1410.0

	NASA Engineering and Safety Center Technical Assessment Report	Document #: NESC-RP-12-00783	Version: 1.0
Title: Empirical Model Development for Predicting Shock Response on Composite Materials Subjected to Pyroshock Loading		Page #: 68 of 123	

The results from the statistical analysis are graphically presented in Figure 7.3.6.2-1 for the type of panel (and whether it was acoustically damped) versus distance from the source shock. Of note, regardless of the panel type, the change in frequency breakpoint is relatively flat at mid-panel distances (2 ft to 5 ft).

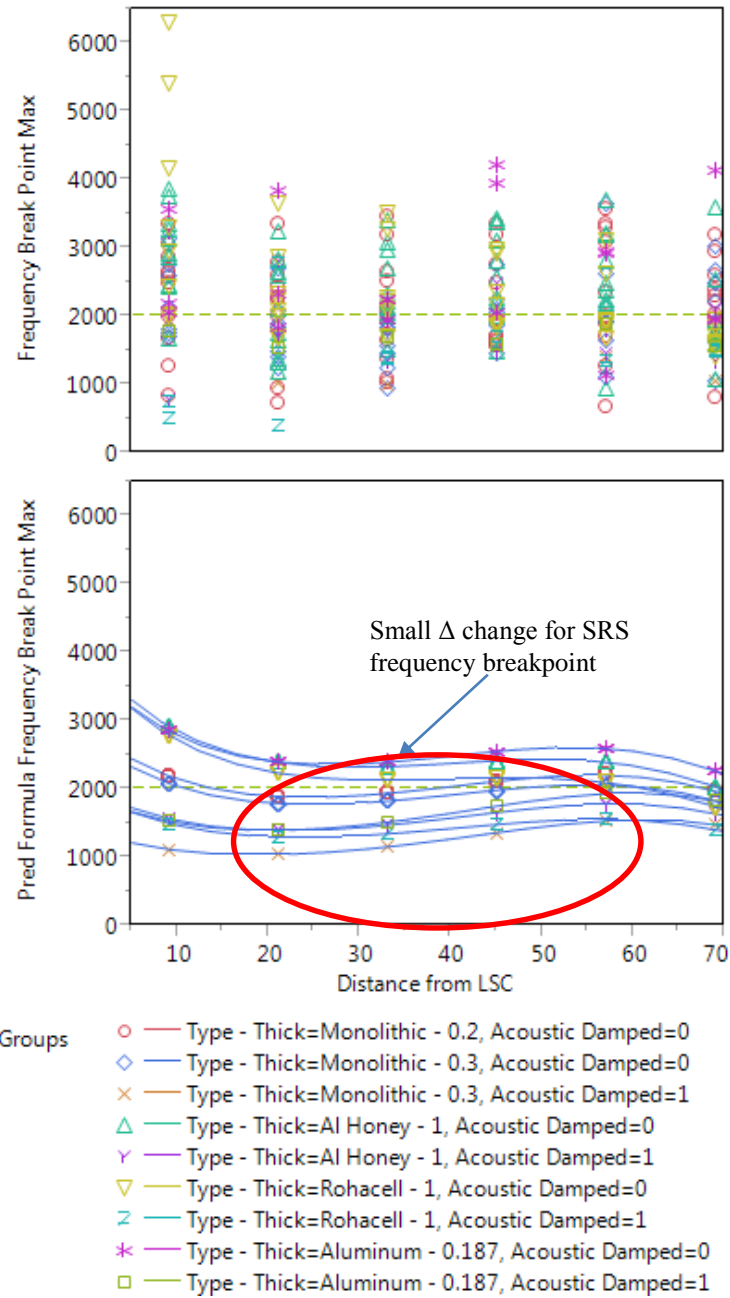



Figure 7.3.6.2-1. Predicted Frequency Breakpoint versus Distance by Panel Type

	NASA Engineering and Safety Center Technical Assessment Report	Document #:	Version:
		NESC-RP-12-00783	1.0
Title:		Page #:	
Empirical Model Development for Predicting Shock Response on Composite Materials Subjected to Pyroshock Loading		69 of 123	

The SRS frequency breakpoint was further evaluated to discern a difference in the SRS frequency breakpoint with regard to the type of ply used for the monolithic composite panels. As illustrated in Figure 7.3.6.2-2, the ply type showed little effect in the average SRS frequency breakpoint.

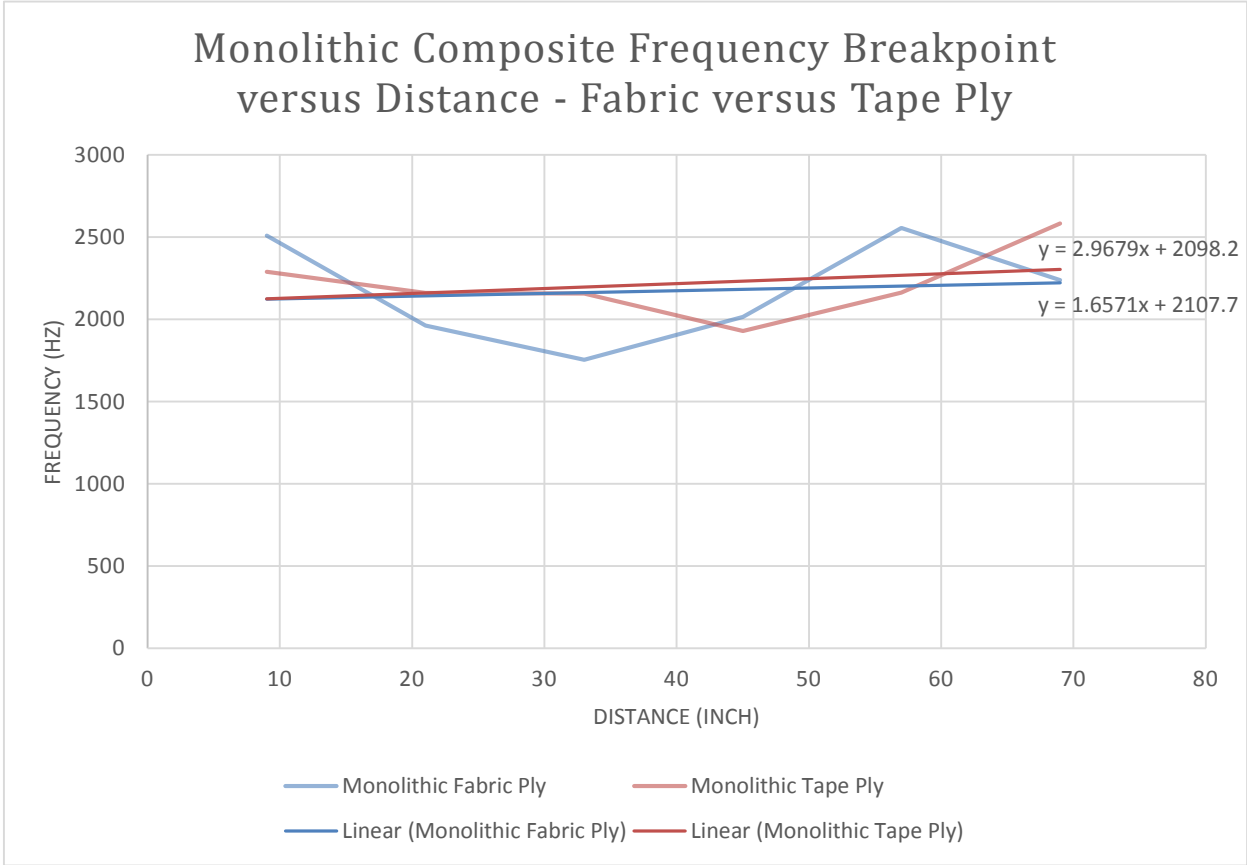


Figure 7.3.6.2-2. SRS Frequency Breakpoint – Ply Type Evaluation

The SRS frequency breakpoint was further analyzed by fill type for the composite sandwich panel types (i.e., Al honeycomb versus ROHACELL[®] foam). Figures 7.3.6.2-3 and 7.3.6.2-4 illustrate the change in the frequency breakpoint for the Al honeycomb sandwich composite panels, which was small (similar to the monolithic composite panels), and the ROHACELL[®] foam sandwich panels showed a slight decrease (~800 Hz over a distance of 60 inches) in frequency breakpoint with distance from the shock source. The frequency breakpoint data were evaluated both with and without the composite LSC plate data (from Group III) and the data at the 69-inch location. The composite LSC data and the data at the 69-inch location artificially elevated the frequency breakpoint, which on average was 2500 Hz (regardless of sandwich fill type) as compared to 2100 Hz for the monolithic composite panels.



Title:

Empirical Model Development for Predicting Shock Response on Composite Materials Subjected to Pyroshock Loading

Page #:
70 of 123

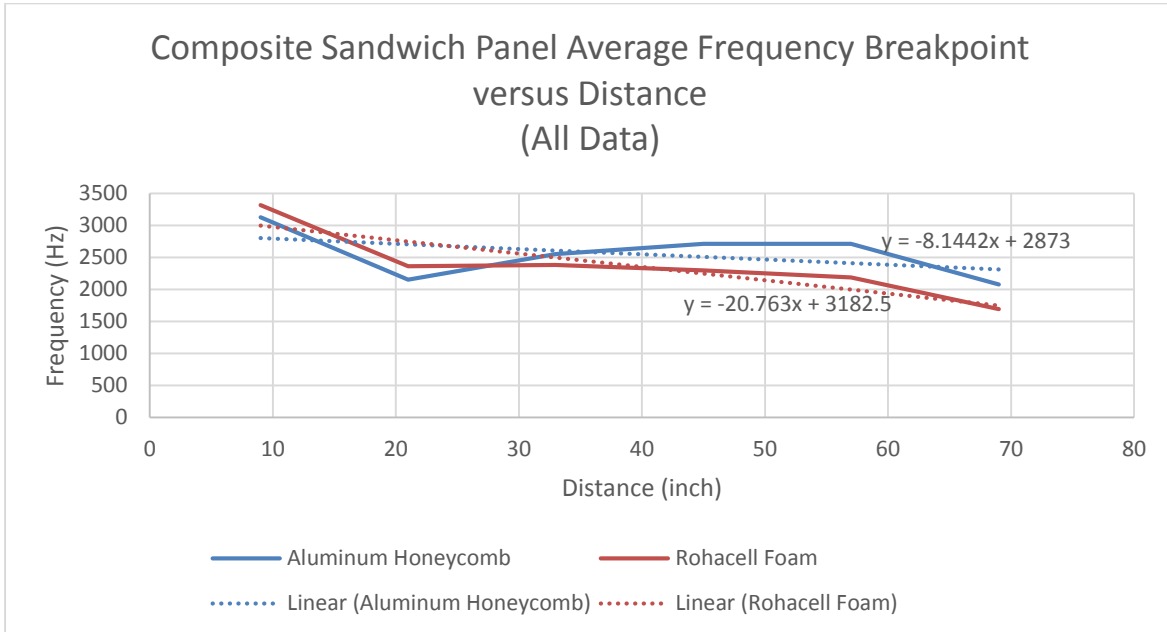


Figure 7.3.6.2-3. SRS Frequency Breakpoint Composite Sandwich Fill Evaluation (all data)

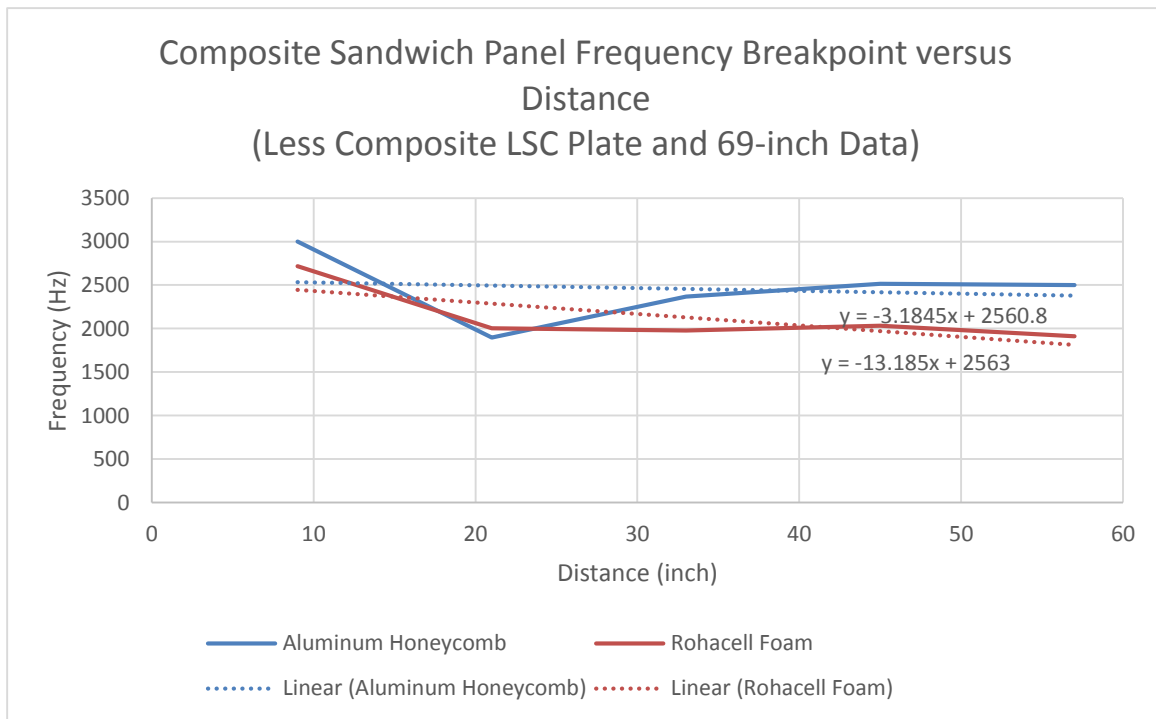



Figure 7.3.6.2-4. SRS Frequency Breakpoint Composite Sandwich Fill Evaluation (less 69-inch data and composite LSC plate data)

	NASA Engineering and Safety Center Technical Assessment Report	Document #: NESC-RP-12-00783	Version: 1.0
Title: Empirical Model Development for Predicting Shock Response on Composite Materials Subjected to Pyroshock Loading		Page #: 71 of 123	

7.3.6.3 SRS Peak Acceleration

The SRS peak acceleration is the plateau region of the SRS beyond the frequency breakpoint within the SRS frequency domain. The peak acceleration from the SRS is also commonly referred to as the maximum acceleration and the two terms are used interchangeably herein. The statistical analysis from the data output of the SRS algorithm indicated the significant factors to be distance from the shock source, the explosive core load of the LSC used to induce the shock, and the thickness of the monolithic composite panel. The predictive equations from the SRS algorithm data output statistical analysis by panel type and core load are listed below.

For Monolithic 0.2” Thick panels at Core Load = 10 gpf:

Maximum SRS Acceleration

$$\begin{aligned}
 &= \text{Exp}(9.12264279357447 \\
 &+ -0.175906636393387 * ((\text{Distance from LSC} - 39) / 30) \\
 &+ 0.239841649170964 \\
 &+ -0.0684974241978297 \\
 &+ ((\text{Distance from LSC} - 39) / 30) * 0.0946234438399386 \\
 &+ -((\text{Distance from LSC} - 39) / 30) * 0.0323247729199656 \\
 &+ ((\text{Distance from LSC} - 39) / 30) * (((\text{Distance from LSC} - 39) / 30) * 0.186658985688534))
 \end{aligned}$$

For Monolithic 0.2” Thick panels at Core Load = 22 gpf:


Maximum SRS Acceleration

$$\begin{aligned}
 &= \text{Exp}(9.12264279357447 \\
 &+ -0.175906636393387 * ((\text{Distance from LSC} - 39) / 30) \\
 &+ 0.239841649170964 \\
 &+ 0.0684974241978297 \\
 &+ ((\text{Distance from LSC} - 39) / 30) * 0.0946234438399386 \\
 &+ ((\text{Distance from LSC} - 39) / 30) * 0.0323247729199656 \\
 &+ ((\text{Distance from LSC} - 39) / 30) * (((\text{Distance from LSC} - 39) / 30) * 0.186658985688534))
 \end{aligned}$$

For Monolithic 0.3” Thick panels at Core Load = 10 gpf:

Maximum SRS Acceleration

$$\begin{aligned}
 &= \text{Exp}(9.12264279357447 \\
 &+ -0.175906636393387 * ((\text{Distance from LSC} - 39) / 30) \\
 &+ -0.0259617976444534 \\
 &+ -0.0684974241978297 \\
 &+ ((\text{Distance from LSC} - 39) / 30) * 0.0857940847197687 \\
 &+ -((\text{Distance from LSC} - 39) / 30) * 0.0323247729199656 \\
 &+ ((\text{Distance from LSC} - 39) / 30) * (((\text{Distance from LSC} - 39) / 30) * 0.186658985688534))
 \end{aligned}$$

	NASA Engineering and Safety Center Technical Assessment Report	Document #: NESC-RP-12-00783	Version: 1.0
Title: Empirical Model Development for Predicting Shock Response on Composite Materials Subjected to Pyroshock Loading		Page #: 72 of 123	

For Monolithic 0.3” Thick panels at Core Load = 22 gpf:


Maximum SRS Acceleration
 = Exp (9.12264279357447
 + -0.175906636393387 * ((Distance from LSC - 39) / 30)
 + -0.0259617976444534
 + 0.0684974241978297
 + ((Distance from LSC - 39) / 30) * 0.0857940847197687
 + ((Distance from LSC - 39) / 30) * 0.0323247729199656
 + ((Distance from LSC - 39) / 30) * (((Distance from LSC - 39) / 30) * 0.186658985688534))

For Al Honeycomb panels at Core Load = 10 gpf:

Maximum SRS Acceleration
 = Exp (9.12264279357447
 + -0.175906636393387 * ((Distance from LSC - 39) / 30)
 + -0.114859502597656
 + -0.0684974241978297
 + ((Distance from LSC - 39) / 30) * -0.0900791110938465
 + -((Distance from LSC - 39) / 30) * 0.0323247729199656
 + ((Distance from LSC - 39) / 30) * (((Distance from LSC - 39) / 30) * 0.186658985688534))

For Al Honeycomb panels at Core Load = 22 gpf:

Maximum SRS Acceleration
 = Exp(
 9.12264279357447
 + -0.175906636393387 * ((Distance from LSC - 39) / 30)
 + -0.114859502597656
 + 0.0684974241978297
 + ((Distance from LSC - 39) / 30) * -0.0900791110938465
 + ((Distance from LSC - 39) / 30) * 0.0323247729199656
 + ((Distance from LSC - 39) / 30) * (((Distance from LSC - 39) / 30) * 0.186658985688534))

	NASA Engineering and Safety Center Technical Assessment Report	Document #: NESC-RP-12-00783	Version: 1.0
Title: Empirical Model Development for Predicting Shock Response on Composite Materials Subjected to Pyroshock Loading		Page #: 73 of 123	

For ROHACELL® panels at Core Load = 10 gpf:

$$\begin{aligned}
 &\text{Maximum SRS Acceleration} \\
 &= \text{Exp } (9.12264279357447 \\
 &+ -0.175906636393387 * ((\text{Distance from LSC} - 39) / 30) \\
 &+ -0.158934902223547 \\
 &+ -0.0684974241978297 \\
 &+ ((\text{Distance from LSC} - 39) / 30) * -0.155745103509068 \\
 &+ -((\text{Distance from LSC} - 39) / 30) * 0.0323247729199656 \\
 &+ ((\text{Distance from LSC} - 39) / 30) * (((\text{Distance from LSC} - 39) / 30) * 0.186658985688534))
 \end{aligned}$$

For ROHACELL® panels at Core Load = 22 gpf:


$$\begin{aligned}
 &\text{Maximum SRS Acceleration} \\
 &= \text{Exp } (9.12264279357447 \\
 &+ -0.175906636393387 * ((\text{Distance from LSC} - 39) / 30) \\
 &+ -0.158934902223547 \\
 &+ 0.0684974241978297 \\
 &+ ((\text{Distance from LSC} - 39) / 30) * -0.155745103509068 \\
 &+ ((\text{Distance from LSC} - 39) / 30) * 0.0323247729199656 \\
 &+ ((\text{Distance from LSC} - 39) / 30) * (((\text{Distance from LSC} - 39) / 30) * 0.186658985688534))
 \end{aligned}$$

For Al panel at Core Load = 10 gpf:

$$\begin{aligned}
 &\text{Maximum SRS Acceleration} \\
 &= \text{Exp } (9.12264279357447 \\
 &+ -0.175906636393387 * ((\text{Distance from LSC} - 39) / 30) \\
 &+ 0.059914553294692 \\
 &+ -0.0684974241978297 \\
 &+ ((\text{Distance from LSC} - 39) / 30) * 0.0654066860432069 \\
 &+ -((\text{Distance from LSC} - 39) / 30) * 0.0323247729199656 \\
 &+ ((\text{Distance from LSC} - 39) / 30) * (((\text{Distance from LSC} - 39) / 30) * 0.186658985688534))
 \end{aligned}$$

For Al panel at Core Load = 22 gpf:

$$\begin{aligned}
 &\text{Maximum SRS Acceleration} \\
 &= \text{Exp } (9.12264279357447 \\
 &+ -0.175906636393387 * ((\text{Distance from LSC} - 39) / 30) \\
 &+ 0.059914553294692 \\
 &+ -0.0684974241978297 \\
 &+ ((\text{Distance from LSC} - 39) / 30) * 0.0654066860432069 \\
 &+ ((\text{Distance from LSC} - 39) / 30) * 0.0323247729199656 \\
 &+ ((\text{Distance from LSC} - 39) / 30) * (((\text{Distance from LSC} - 39) / 30) * 0.186658985688534))
 \end{aligned}$$

	NASA Engineering and Safety Center Technical Assessment Report	Document #: NESC-RP-12-00783	Version: 1.0
Title: Empirical Model Development for Predicting Shock Response on Composite Materials Subjected to Pyroshock Loading		Page #: 74 of 123	

The results from the statistical analysis predictive equations are graphically presented in Figure 7.3.6.3-1 and tabulated in Table 7.3.6.3-1.

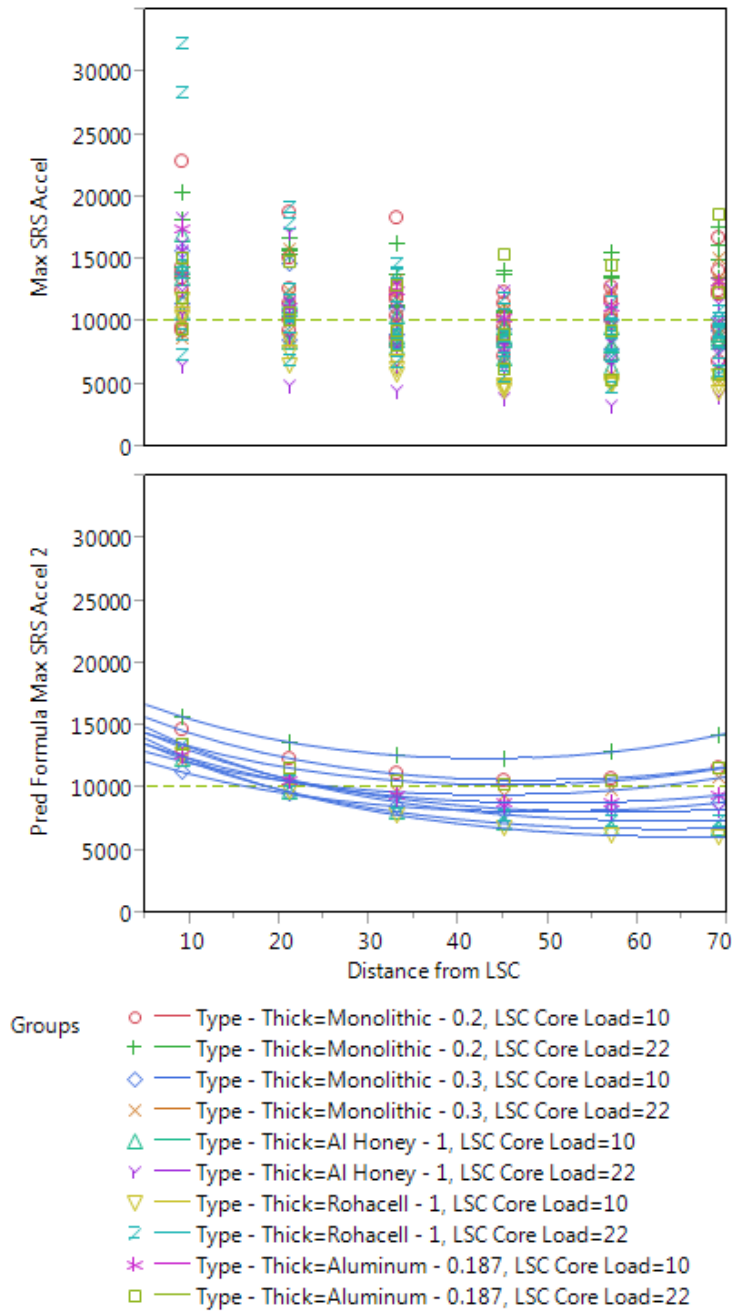


Figure 7.3.6.3-1. Predicted SRS Peak Acceleration versus Distance by Panel Type


	NASA Engineering and Safety Center Technical Assessment Report	Document #:	Version:
		NESC-RP-12-00783	1.0
Title:		Page #:	
Empirical Model Development for Predicting Shock Response on Composite Materials Subjected to Pyroshock Loading		75 of 123	

Table 7.3.6.3-1. Predicted Peak Acceleration Values by Panel Material Type


Factor		Predicted Peak Acceleration by Distance from LSC					
Type - Thick	LSC Core Load	9	21	33	45	57	69
Al Honey - 1	10	12385.2	9754.4	8155.2	7237.9	6819.2	6820.1
Al Honey - 1	22	13314.4	10760.9	9232.4	8408.6	8129.7	8343.8
Al - 0.187	10	12626.4	10582.4	9415.3	8892.5	8915.6	9489.1
Al - 0.187	22	13573.7	11674.4	10659.0	10330.8	10629.1	11609.0
Monolithic - 0.2	10	14680.2	12448.4	11205.7	10707.8	10861.9	11696.4
Monolithic - 0.2	22	15781.6	13733.0	12685.8	12439.8	12949.4	14309.6
Monolithic - 0.3	10	11353.5	9593.5	8605.3	8194.0	8282.7	8887.5
Monolithic - 0.3	22	12205.3	10583.5	9742.0	9519.4	9874.4	10873.1
ROHACELL® - 1	10	12655.5	9708.9	7906.8	6835.5	6273.1	6111.3
ROHACELL® - 1	22	13605.0	10710.7	8951.1	7941.1	7478.6	7476.6

It is notable the tabulated peak acceleration, for any given panel type, does not correspond well with the peak accelerations that were predicted for the 10 grains per foot (gpf) and 22 gpf LSC as shown in Figures 7.2.5.2-1 and 7.2.5.2-2, respectively. The most likely reason is the 0.125-inch Al thick LSC plate used in the test setup is close to the maximum thickness for Al the 10-gpf LSC is capable of severing. Post-test visual examination of the LSC plate using the 10-gpf LSC typically showed approximately 50% of the plate cut by the LSC jet and the remaining 50% fracture from the explosive detonation. (Note: Evidence of fracture of up to 50% of the LSC target thickness is expected when near the upper thickness limitation of the LSC is reached). The 22-gpf LSC fully cut the LSC plate with no visual evidence of fracture meaning the excess energy of the 22-gpf LSC is lost into the atmosphere and not transmitted into the LSC panel as shock. Excerpted below from *NASA-HDBK-7005* is the guideline specified for source shock energy scaling, which includes as a caveat with regard to excess explosive energy.

5.3.4.1 Source Energy Scaling. Letting E_r and E_n denote the total explosive energy released by the pyrotechnic device on the reference and new spacecraft, respectively, the shock response spectrum at all frequencies is scaled from the reference to the new vehicle by

$$SRS_n(D) = SRS_r(D) \sqrt{E_n/E_r} \quad (5.77)$$

where SRS_r and SRS_n are the shock response spectra for the reference and new spacecraft, respectively, at the same distance D from the pyrotechnic source. Caution should be exercised in the utilization of Equation (5.77) since, in many cases, an excess of source energy beyond that required to cause structural separation will not increase the shock transmission, but instead will generate an increased shock or blast wave that will be transmitted into the atmosphere or vacuum adjacent to the structure. This excess energy may not be as effective in

	NASA Engineering and Safety Center Technical Assessment Report	Document #: NESC-RP-12-00783	Version: 1.0
Title: Empirical Model Development for Predicting Shock Response on Composite Materials Subjected to Pyroshock Loading		Page #: 76 of 123	

generating structural response. Thus, when $E_n > E_r$, the application of Equation (5.77) may cause an over-prediction of the pyroshock environment. Similarly, an under-prediction may result when $E_n < E_r$.

The peak acceleration versus distance for the four main types of composite panels evaluated for this task, (two thicknesses of monolithic composite panels and the two sandwich panels with different core materials) were evaluated. Figure 7.3.6.3-2 shows the evaluation of the monolithic composite panels with regard to both the LSC explosive core load and the thickness of the composite material. The peak acceleration decreases with distance from the source shock ranging from 24 g to 100 g per inch with the exception of the 0.3-inch-thick composite panel and the 22-gpf LSC, which showed little attenuation of the shock with distance. Further evaluation of the 0.3-inch-thick composite panel with the 22-gpf LSC was performed on a randomly selected test and the results from this evaluation indicated the enveloping SRS algorithm, which captures highest peak acceleration within the plateau region of the SRS, for this particular test case, resulted in little or no attenuation of the shock with distance. Figure 7.3.6.3-3 and Figure 7.3.6.3-4 show the peak acceleration versus distance and the median peak acceleration percentile remaining with distance for the Group I, re-test of test 2 results, respectively.



NASA Engineering and Safety Center Technical Assessment Report

Document #:
**NESC-RP-
12-00783**

Version:
1.0

Title:

Empirical Model Development for Predicting Shock Response on Composite Materials Subjected to Pyroshock Loading

Page #:
77 of 123

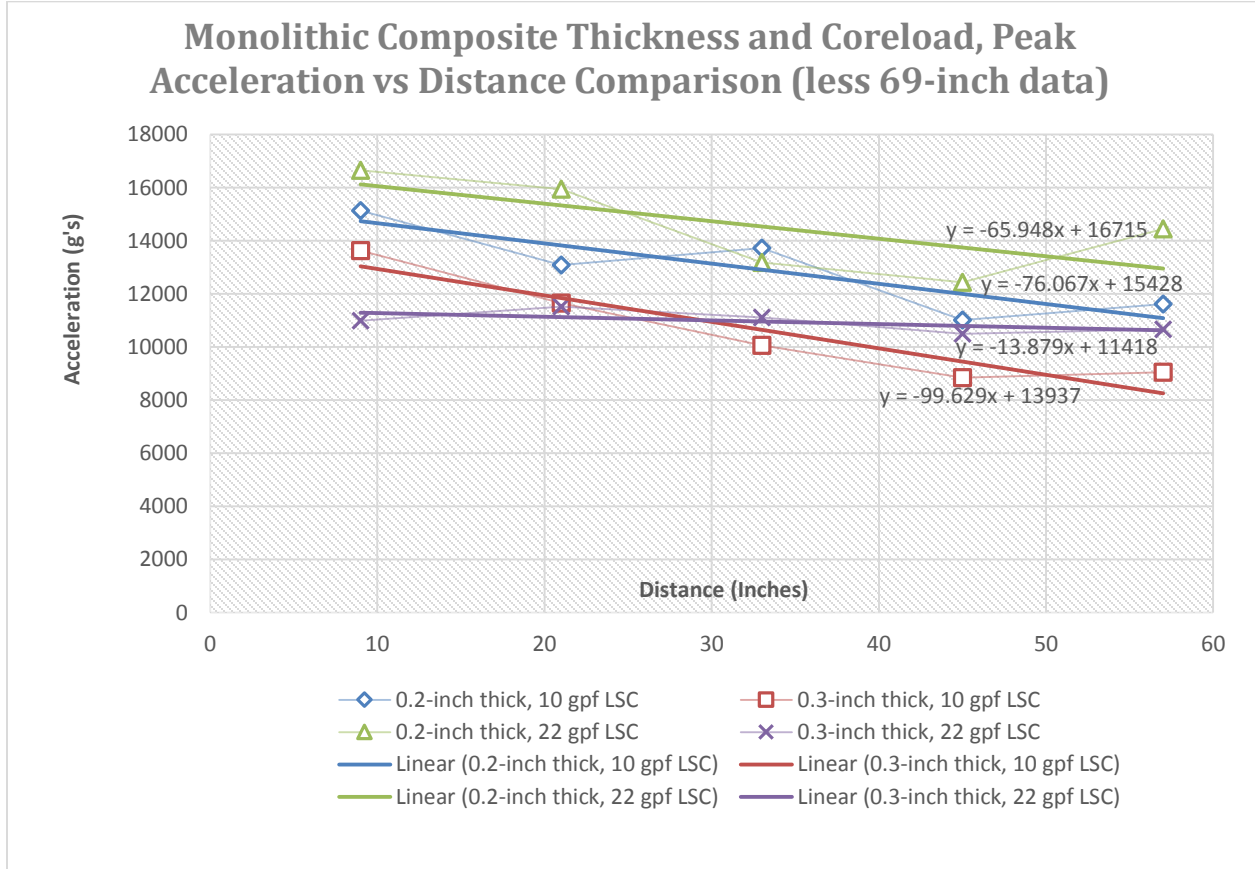


Figure 7.3.6.3-2. Monolithic Composite Panel Peak Acceleration with Distance Comparison



NASA Engineering and Safety Center Technical Assessment Report

Document #:
**NESC-RP-
12-00783**

Version:
1.0

Title:

**Empirical Model Development for Predicting Shock Response on
Composite Materials Subjected to Pyroshock Loading**

Page #:
78 of 123

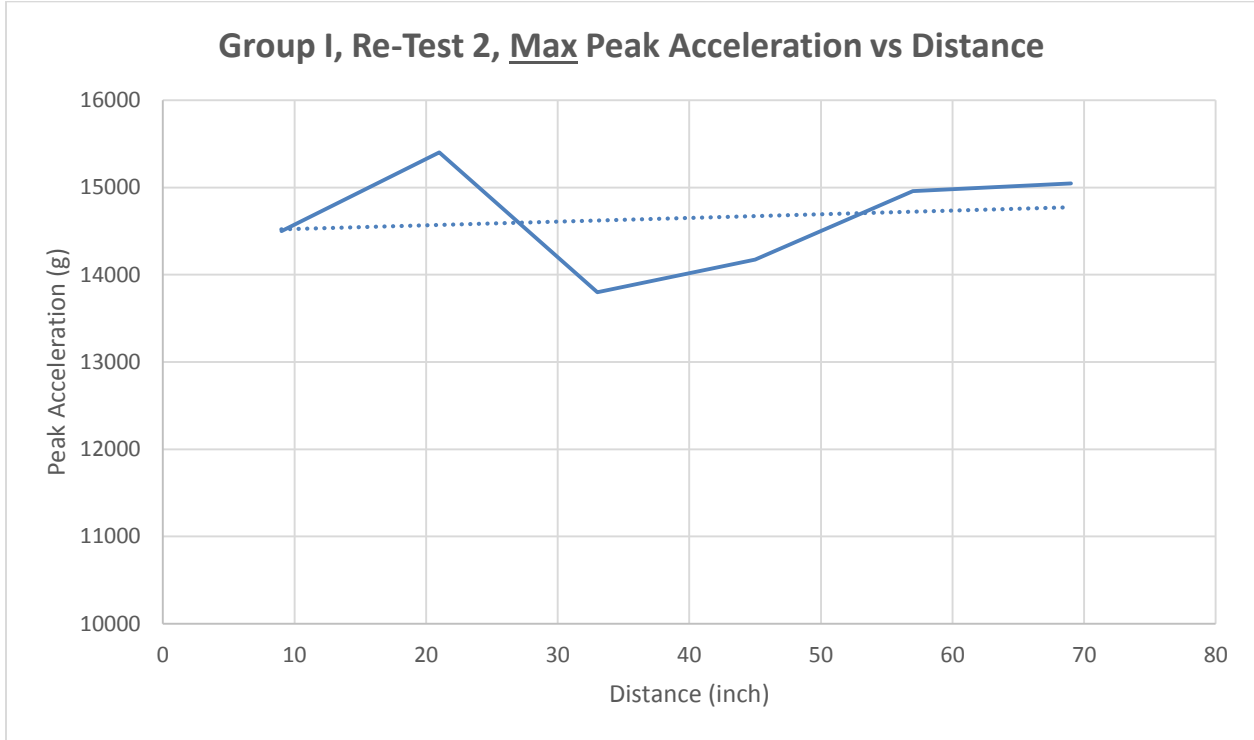



Figure 7.3.6.3-3. Peak Acceleration versus Distance, Group I Re-Test 2

	NASA Engineering and Safety Center Technical Assessment Report	Document #: NESC-RP-12-00783	Version: 1.0
Title: Empirical Model Development for Predicting Shock Response on Composite Materials Subjected to Pyroshock Loading		Page #: 79 of 123	

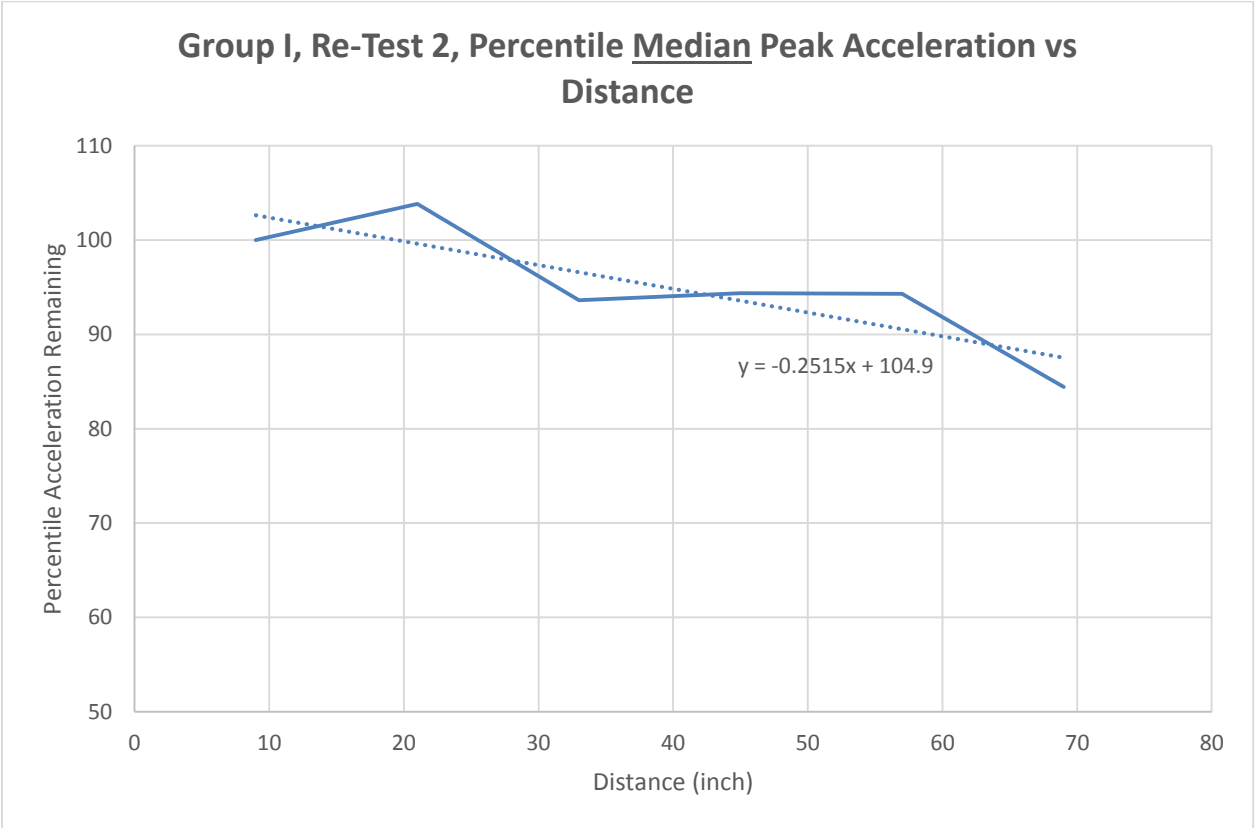


Figure 7.3.6.3-4. Monolithic Composite Group I, Re-Test 2, Percent Median Peak Acceleration versus Distance

Further evaluations performed for the SRS peak acceleration included fabric versus tape ply, orientation of ply layup (unidirectional versus quasi-isotropic), and monolithic versus sandwich composite configurations. Figure 7.3.6.3-5 provides the peak acceleration evaluation results for comparison of the two types of ply used and Figure 7.3.6.3-6 illustrates the evaluation of the peak acceleration with regard to the direction of the ply layup. Figure 7.3.6.3-7 shows the peak acceleration evaluation of the monolithic composite panel with regard to thickness of the composite panel (i.e., number of plies) and Figure 7.3.6.3-8 provides the peak acceleration test results of the monolithic composite panels versus the sandwich composite panel test results.



NASA Engineering and Safety Center Technical Assessment Report

Document #:
**NESC-RP-
12-00783**

Version:
1.0

Title:

Empirical Model Development for Predicting Shock Response on Composite Materials Subjected to Pyroshock Loading

Page #:
80 of 123

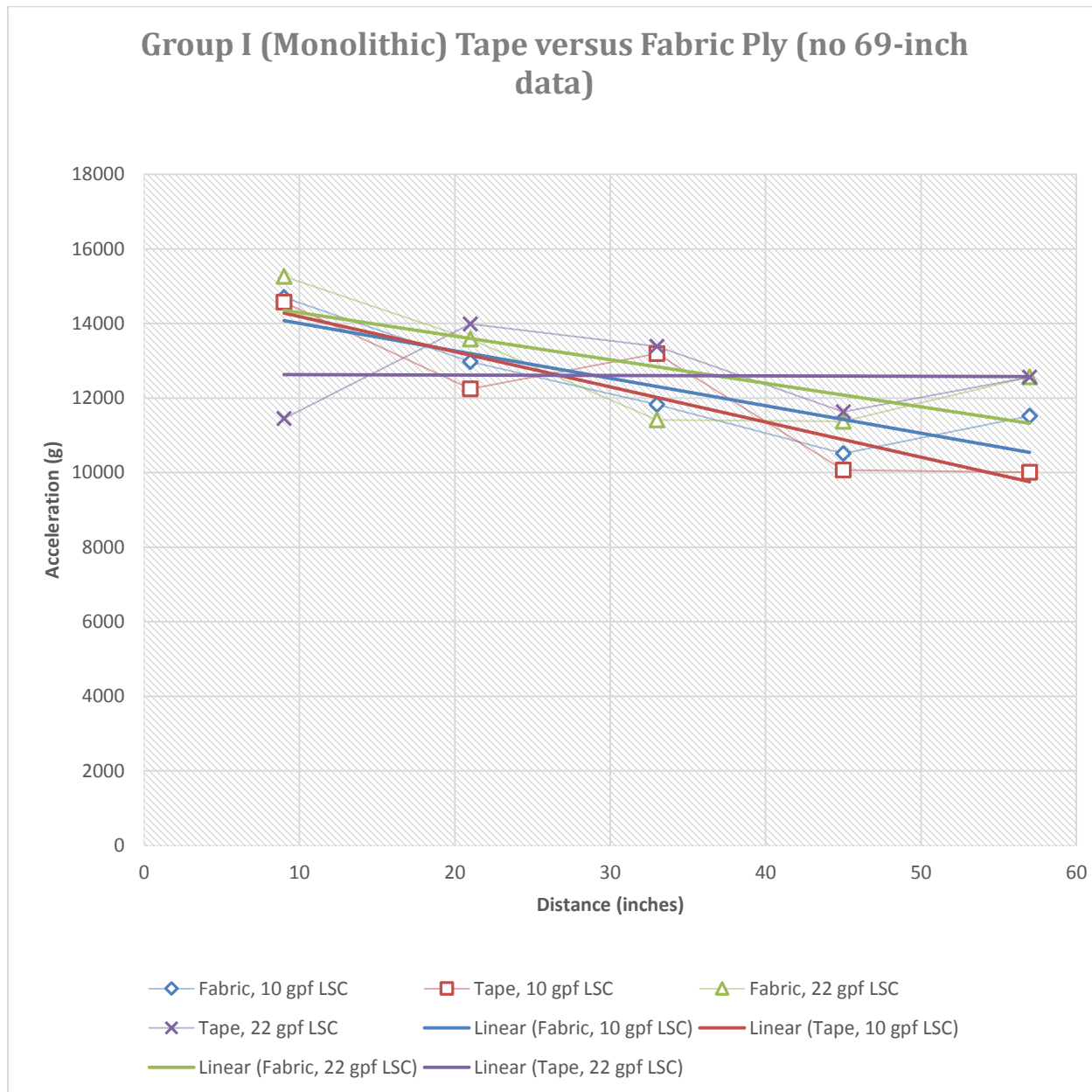


Figure 7.3.6.3-5. Peak Acceleration – Tape versus Fabric Ply



NASA Engineering and Safety Center Technical Assessment Report

Document #:
**NESC-RP-
12-00783**

Version:
1.0

Title:

Empirical Model Development for Predicting Shock Response on Composite Materials Subjected to Pyroshock Loading

Page #:
81 of 123

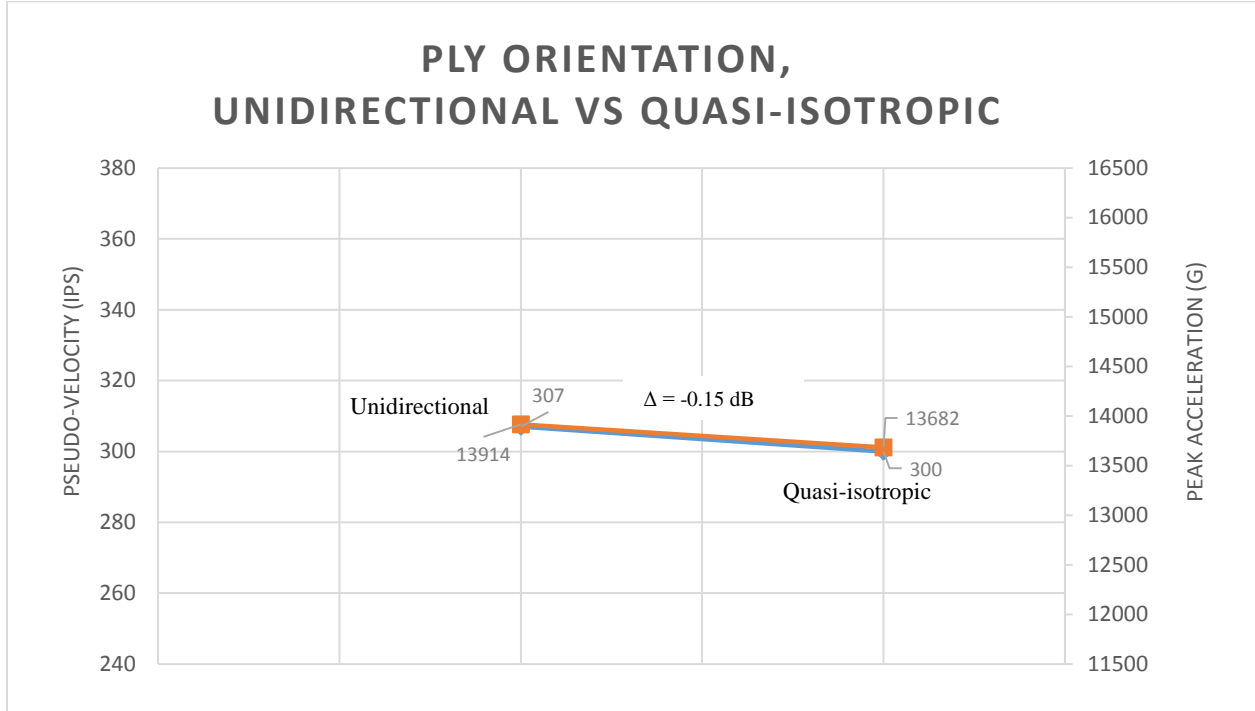


Figure 7.3.6.3-6. Comparison of Ply Layup Direction –Peak Acceleration and PV



NASA Engineering and Safety Center Technical Assessment Report

Document #:
**NESC-RP-
12-00783**

Version:
1.0

Title:

Empirical Model Development for Predicting Shock Response on Composite Materials Subjected to Pyroshock Loading

Page #:
82 of 123

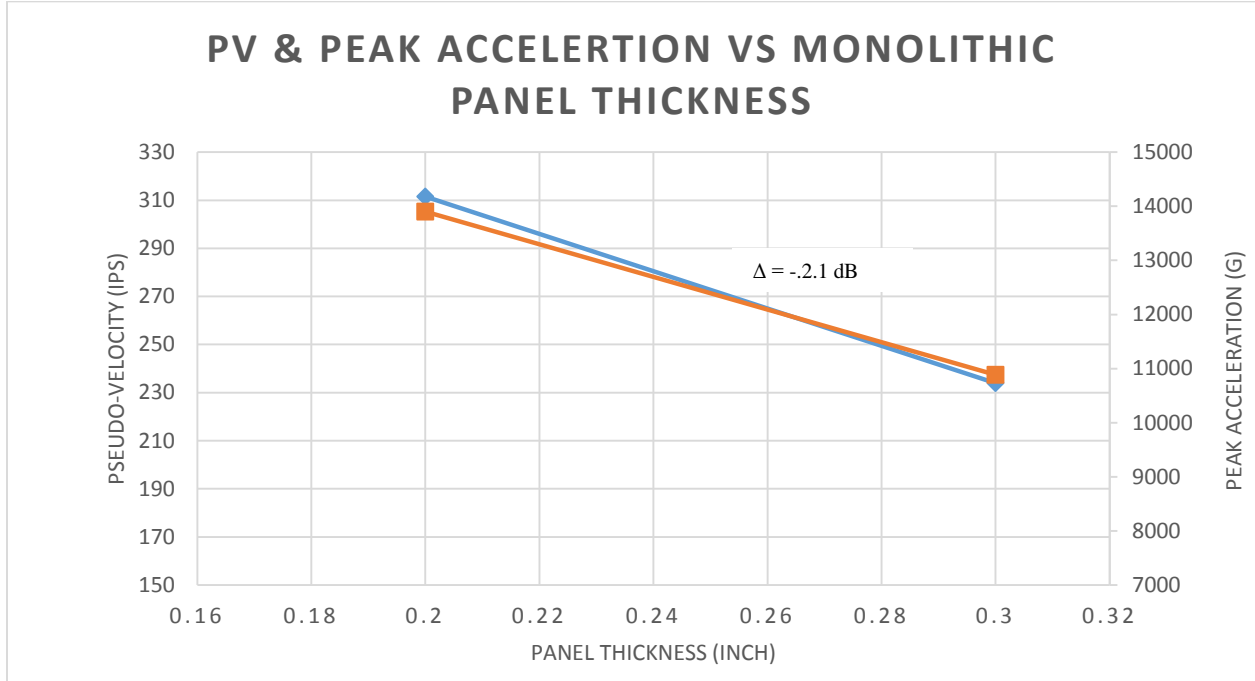



Figure 7.3.6.3-7. Comparison of Monolithic Composite Panel Thickness – Peak Acceleration and PV

	NASA Engineering and Safety Center Technical Assessment Report	Document #:	Version:
		NESC-RP-12-00783	1.0
Title:		Page #:	
Empirical Model Development for Predicting Shock Response on Composite Materials Subjected to Pyroshock Loading		83 of 123	

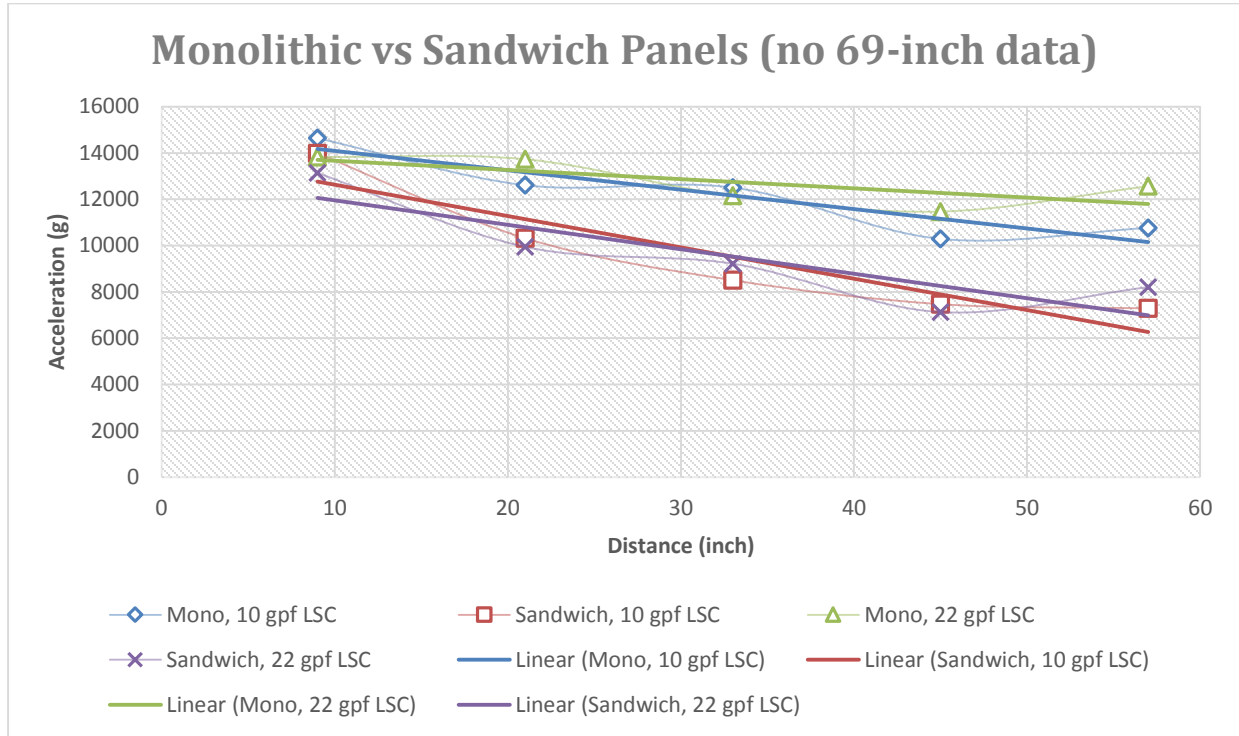


Figure 7.3.6.3-8. Comparison of Monolithic Composite Panel and Sandwich Composite Panel – Peak Acceleration versus Distance

- Some general conclusions that may be drawn from Figures 7.3.6.3-5 through 7.3.6.3-8 include:
- The type of ply (tape or fabric) is not a significant factor with regard to peak acceleration.
 - There is little difference in the peak acceleration due to the direction of the ply layup.
 - The change in amount of peak acceleration attenuation with distance is not significantly different based upon the thickness of the monolithic composite.
 - The change in the peak acceleration attenuation between the monolithic composite and the sandwich filled composite is significantly different with a given similar source shock.

Given the limitation of performing the characterization of the composite material for pyroshock using flat panels, the percentile of the remaining shock with distance was evaluated since it is an invaluable tool for predicting the MEFÉ at a given distance from the shock source. The data provided herein are limited to approximately 48 inches from the shock source due to the limited size of the test panels.

The predicted peak acceleration generated from the statistical analysis from the SRS algorithm output (reference Table 7.3.6.3-1) was used to generate graphical representations of the percentile of the shock remaining at a given distance. Figures 7.3.6.3-9 through 7.3.6.3-12 illustrate the results from this evaluation for the compilation of each panel type, the monolithic composite panels, the Al honeycomb sandwich composite panels, and the ROHACELL® foam

sandwich composite panels, respectively. All of the data for this evaluation was normalized for the 9-inch data to be set at 100% and the data at distances further from the shock source shown as a percentile of the 9-inch data.

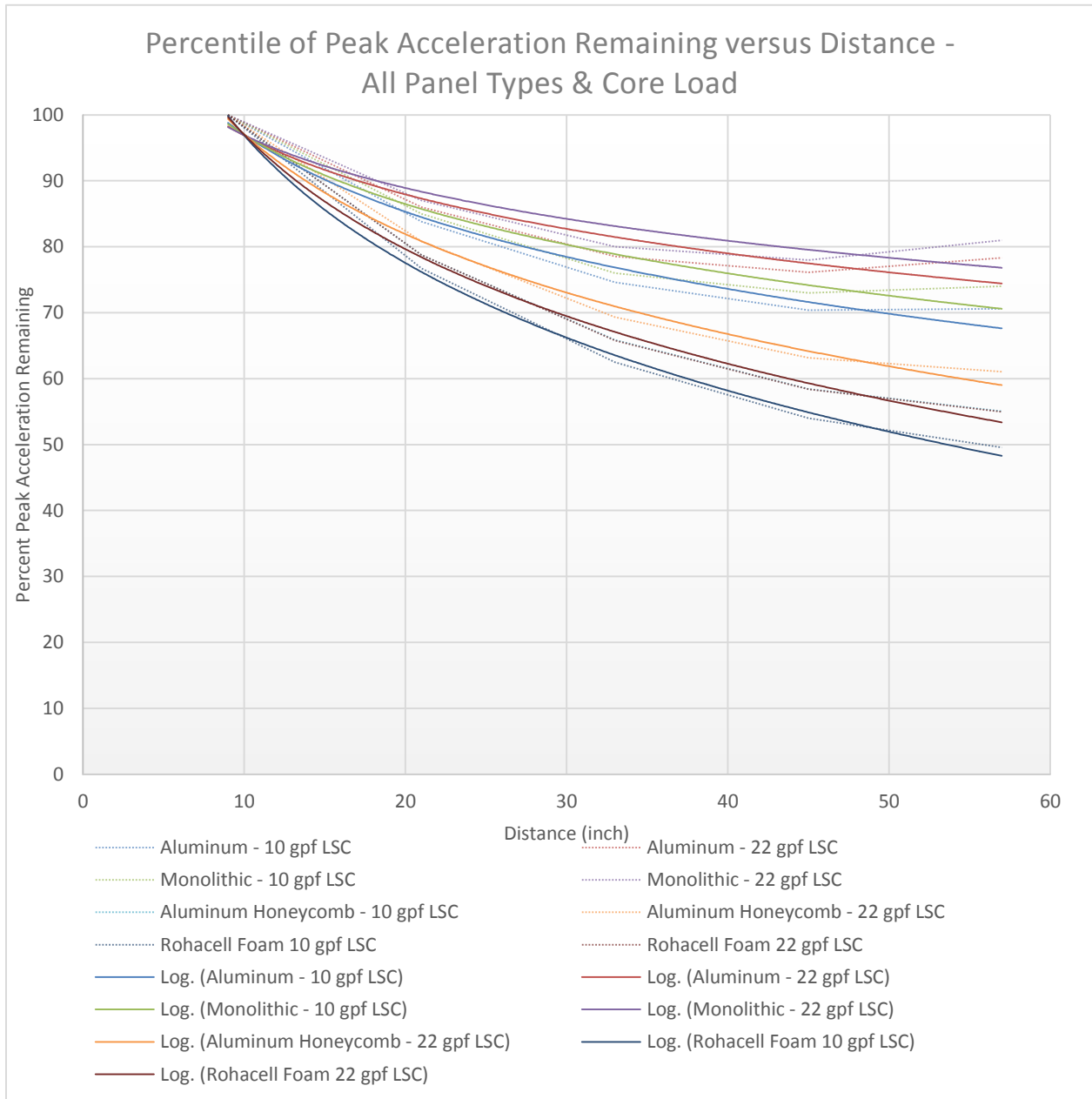


Figure 7.3.6.3-9. Percentile of Shock Remaining – All Panel Types



NASA Engineering and Safety Center Technical Assessment Report

Document #:
**NESC-RP-
12-00783**

Version:
1.0

Title:

**Empirical Model Development for Predicting Shock Response on
Composite Materials Subjected to Pyroshock Loading**

Page #:
85 of 123

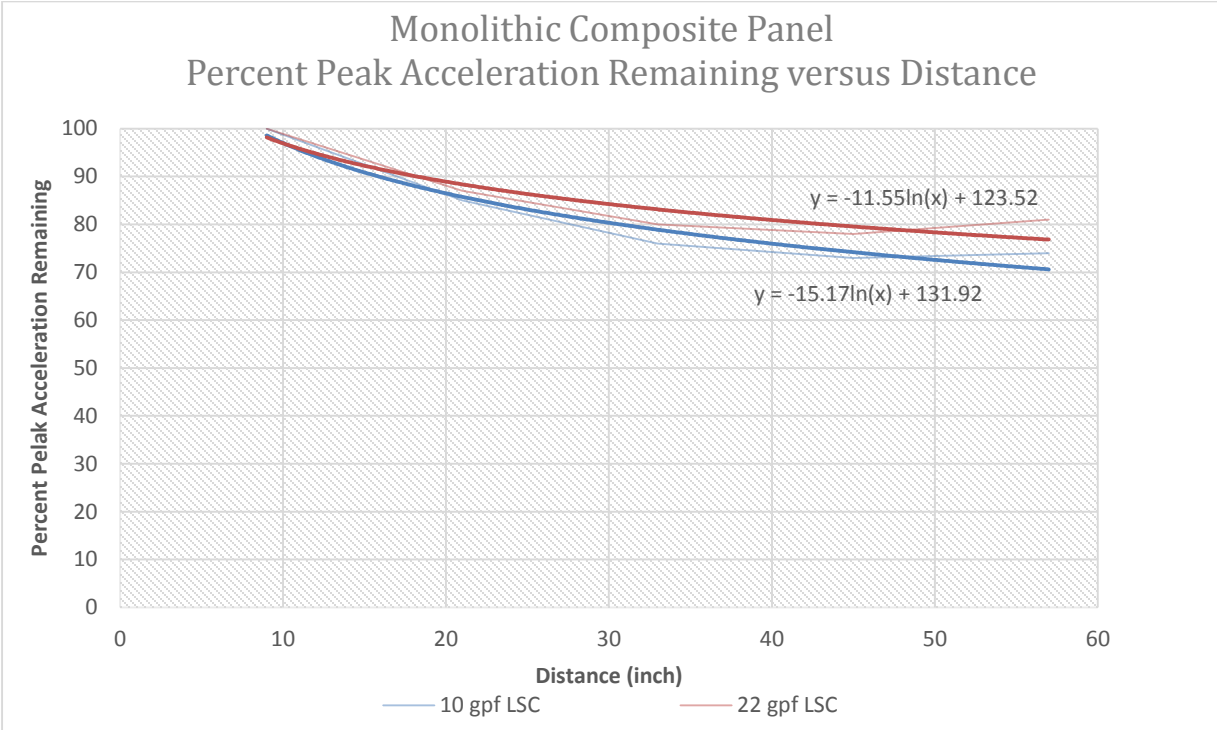


Figure 7.3.6.3-10. Percentile of Shock Remaining - Monolithic Composite Panel



NASA Engineering and Safety Center Technical Assessment Report

Document #:
**NESC-RP-
12-00783**

Version:
1.0

Title:

Empirical Model Development for Predicting Shock Response on Composite Materials Subjected to Pyroshock Loading

Page #:
86 of 123

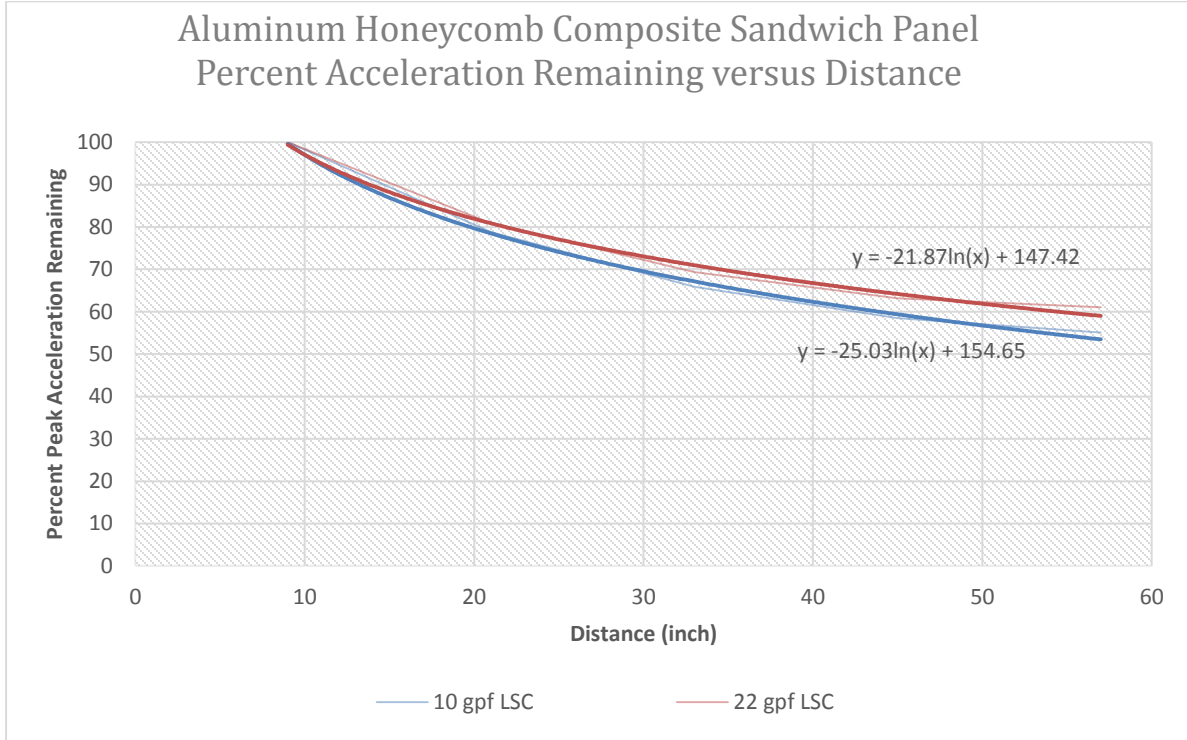



Figure 7.3.6.3-11. Percentile of Shock Remaining – Al Honeycomb Composite Sandwich Panel

	NASA Engineering and Safety Center Technical Assessment Report	Document #: NESC-RP-12-00783	Version: 1.0
Title: Empirical Model Development for Predicting Shock Response on Composite Materials Subjected to Pyroshock Loading		Page #: 87 of 123	

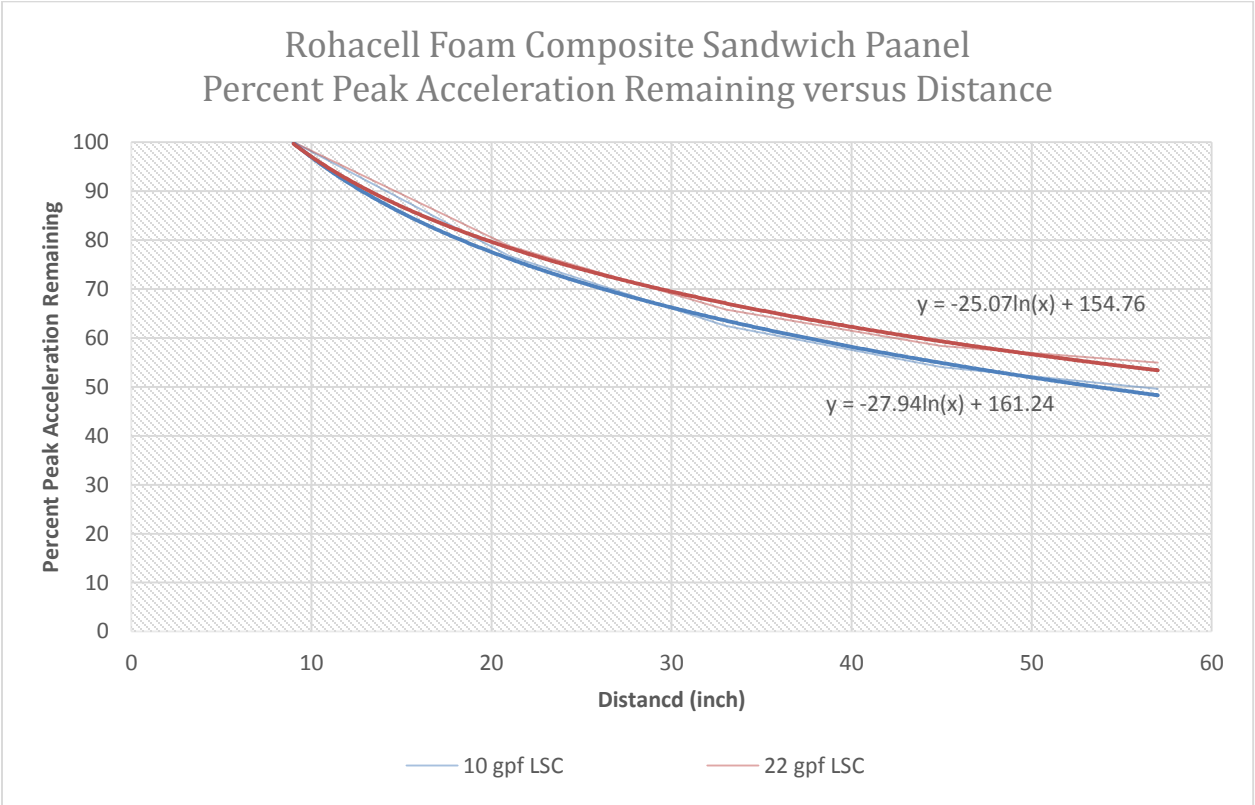


Figure 7.3.6.3-12. Percentile of Shock Remaining – ROHACELL® Foam Composite Sandwich Panel

NASA-CR-116406, *Pyrotechnic Shock Design Guidelines Manual*, prepared by Martin Marietta, does include a graph for honeycomb percentile of shock remaining.

For reference, Figure 7.3.6.3-13 illustrates the Martin Marietta data in comparison with the data collected, reduced, and analyzed for this task. The figure shows the reduction of the shock over distance documented in NASA-CR-116406 and the Al honeycomb test panel data to be slightly greater based upon the testing performed for this task assessment, but the attenuation slopes (log) to be comparable.

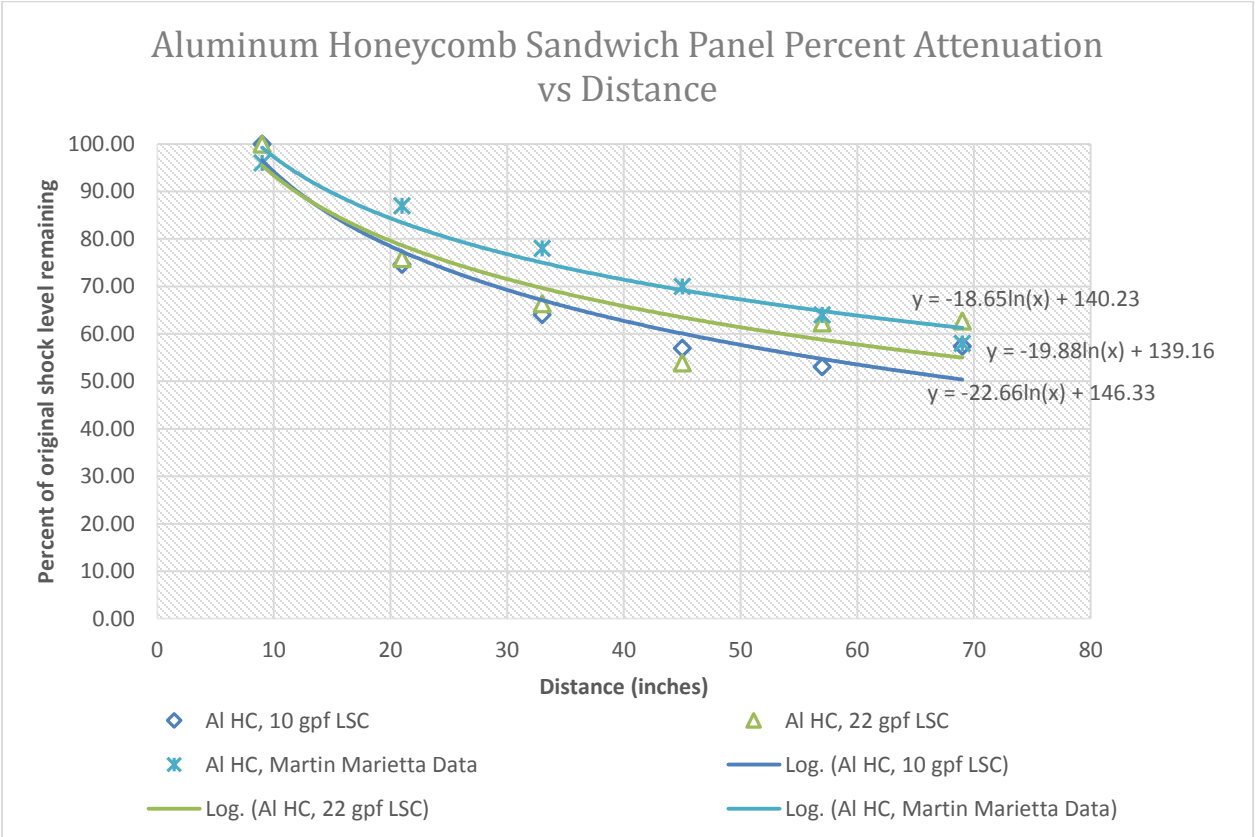



Figure 7.3.6.3-13. Percentile of Shock Remaining- Comparison of Martin Marietta Data with AI Honeycomb Sandwich Panel Data

7.3.7 PV Evaluation

The PVRs may be regarded as the second most common method for characterizing the shock environment in the aerospace industry. ANSI/ASA S2.62-20098, *Shock Test Requirements for Equipment in a Rugged Shock Environment*, specifies shock severity levels according to the plateau level on the PVRs plotted on 4CP or displayed as a four coordinate plot. The maximum PV may be calculated directly from the PV curve without further algorithm processing. The data output from the maximum PV was not empirically modeled since no factors were determined, which correlated meaningfully from the statistical analysis. To evaluate the mean PV the data from the algorithm was imported to Excel[®] and a graph of each test data set was generated. From the graph the frequency band was chosen for the PV plateau, the values averaged and new plots generated for the mean PV at each of the accelerometer distances from the shock source. Then the data were normalized from the 9-inch data set to produce plots of the percentile PV remaining with distance in a similar manner to the evaluation of the SRS peak acceleration data.

	NASA Engineering and Safety Center Technical Assessment Report	Document #: NESC-RP-12-00783	Version: 1.0
Title: Empirical Model Development for Predicting Shock Response on Composite Materials Subjected to Pyroshock Loading		Page #: 89 of 123	

The results from this evaluation for the monolithic composite panels are shown in Figures 7.3.7-1 and 7.3.7-2 for the 0.2-inch-thick monolithic composite panels and Figures 7.3.7-3 and 7.3.7-4 for the 0.3-inch-thick monolithic composite panels, respectively.

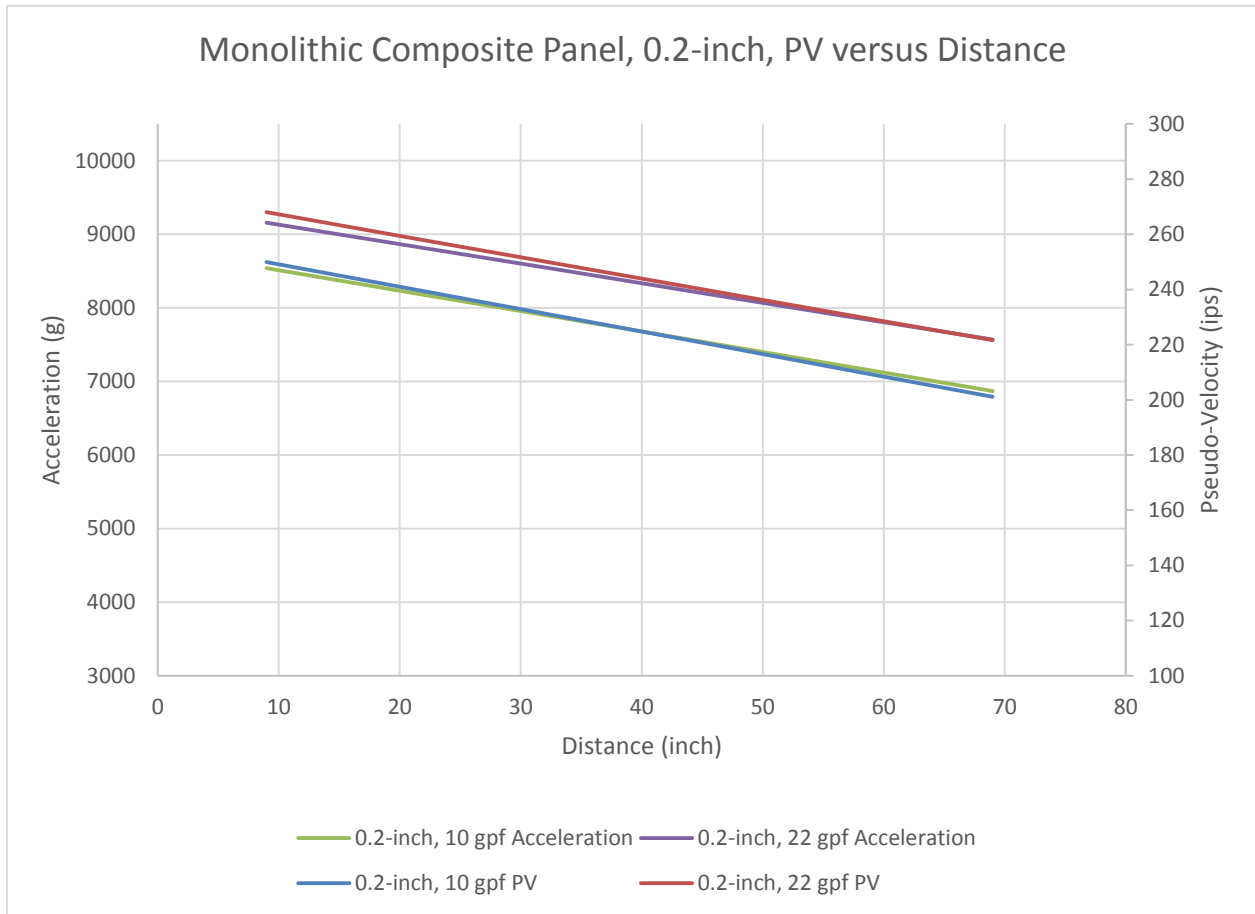


Figure 7.3.7-1. Mean PV versus Distance, 0.2-inch-thick Monolithic Composite Panel



NASA Engineering and Safety Center Technical Assessment Report

Document #:
**NESC-RP-
12-00783**

Version:
1.0

Title:

Empirical Model Development for Predicting Shock Response on Composite Materials Subjected to Pyroshock Loading

Page #:
90 of 123

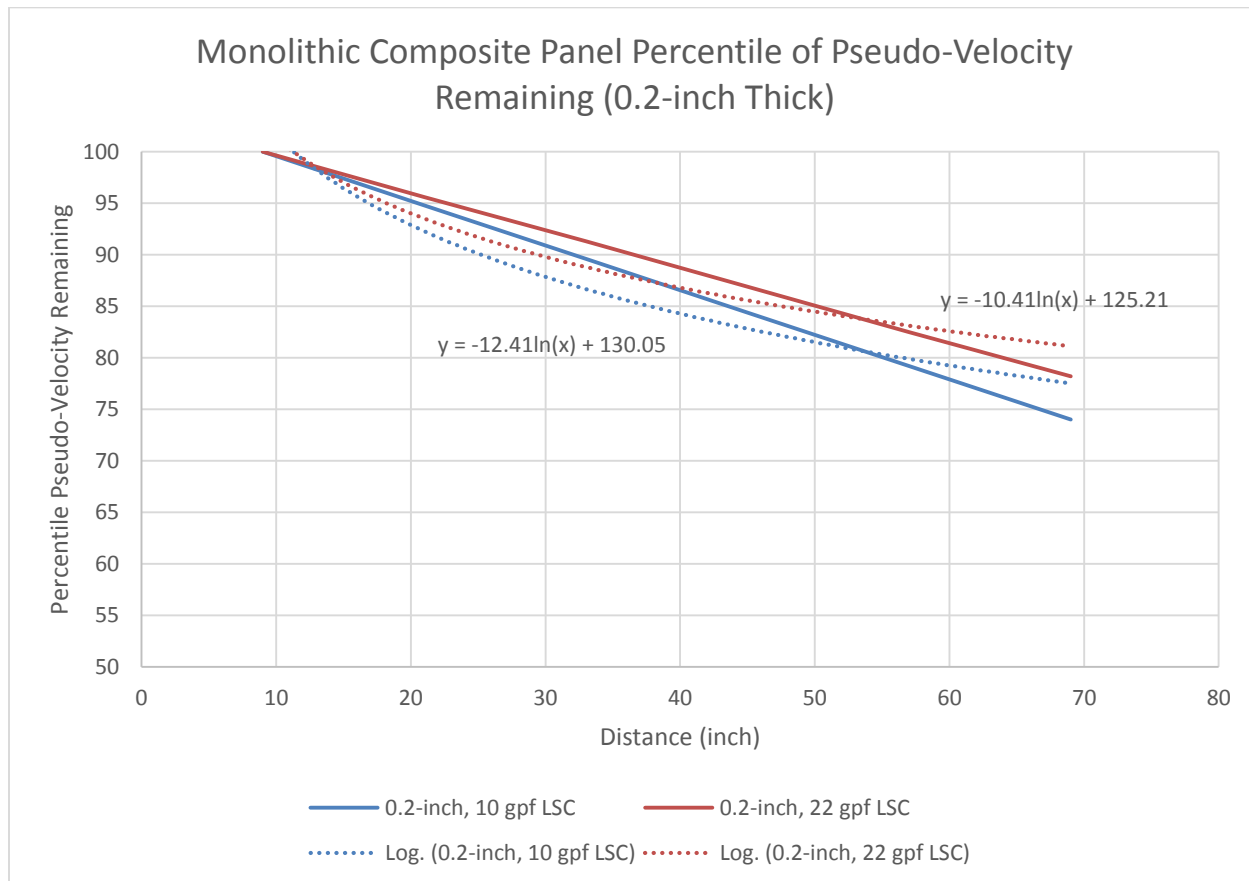


Figure 7.3.7-2. Percentile of PV Remaining versus Distance, 0.2-inch-thick Monolithic Composite Panel



NASA Engineering and Safety Center Technical Assessment Report

Document #:
**NESC-RP-
12-00783**

Version:
1.0

Title:

**Empirical Model Development for Predicting Shock Response on
Composite Materials Subjected to Pyroshock Loading**

Page #:
91 of 123

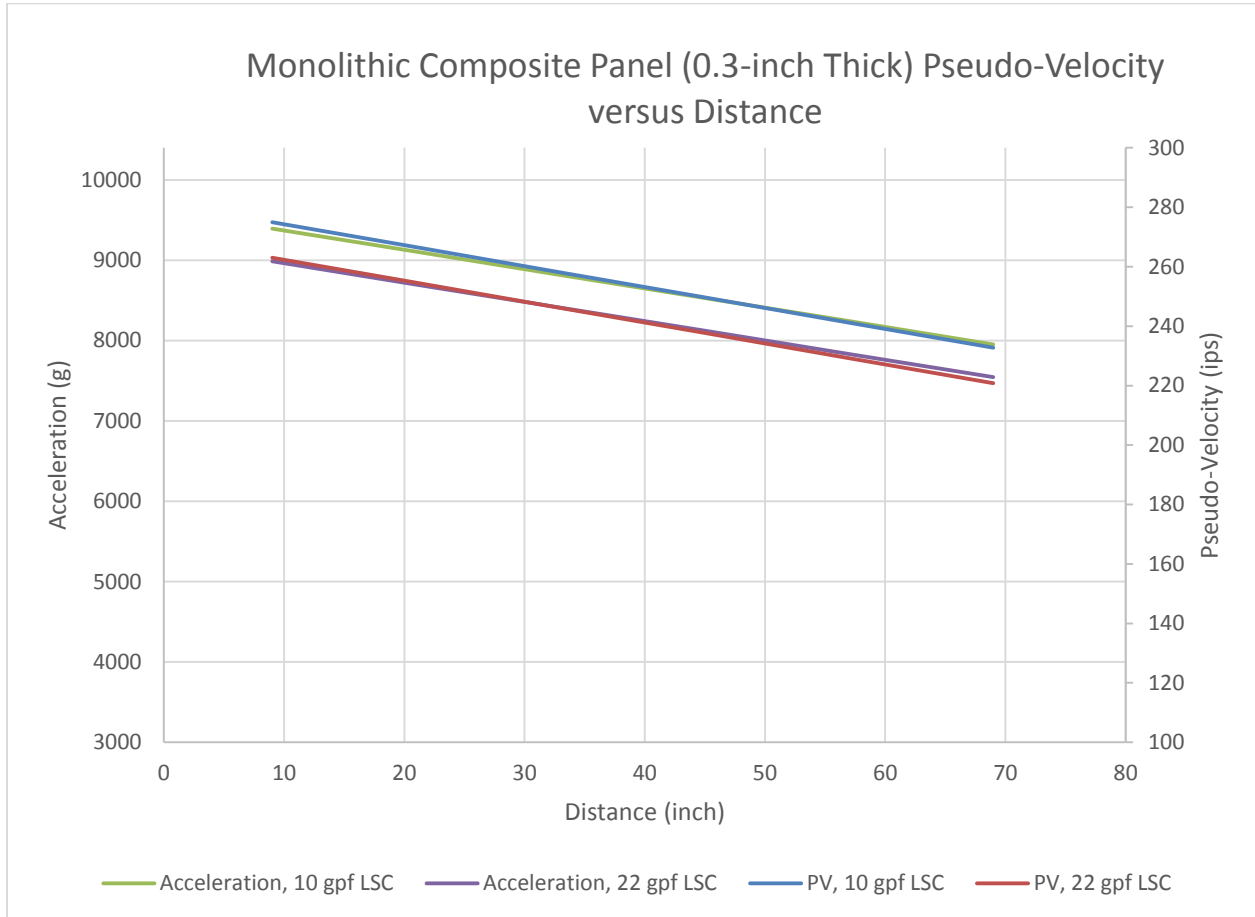


Figure 7.3.7-3. Mean PV versus Distance, 0.3-inch-thick Monolithic Composite Panel



NASA Engineering and Safety Center Technical Assessment Report

Document #:
**NESC-RP-
12-00783**

Version:
1.0

Title:

Empirical Model Development for Predicting Shock Response on Composite Materials Subjected to Pyroshock Loading

Page #:
92 of 123

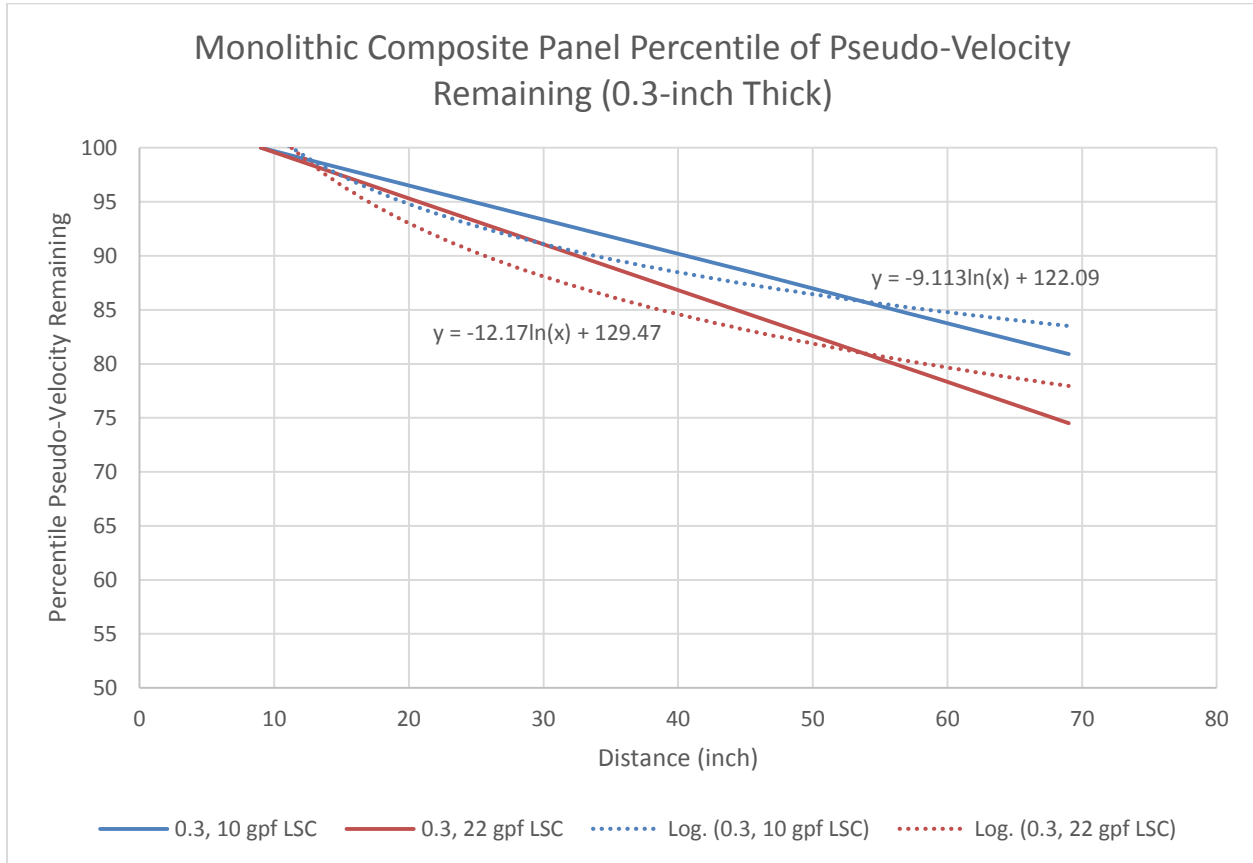


Figure 7.3.7-4. Percentile of PV Remaining versus Distance, 0.3-inch-thick Monolithic Composite Panel

The results from the mean PV for the composite sandwich panels are presented similarly in Figures 7.3.7-5 through 7.3.7-8 for the Al honeycomb sandwich panels and the ROHACELL[®] foam sandwich panels.



NASA Engineering and Safety Center Technical Assessment Report

Document #:
**NESC-RP-
12-00783**

Version:
1.0

Title:

Empirical Model Development for Predicting Shock Response on Composite Materials Subjected to Pyroshock Loading

Page #:
93 of 123

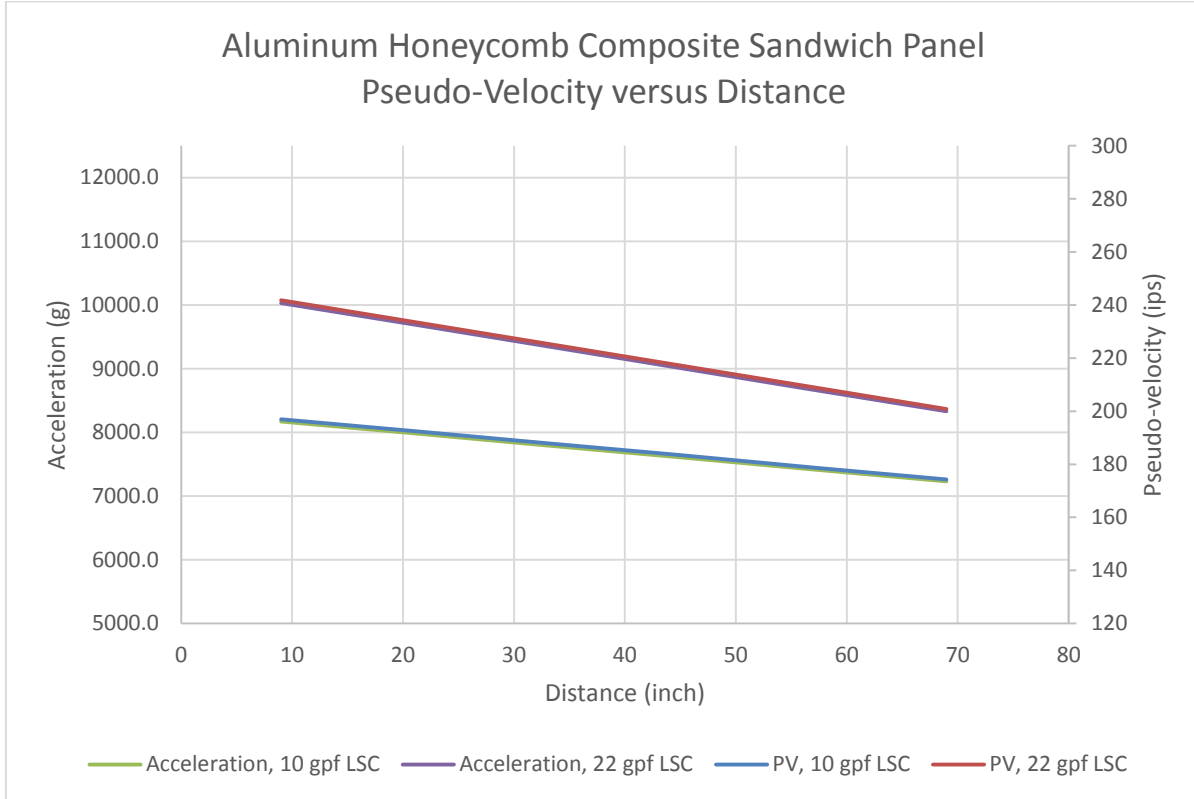


Figure 7.3.7-5. Mean PV versus Distance, Al Honeycomb Composite Sandwich Panel



NASA Engineering and Safety Center Technical Assessment Report

Document #:
**NESC-RP-
12-00783**

Version:
1.0

Title:

Empirical Model Development for Predicting Shock Response on Composite Materials Subjected to Pyroshock Loading

Page #:
94 of 123

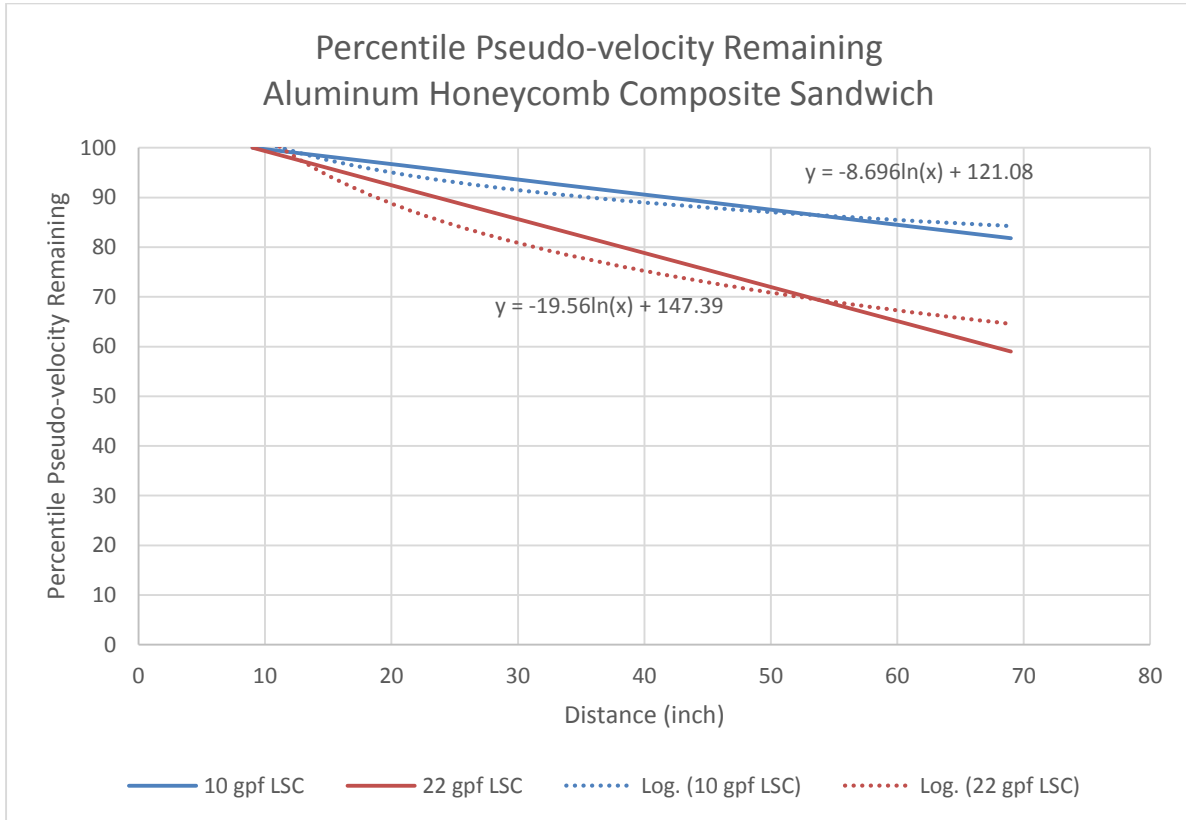


Figure 7.3.7-6. Percentile of PV Remaining versus Distance, Al Honeycomb Composite Sandwich Panel



NASA Engineering and Safety Center Technical Assessment Report

Document #:
**NESC-RP-
12-00783**

Version:
1.0

Title:

**Empirical Model Development for Predicting Shock Response on
Composite Materials Subjected to Pyroshock Loading**

Page #:
95 of 123

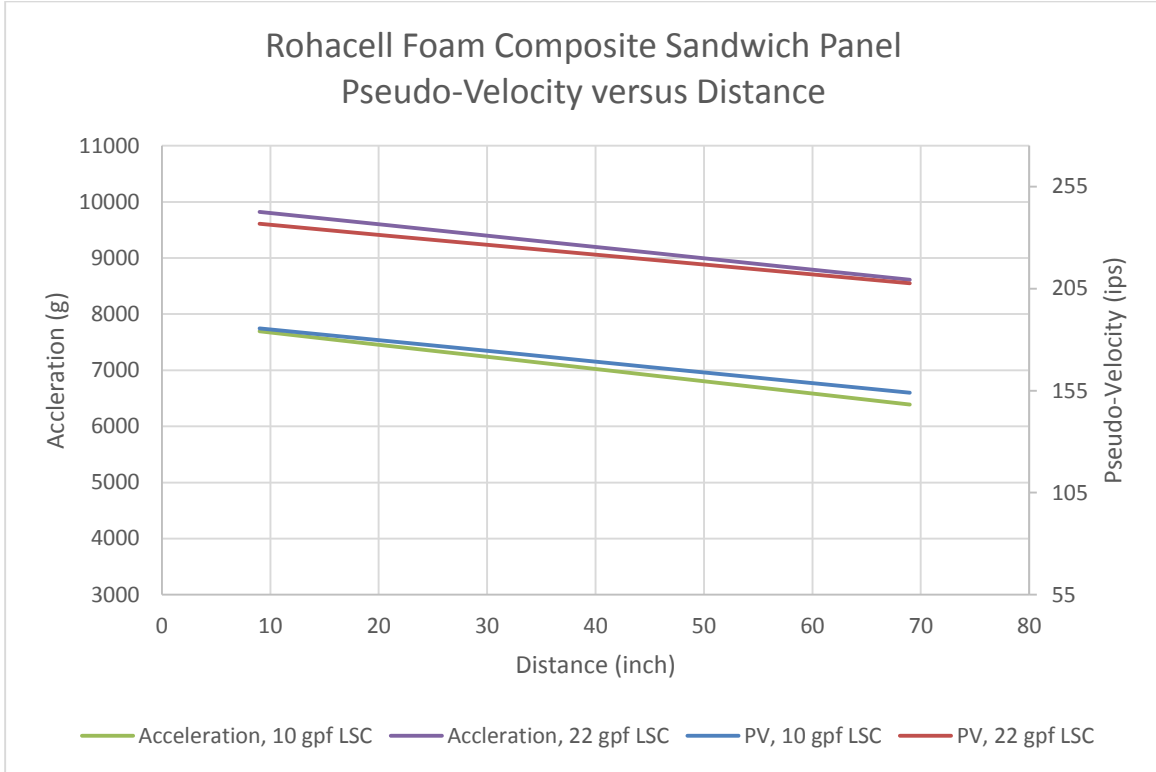



Figure 7.3.7-7. Mean PV versus Distance, ROHACELL® Foam Composite Sandwich Panel

	NASA Engineering and Safety Center Technical Assessment Report	Document #:	Version:
		NESC-RP-12-00783	1.0
Title:		Page #:	
Empirical Model Development for Predicting Shock Response on Composite Materials Subjected to Pyroshock Loading		96 of 123	

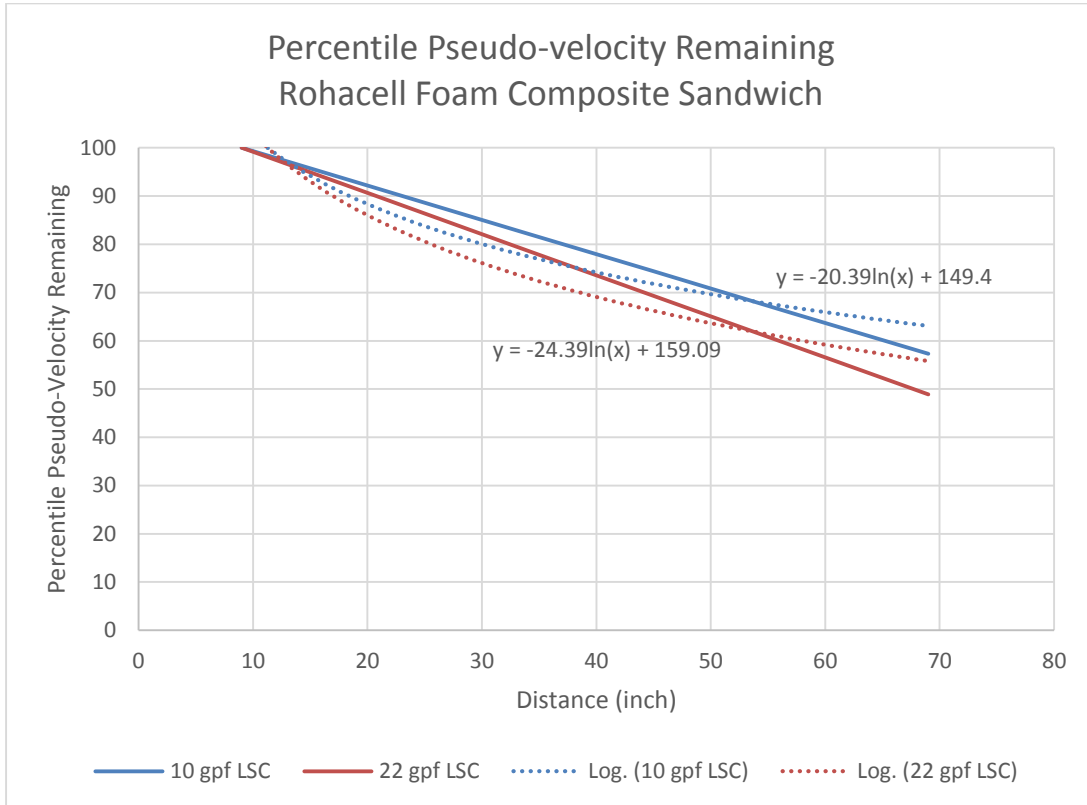



Figure 7.3.7-8. Percentile of PV Remaining versus Distance, ROHACELL® Foam Composite Sandwich Panel

The acceleration values shown in the PV figures (Figures 7.3.7-1, 7.3.7-3, 7.3.7-5, and 7.3.7-7) are for reference only since acceleration and PV are frequency interdependent. (Note that velocity = acceleration/ $2\pi f$, where f is the natural frequency). The PV was not statistically analyzed with the exception for calculating an overall mean of the PV induced into the composite materials, which was 264 inches per second (ips). The acceleration was calculated from the corresponding PV and a constant frequency (2100 Hz for the monolithic composite panels and 2560 Hz for the sandwich composite panels) was used in the calculations. Overall, the attenuation of the PV corresponds well with the distance peak acceleration attenuation except for the Al honeycomb sandwich panel with the 10-gpf LSC (reference Figure 7.3.7-6). The attenuation of the Al honeycomb with 10-gpf LSC was similar to the percentile attenuation of the monolithic composite panels. One notable difference between the peak acceleration percentile attenuation and the PV percentile attenuation is the sandwich composite panels and the 0.3-inch-thick monolithic composite panels had less attenuation with the 10-gpf LSC as compared to the 22-gpf LSC, which is the opposite for the percentile peak acceleration attenuation.

	NASA Engineering and Safety Center Technical Assessment Report	Document #: NESC-RP-12-00783	Version: 1.0
Title: Empirical Model Development for Predicting Shock Response on Composite Materials Subjected to Pyroshock Loading		Page #: 97 of 123	

7.3.8 ESD Evaluation

Section 2.2.9 of NASA-HDBK-7005 provides a definition of energy spectra as follows:

2.2.9 Energy Spectra. A transient random environment represented by the signal $x(t)$ is sometimes described in the frequency domain by an energy spectral density function (usually called an energy spectrum where the term “energy” evolves from an electrical analogy), which is given by

$$E_{xx}(f) = 2 E [|X(f,T)|^2] ; f > 0 \quad (2.12)$$

where $X(f,T)$ is defined in Equation (2.1), $E[]$ denotes expected value of $[]$, and the factor of 2 is needed to obtain a one-sided spectrum with values at positive frequencies only.

$$X(f,T) = \int_0^T x(t) e^{-j2\pi ft} dt ; Y(f,T) = \int_0^T y(t) e^{-j2\pi ft} dt \quad (2.1)$$

Although the energy spectrum is computed only at the discrete frequencies, the exact energy spectrum can be interpolated from these discrete values. The units for the energy spectral density are similar to acceleration spectral density commonly used for characterizing random vibration spectra, $g^2\text{-sec/Hz}$. ESD is not particularly useful for determination of a shock MEF, but can be a useful tool for evaluation of the shock energy with respect to frequency, especially for component failure analysis. The maximum energy, calculated from the shocks induced into the composite material, occurred at a wide range of frequencies (from less than 400 Hz to greater than 5000 Hz) depending upon the composite material type, the LSC explosive core load, and the location of the accelerometer. Some examples of ESD plots are shown in Figures 7.3.8-1 through 7.3.8-3 for each of the types of composite panels and with a core load of 10-gpf LSC.



NASA Engineering and Safety Center Technical Assessment Report

Document #:
**NESC-RP-
12-00783**

Version:
1.0

Title:

**Empirical Model Development for Predicting Shock Response on
Composite Materials Subjected to Pyroshock Loading**

Page #:
98 of 123

NEST1-02_048 - Ch 6

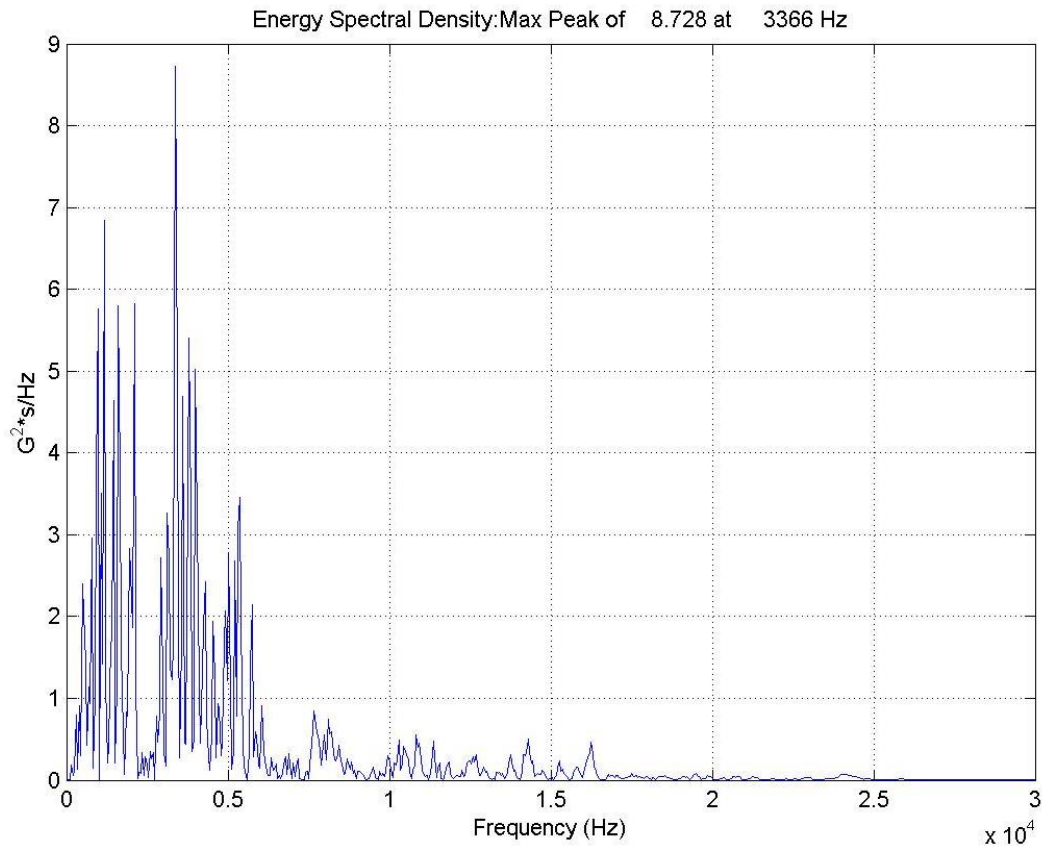


Figure 7.3.8-1. ESD Plot – 0.2-inch Monolithic Panel, 10-gpf LSC



NASA Engineering and Safety Center Technical Assessment Report

Document #:
**NESC-RP-
12-00783**

Version:
1.0

Title:

Empirical Model Development for Predicting Shock Response on Composite Materials Subjected to Pyroshock Loading

Page #:
99 of 123

NEST2-11_048 - Ch 2

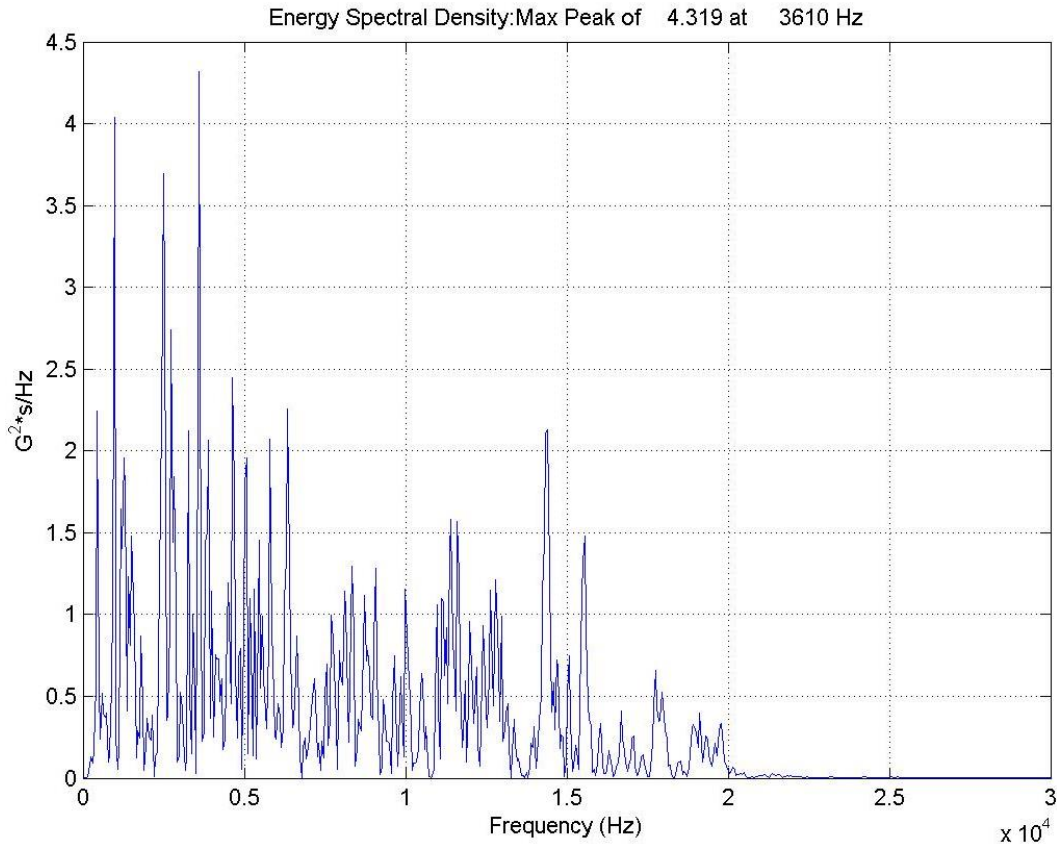



Figure 7.3.8-2. ESD Plot – Al Honeycomb Composite Sandwich Panel, 10-gpf LSC

	NASA Engineering and Safety Center Technical Assessment Report	Document #:	Version:
		NESC-RP-12-00783	1.0
Title:		Page #:	
Empirical Model Development for Predicting Shock Response on Composite Materials Subjected to Pyroshock Loading		100 of 123	

NEST2-13_048 - Ch 4

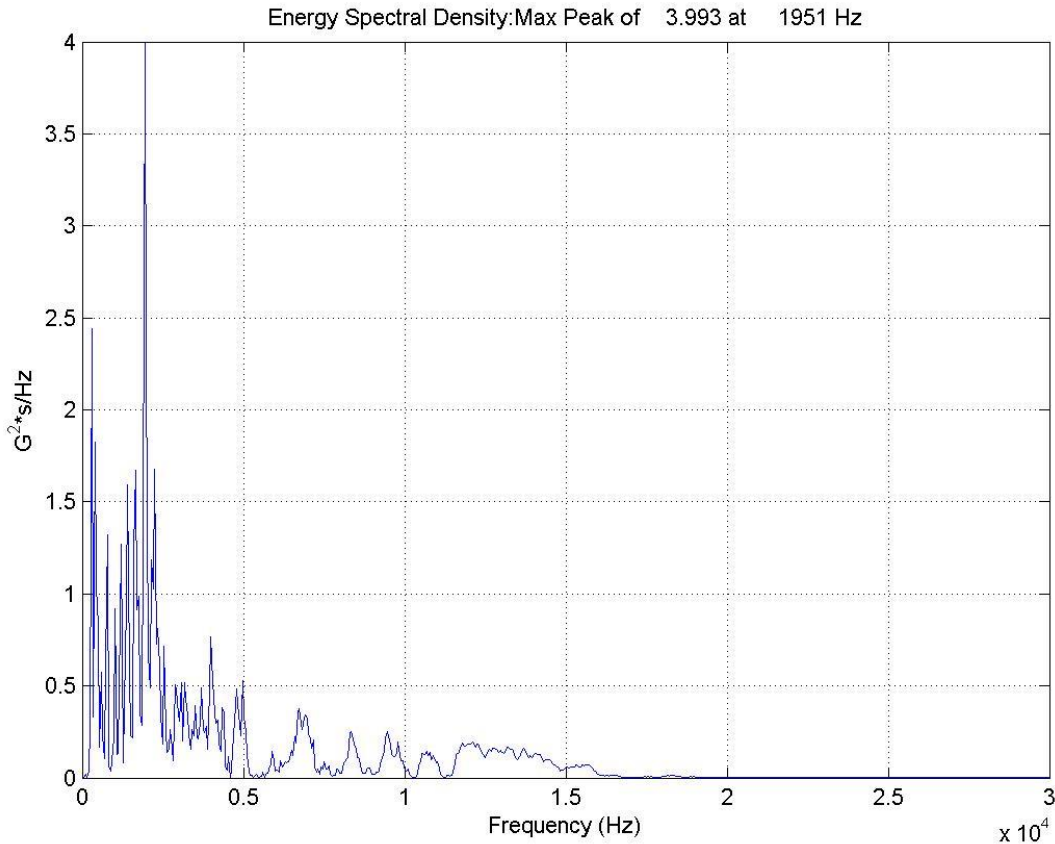



Figure 7.3.8-3. ESD Plot – ROHACELL® Foam Composite Sandwich Panel, 10-gpf LSC

The maximum ESD was statistically analyzed and the following significant factors were determined:

- If an Al or composite LSC, plate was used.
- The location of the accelerometers (top row versus bottom row).

The Al was more efficient in coupling the shock energy through the bolted joint to the composite panel than a composite-to-composite interface. The top row of accelerometers rather consistently showed higher maximum energies, at a given location down the test panel, than the lower row of accelerometers, which was likely an artifact of the test setup. The LSC was always initiated from below the test panel; therefore, the detonation wave was traveling from the bottom of the test panel to the top of the test panel. The shock wave likely vectored across the panel, hence the higher maximum energies calculated from the top row of accelerometers. The predictive equation for maximum ESD based upon the explosive core load, whether a LSC plate was Al or composite, and the distance from the shock source is listed below.

	NASA Engineering and Safety Center Technical Assessment Report	Document #:	Version:
		NESC-RP-12-00783	1.0
Title:		Page #:	
Empirical Model Development for Predicting Shock Response on Composite Materials Subjected to Pyroshock Loading		101 of 123	

Maximum ESD
 =Exp(1.88508105265126
 + -0.00428823884622233 * Distance from LSC
 + (LSC Core Load,
 If 10, -0.181783869892254,
 If 22, 0.181783869892254)
 + (Distance from LSC - 39.0223048327138) * (LSC Core Load,
 If 10, 0.00174623217523917,
 If 22, -0.00174623217523917)
 + (Distance from LSC - 39.0223048327138) * ((Distance from LSC - 39.0223048327138) * -
 0.000177622933837467)
 + (Aluminum LSC Plate,
 If 0, -0.550041910060047,
 If 1, 0.550041910060047))

The predictive results for the maximum ESD with regard to the type of LSC plate used and LSC core load versus distance is tabulated in Table 7.3.8-1.

Table 7.3.8-1. Predicted Maximum ESD

Factors			Prediction at Distance from LSC					
LSC Core Load	Al LSC Plate	LSC Plate	9	21	33	45	57	69
10	0	<i>Fabric Composite</i>	2.465	2.649	2.704	2.623	2.418	2.117
10	1	<i>Al</i>	7.405	7.958	8.124	7.881	7.264	6.361
22	0	<i>Fabric Composite</i>	3.938	4.057	3.972	3.695	3.266	2.743
22	0	<i>Tape Composite</i>	3.938	4.057	3.972	3.695	3.266	2.743
22	1	<i>Al</i>	11.830	12.190	11.935	11.10 2	9.813	8.240

A graphical representation of the statistically predicted maximum ESD for type of LSC plate and LSC explosive core load is shown in Figure 7.3.8-4.



Title:

Empirical Model Development for Predicting Shock Response on Composite Materials Subjected to Pyroshock Loading

Page #:
102 of 123

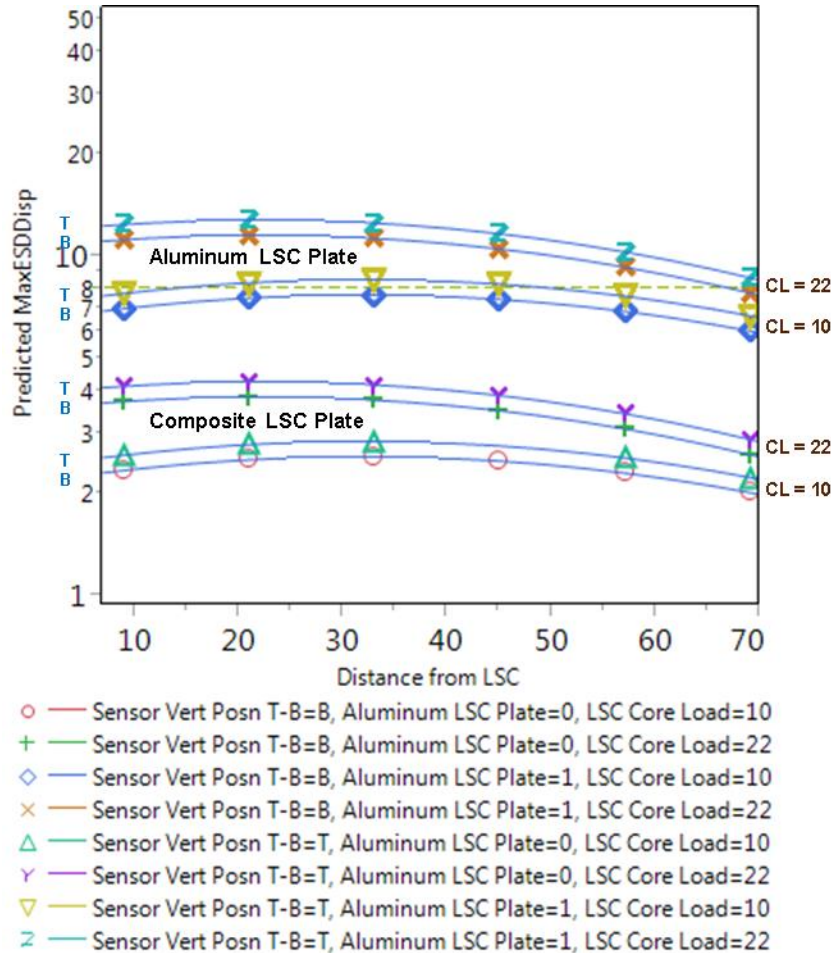


Figure 7.3.8-4. Maximum Predicted ESD – LSC Plate Type and LSC Explosive Core Load

7.3.9 Time History, Velocity, and Displacement

The acceleration, velocity, and displacement for each of the accelerometers for each test was generated from the post-processed data. Generation of the time histories allows the data to be scrutinized to verify data “quality” (i.e., free of zero-shifts and offsets). The velocity and displacement time histories are examined to ensure they are consistent with the acceleration time history. The time histories are qualitatively scrutinized and therefore post-processing statistical analysis is required. Examples of acceleration, velocity, and displacement time histories for the monolithic and composite sandwich test panels are shown in Figures 7.3.9-1 through 7.3.9-3, respectively. The results from evaluation of the time histories for each of the accelerometers, for each test, verified the accelerometer data was indeed quality data.



NASA Engineering and Safety Center Technical Assessment Report

Document #:
**NESC-RP-
12-00783**

Version:
1.0

Title:

Empirical Model Development for Predicting Shock Response on Composite Materials Subjected to Pyroshock Loading

Page #:
103 of 123

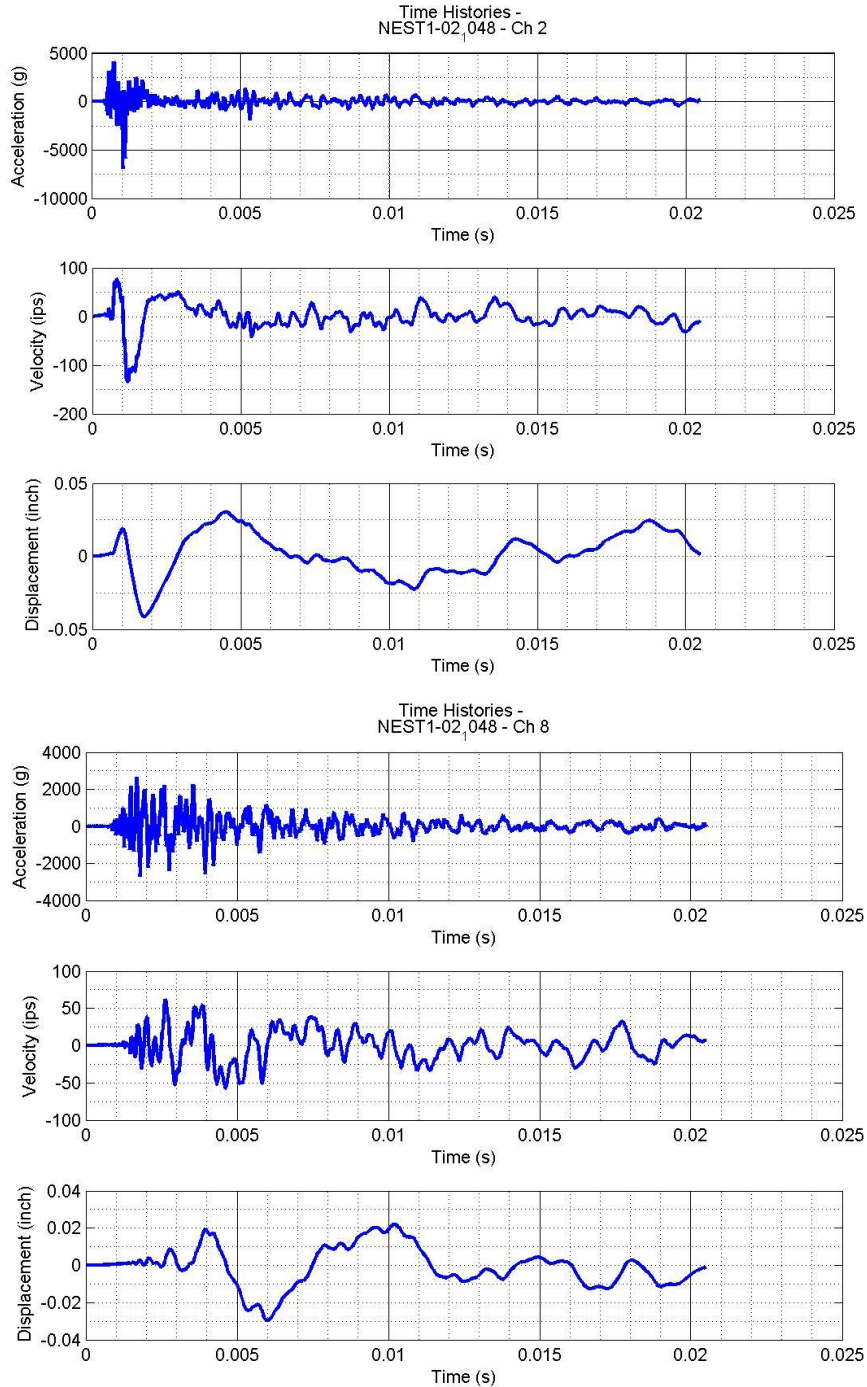


Figure 7.3.9-1. Time Histories for Group I, Test 2, Monolithic Composite Panel – Accelerometers 2 and 8



NASA Engineering and Safety Center Technical Assessment Report

Document #:
**NESC-RP-
12-00783**

Version:
1.0

Title:

Empirical Model Development for Predicting Shock Response on Composite Materials Subjected to Pyroshock Loading

Page #:
104 of 123

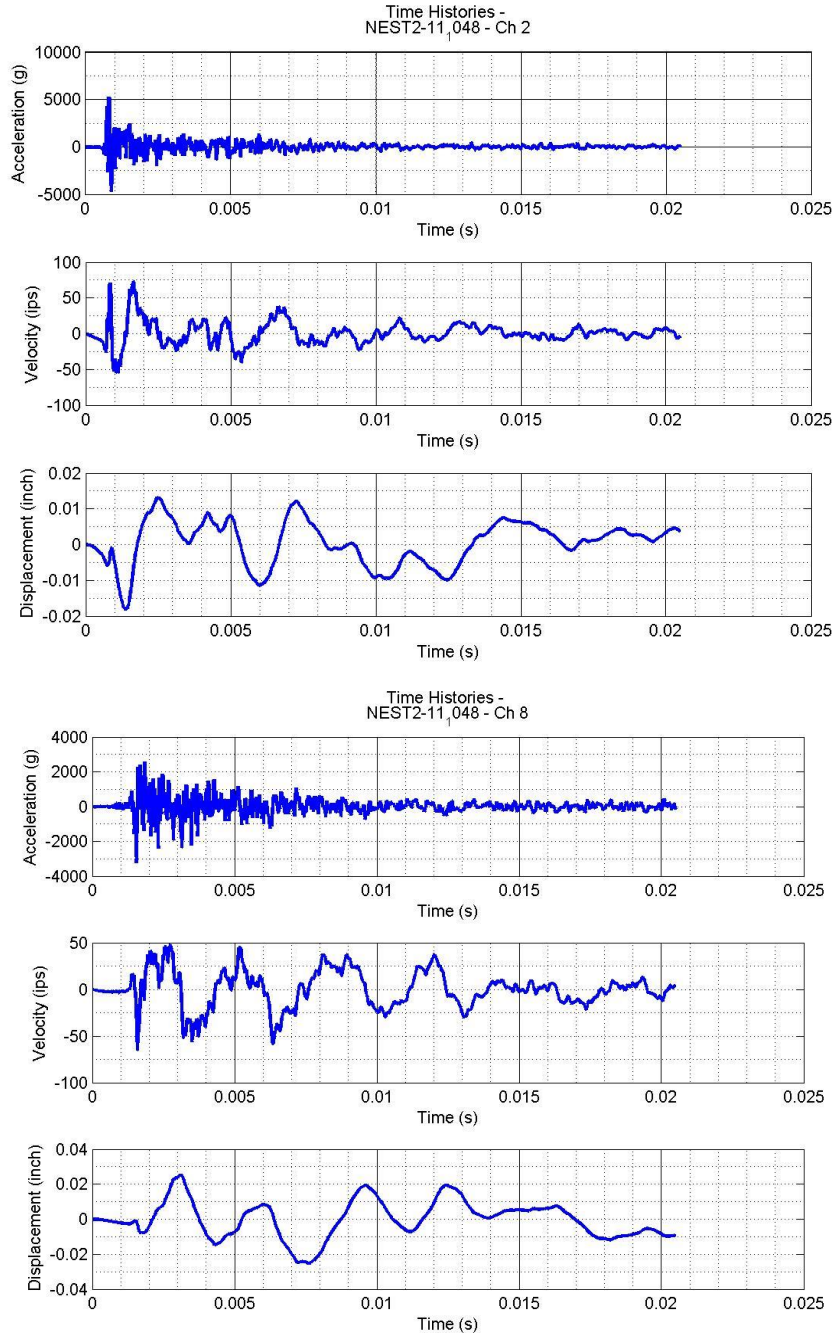


Figure 7.3.9-2. Time Histories for Group II, Test 11, Al Honeycomb Sandwich Composite Panel – Accelerometers 2 and 8



NASA Engineering and Safety Center Technical Assessment Report

Document #:
**NESC-RP-
12-00783**

Version:
1.0

Title:

Empirical Model Development for Predicting Shock Response on Composite Materials Subjected to Pyroshock Loading

Page #:
105 of 123

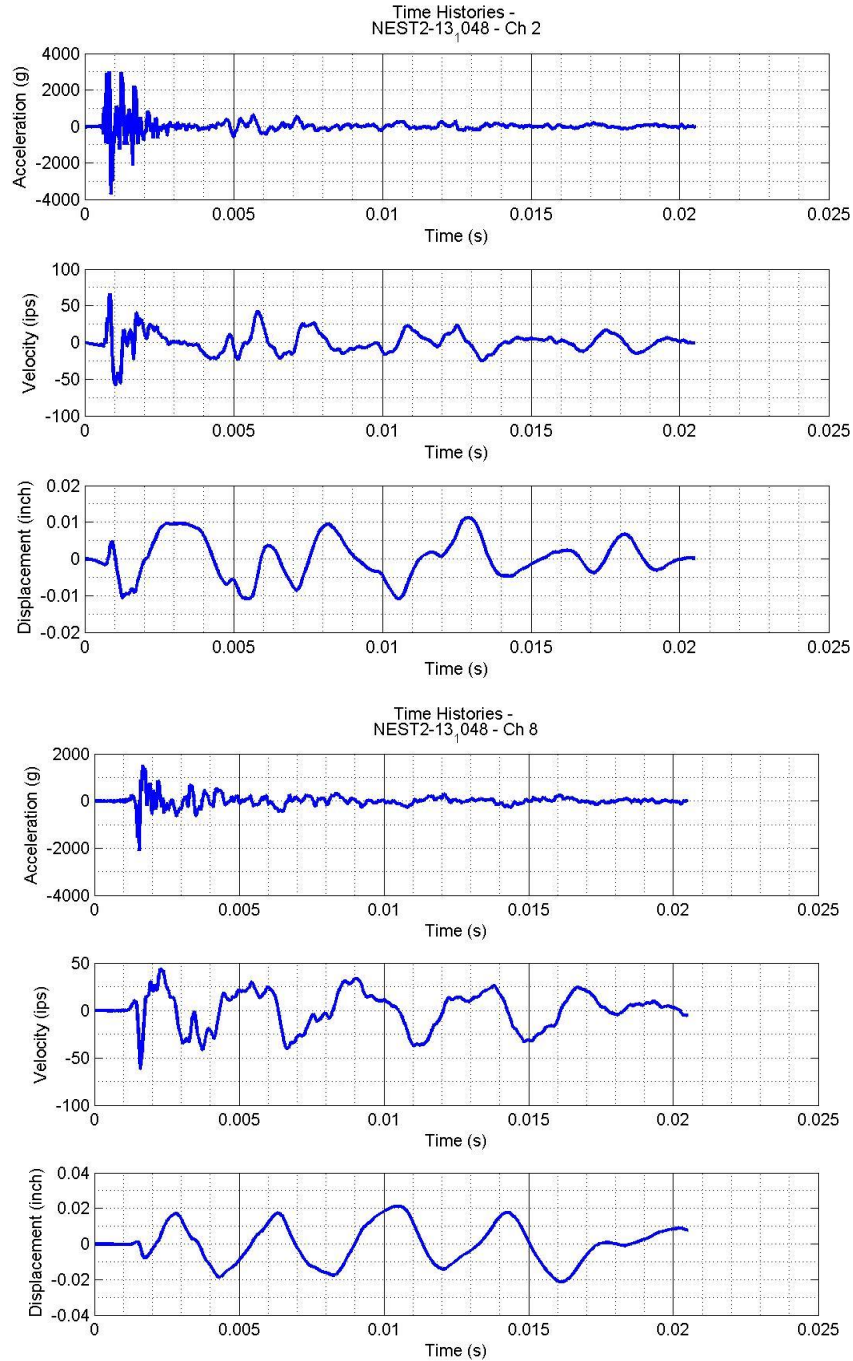



Figure 7.3.9-3. Time Histories for Group II, Test 13, ROHACELL® Foam Sandwich Composite Panel – Accelerometers 2 and 8

	NASA Engineering and Safety Center Technical Assessment Report	Document #: NESC-RP-12-00783	Version: 1.0
Title: Empirical Model Development for Predicting Shock Response on Composite Materials Subjected to Pyroshock Loading		Page #: 106 of 123	

7.3.10 Temporal Moments

David O. Smallwood, *Sandia National Laboratories*, developed a method to characterize shocks in terms of Fourier energy spectrum and temporal moments of the shock (reference Shock and Vibration, Vol 1, No 6, pp 507-527 (1994) © 1994 John Wiley and Son, *Characterization and Simulation of Transient Vibrations Using Band Limited Temporal Moments*). Temporal moments are analogous to the moments of probability density functions. For pyroshock applications the square of the time history is used, which allows relating between the temporal moments and moments with the frequency domain. The i th temporal moment, $m_i(a)$, of a time history, $(x)t$, about a time location, a , is defined as:

$$m_i(a) = \int_{-\infty}^{\infty} (t - a)^i x^2(t) dt.$$

The moments are useful to describe simple time history shapes and to describe envelopes of more complicated shock time histories. The energy moment, referred to as the time history energy, is the integral of the magnitude squared of the time history. The square root of the energy normalized by the root mean square (RMS) duration is referred to as the root energy amplitude and is a convenient way to describe the energy of the shock transient. For this task, the temporal energy (TE) was calculated and statistically evaluated for the monolithic composite panel test results. The results from the evaluation indicated the following significant factors:

- The panel thickness
- The distance from the shock source.

Factors determined not to be significant

- The explosive core load used for inducing the shock
- The type and orientation of the ply used in fabrication of the monolithic composite panel.

General conclusions that may be drawn are:

- Thin panels had higher TE
- TE decreased with increasing distance from the shock source

Figure 7.3.10-1 graphically presents the results of the TE statistical analysis.

Statistical analyses of the TE was *not* performed for sandwich composite panel test results since in practicality TE has seen little use for satisfying shock test requirements. Although, Smallwood proposed its usage in conjunction with the SRS to improve the agreement between the shock test requirement and the laboratory test results as reported in his paper entitled, *A Methodology for Defining Shock Tests Based on Shock Response Spectra and Temporal Moments*, Jerome S. Cap and David O. Smallwood, *Sandia National Laboratories, Mechanical and Thermal Environments Department*. The process proposed by Smallwood was to develop a procedure to implement shock testing defined by both the SRS and the temporal moments. The proposed procedure was to be performed in two phases with the first phase assessing the shock requirement via the SRS and temporal moments, applying the margins to the SRS, temporal

energy and root energy amplitude, and develop the SRS test requirements (straight-line envelope). The second phase is to compute the SRS and temporal moments of the field test data and compare the values with the test requirements. Iteration of the field-testing would be required to be performed until the upper and lower limit specified shock tolerances for both the SRS and temporal moments are met.

As previously stated, the procedural process incorporating temporal moments into specified shock tests requirements has not been adopted within the aerospace community, which extensively uses SRS, nor the structural community or Navy, both of which use PVRS 4CP.

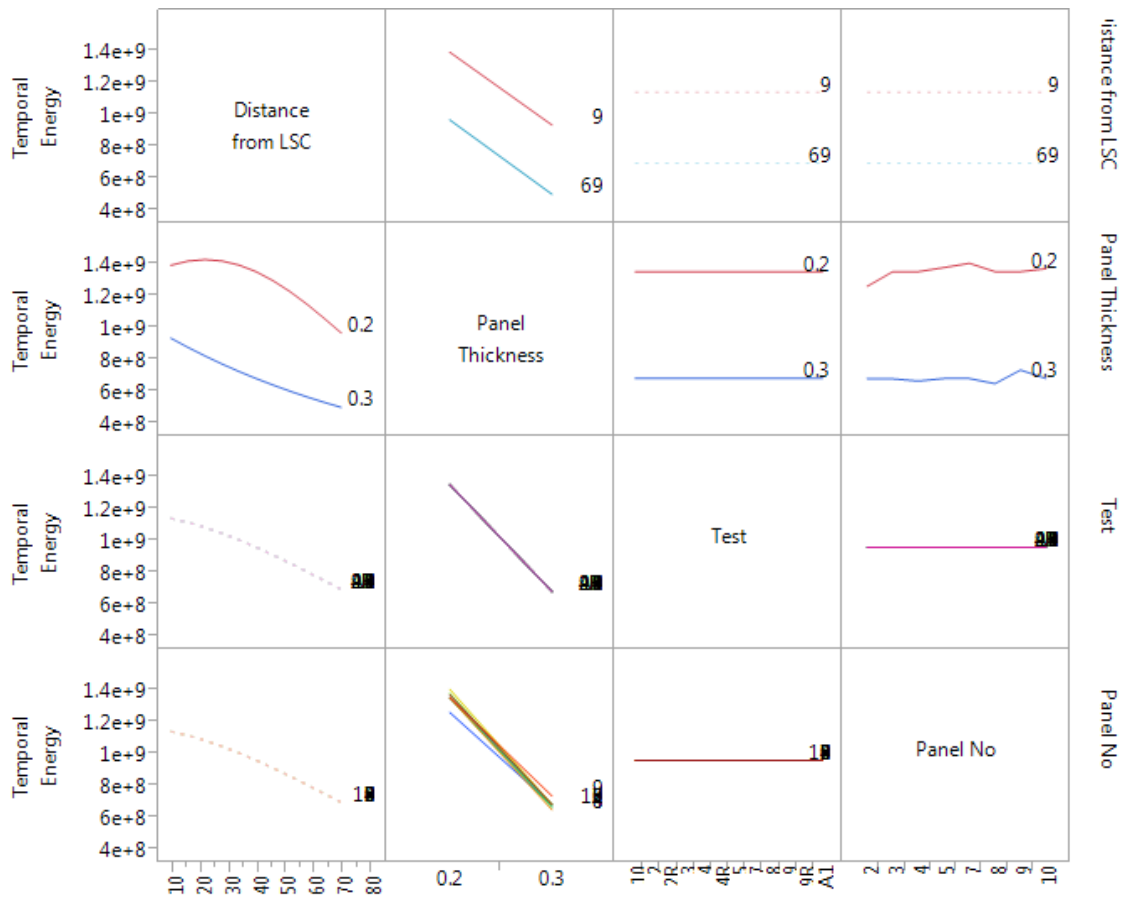



Figure 7.3.10-1. Monolithic Composite Temporal Energy Sensitivities

7.3.11 MEFÉ Prediction Example

For prediction of the MEFÉ, using the guidelines developed from the data evaluation within this report, a hypothetical shock that is characterized as having a peak shock of 8,000 g at 10,000 Hz (similar to a source shock from a 10-gpf linear explosive induced into a 0.19-inch metallic structure) is used as an example for the prediction of the MEFÉ at a distance of 48 inches from

	NASA Engineering and Safety Center Technical Assessment Report	Document #:	Version:
		NESC-RP-12-00783	1.0
Title:		Page #:	
Empirical Model Development for Predicting Shock Response on Composite Materials Subjected to Pyroshock Loading		108 of 123	

the shock source. (Note: The hypothetical source shock is assumed to have been predicted through a bolted interface). The first example will be for the monolithic composite material followed by the Al honeycomb sandwich composite material and then the ROHACELL[®] foam sandwich composite material.

The first step for the prediction is to generate an SRS for source shock. The peak acceleration is given so the two attributes that need to be included are the slope (in dB/oct) and the frequency breakpoint (in Hz). For this exercise Table 7.3.6.1-1 is used for the slope at the 9-inch location, which is 8.9 dB/oct (for all panel types). The second step is to determine the frequency breakpoint. Table 7.3.6.2-1 provides the predicted frequency breakpoint for both the 0.2-inch-thick monolithic composite and the 0.3-inch monolithic composite materials. The median frequency breakpoint for these materials is 2100 Hz. Usage of this value is further substantiated by Figure 7.3.6.2-2. Figure 7.3.11-1 provides the predicted SRS for a monolithic composite material for a given 8,000 g shock.

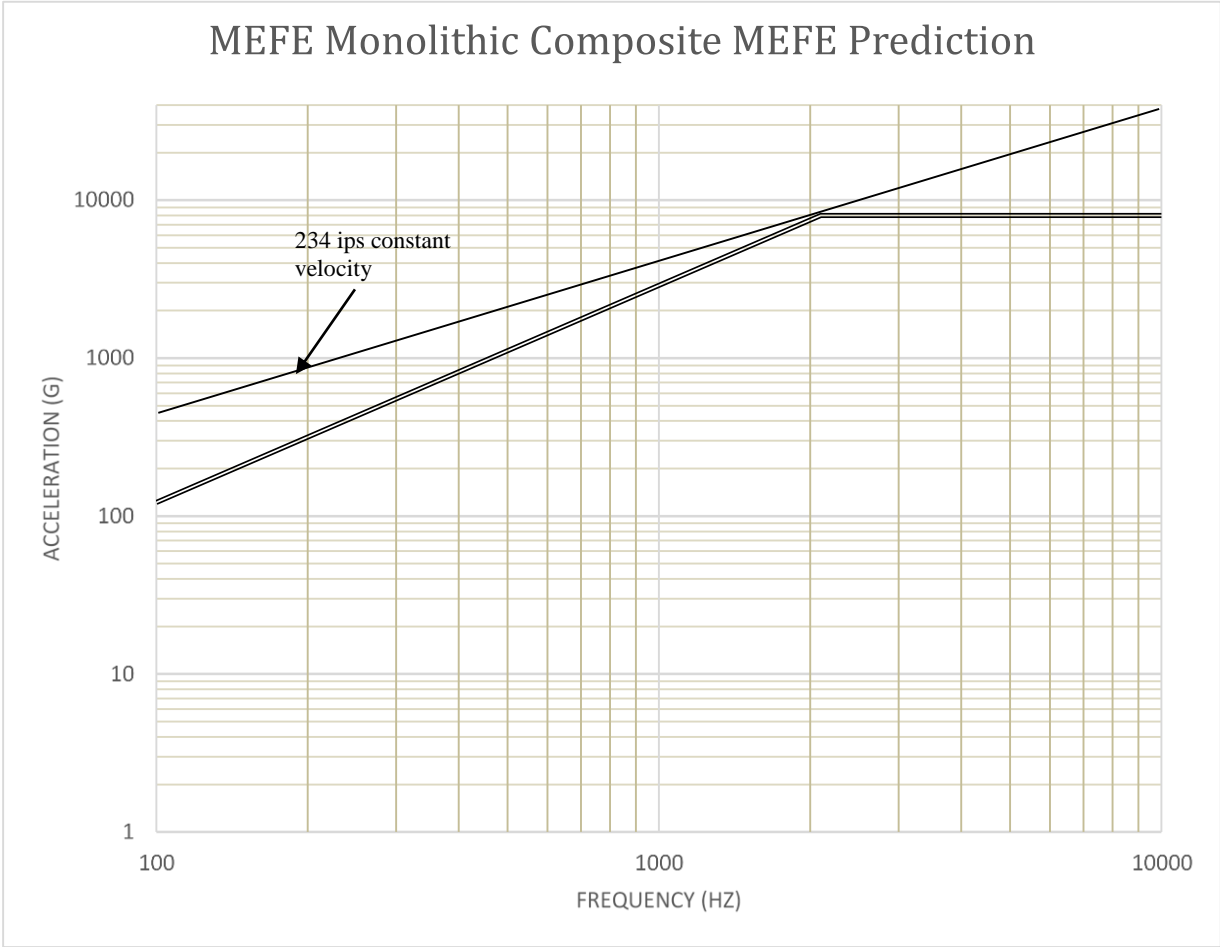



Figure 7.3.11-1. Predictive MEFE, Monolithic Composite

	NASA Engineering and Safety Center Technical Assessment Report	Document #: NESC-RP-12-00783	Version: 1.0
Title: Empirical Model Development for Predicting Shock Response on Composite Materials Subjected to Pyroshock Loading		Page #: 109 of 123	

The predictive MEFE would be defined in tabular format as shown in Table 7.3.11-1.

Table 7.3.11-1. Predictive 8,000 g Shock, Monolithic Composite

Frequency (Hz)	Acceleration (g)
100	122
2100	8000
5000	8000
10000	8000

Of note, the velocity for this predicted shock is 234 ips, which is within the upper half of the moderate range in relative severity.

To predict the shock for a component mounted 48 inches away from the 9-inch location given for the shock source, Figure 7.3.6.3-10 for the 10-gpf LSC is used. At a distance of 48 inches (from the 9-inch location), the percent peak acceleration remaining is approximately 70%. Therefore, the peak acceleration at 48 inches away would be 5,600 g. Given in Section 7.3.6.1 for the evaluation of the SRS slope the slope is held constant for prediction of the attenuated shock spectrum. Referencing back to Table 7.3.6.2-1 for the frequency breakpoint the median value for the monolithic composite at 57 inches is 2067 Hz. The velocity for this shock is 166 ips, which is still considered to be a moderate shock, but on the lower half of the moderate range. The prediction of the MEFE at a distance of 48 inches from the shock source is illustrated in Figure 7.3.11-2.

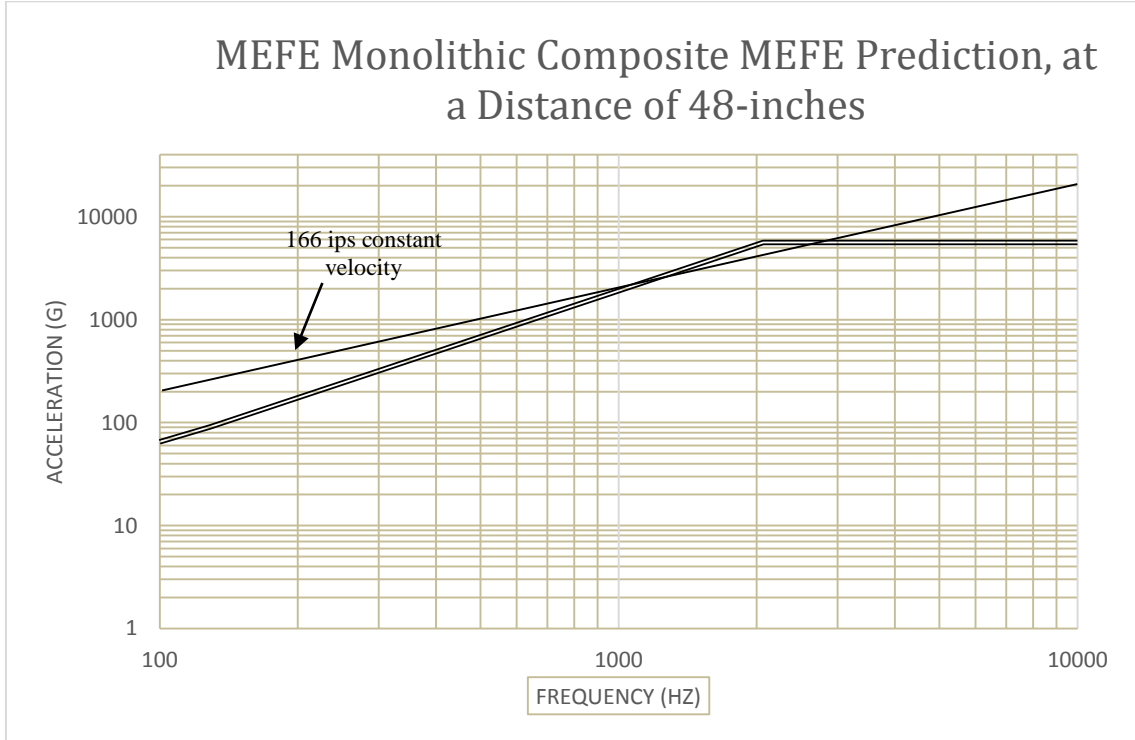


Figure 7.3.11-2. Predicted MEFE Example at 48 inches, Monolithic Composite


The predictive MEFE would be defined in tabular format as shown in Table 7.3.11-2.

Table 7.3.11-2. Predictive 8,000-g Shock Attenuated for 48-inch Distance, Monolithic Composite

Frequency (Hz)	Acceleration (g)
100	65
2067	5600
5000	5600
10000	5600

For reference, the same process is repeated for the Al honeycomb sandwich composite material and the ROHACELL[®] foam sandwich composite material illustrated in Figures 7.3.11-3, 7.3.11-4, 7.3.11-5, and 7.3.11-6, respectively.

For the Al honeycomb sandwich composite, the same slope is used (8.9 dB/oct) and the un-attenuated frequency breakpoint is 2900 Hz per Table 7.3.6.2-1. The 48-inch distance attenuated frequency breakpoint is 2400 Hz per Table 7.3.6.2-1. For the ROHACELL[®] foam sandwich composite the un-attenuated frequency breakpoint is 2800 Hz and the 48-inch distance attenuated frequency breakpoint is 2100 Hz.

	NASA Engineering and Safety Center Technical Assessment Report	Document #: NESC-RP-12-00783	Version: 1.0
Title: Empirical Model Development for Predicting Shock Response on Composite Materials Subjected to Pyroshock Loading		Page #: 111 of 123	

Using Figure 7.3.6.3-11 and the 10-gpf LSC, attenuation line shows 46% attenuation at a distance of 48 inches from the 9-inch location. Using Figure 7.3.6.3-12 and the 10-gpf LSC line, the attenuation is 52% at a distance of 48 inches from the 9-inch location.

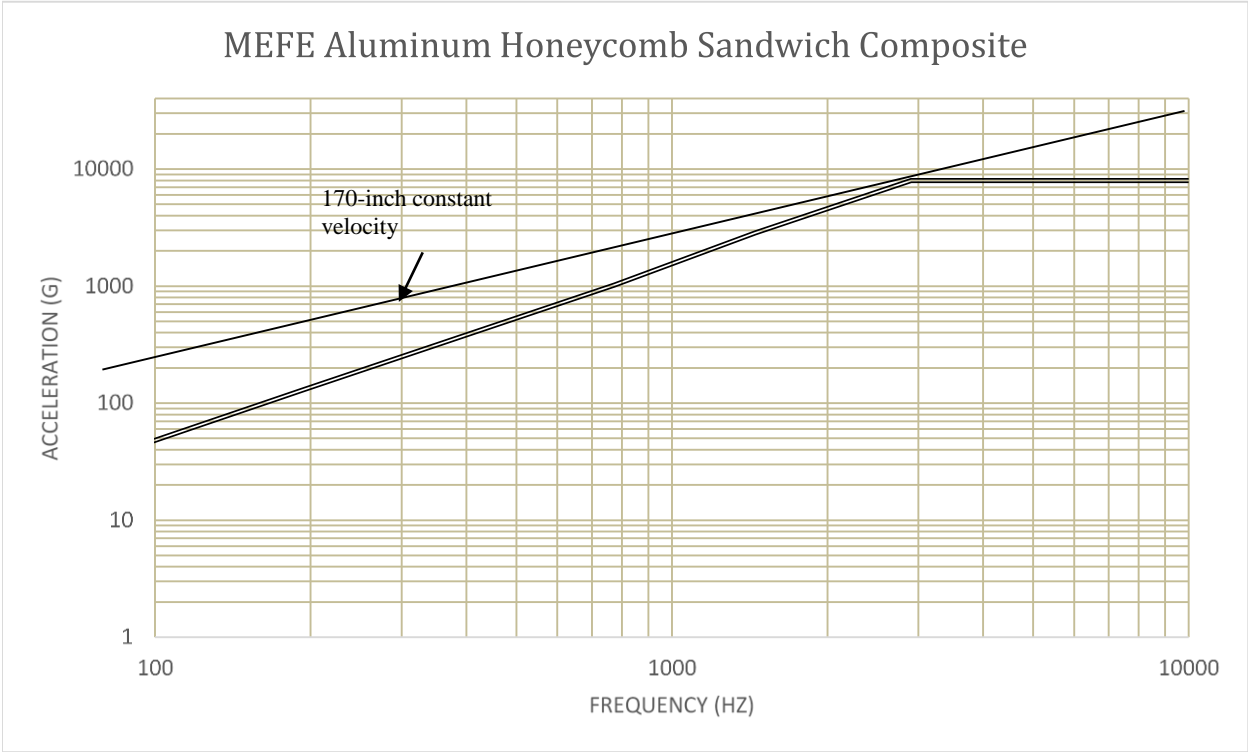


Figure 7.3.11-3. Predicted MEFE, Al Honeycomb



NASA Engineering and Safety Center Technical Assessment Report

Document #:
**NESC-RP-
12-00783**

Version:
1.0

Title:

**Empirical Model Development for Predicting Shock Response on
Composite Materials Subjected to Pyroshock Loading**

Page #:
112 of 123

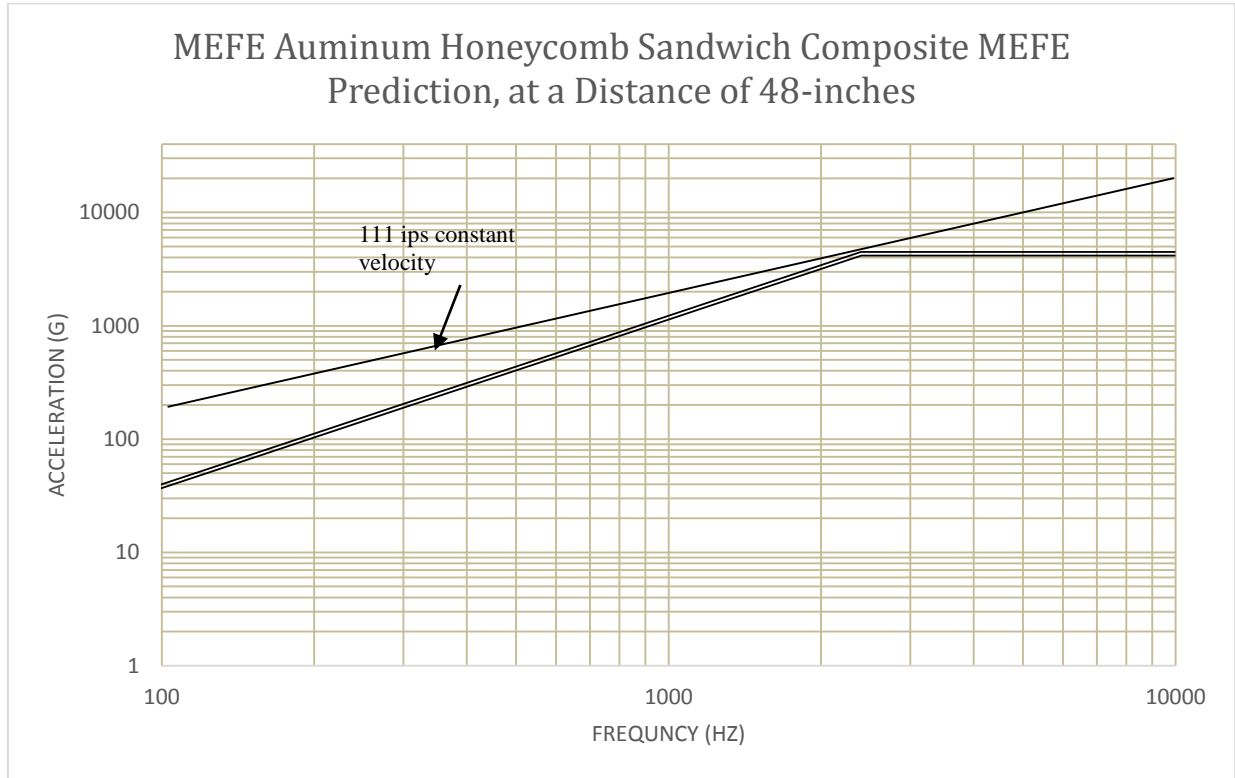


Figure 7.3.11-4. Predicted MEFE at 48-inch Distance, Al Honeycomb



NASA Engineering and Safety Center Technical Assessment Report

Document #:
**NESC-RP-
12-00783**

Version:
1.0

Title:

Empirical Model Development for Predicting Shock Response on Composite Materials Subjected to Pyroshock Loading

Page #:
113 of 123

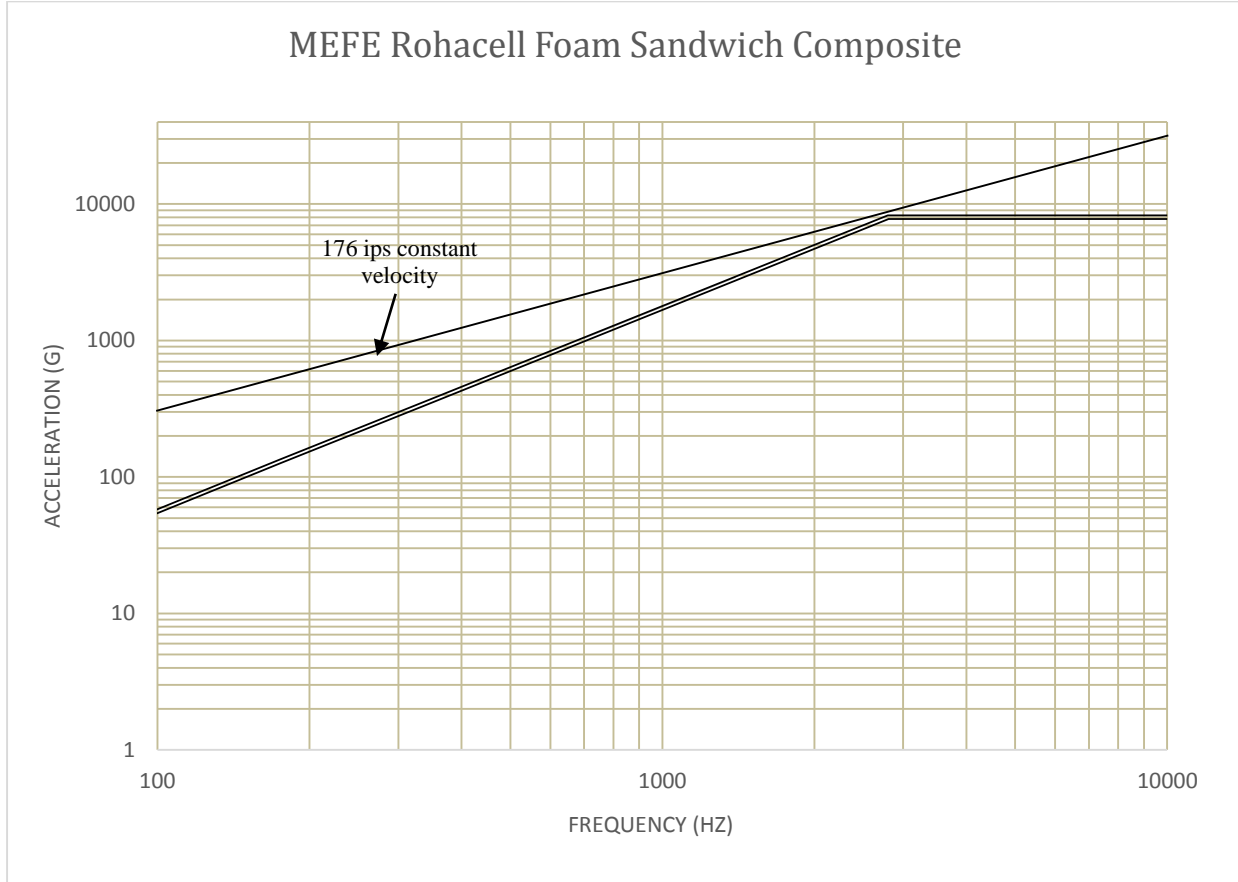



Figure 7.3.11-5. Predicted MEFE, ROHACELL® Foam

	<p align="center">NASA Engineering and Safety Center Technical Assessment Report</p>	<p>Document #: NESC-RP-12-00783</p>	<p>Version: 1.0</p>
<p>Title: Empirical Model Development for Predicting Shock Response on Composite Materials Subjected to Pyroshock Loading</p>		<p>Page #: 114 of 123</p>	

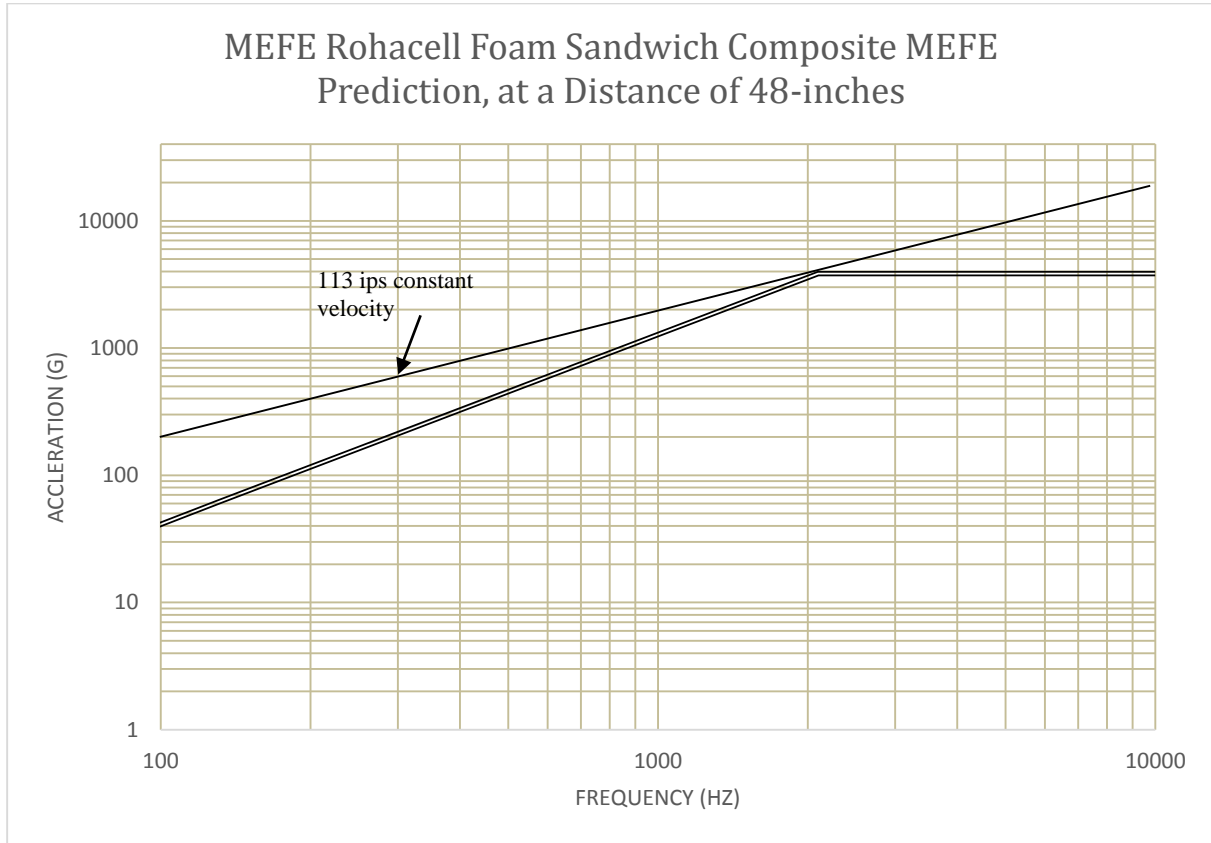


Figure 7.3.11-6. Predicted MEFE at a Distance of 48-inches, ROHACELL® Foam

7.3.12 MAF Qualitative Pyroshock Assessment

MAF has been evaluated to dampen acoustic levels for usage as replacement of fiberglass blankets within a payload fairing, reference NESC TI-12-00811, *NESC Enhanced Melamine Foam Acoustic Tests*. This report evaluated a number of configurations of melamine foam acoustic attenuation properties and one of the more promising configurations (i.e., two layers of 2-inch-thick melamine foam was included as the Group IV test series to evaluate whether the MAF provided additional pyroshock attenuation).

The data from the Group IV tests were qualitatively evaluated for four material types: Al, monolithic composite, Al honeycomb sandwich composite, and ROHACELL® foam sandwich composite, both with and without the melamine foam bonded to the backside (opposite sided of the accelerometer locations) of the test panel. The qualitative evaluation included the three primary attributes of the SRS: slope, frequency breakpoint, and peak acceleration. The results for the evaluation are shown in Figures 7.3.12-1, 7.3.12-2, and 7.3.12-3, for the slope, frequency breakpoint, and peak acceleration, respectively.



NASA Engineering and Safety Center Technical Assessment Report

Document #:
**NESC-RP-
12-00783**

Version:
1.0

Title:

Empirical Model Development for Predicting Shock Response on Composite Materials Subjected to Pyroshock Loading

Page #:
115 of 123

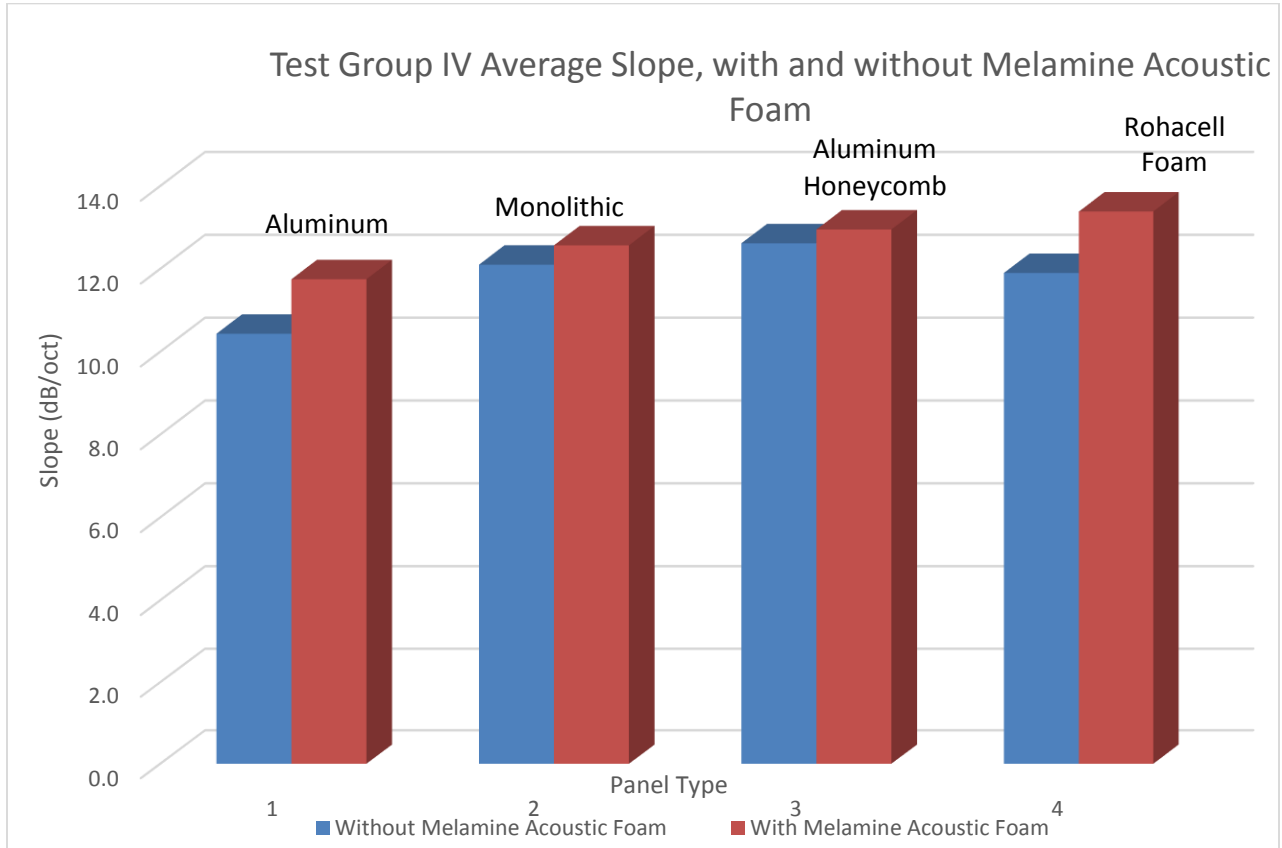


Figure 7.3.12-1. MAF Evaluation, SRS Slope



NASA Engineering and Safety Center Technical Assessment Report

Document #:
**NESC-RP-
12-00783**

Version:
1.0

Title:

Empirical Model Development for Predicting Shock Response on Composite Materials Subjected to Pyroshock Loading

Page #:
116 of 123

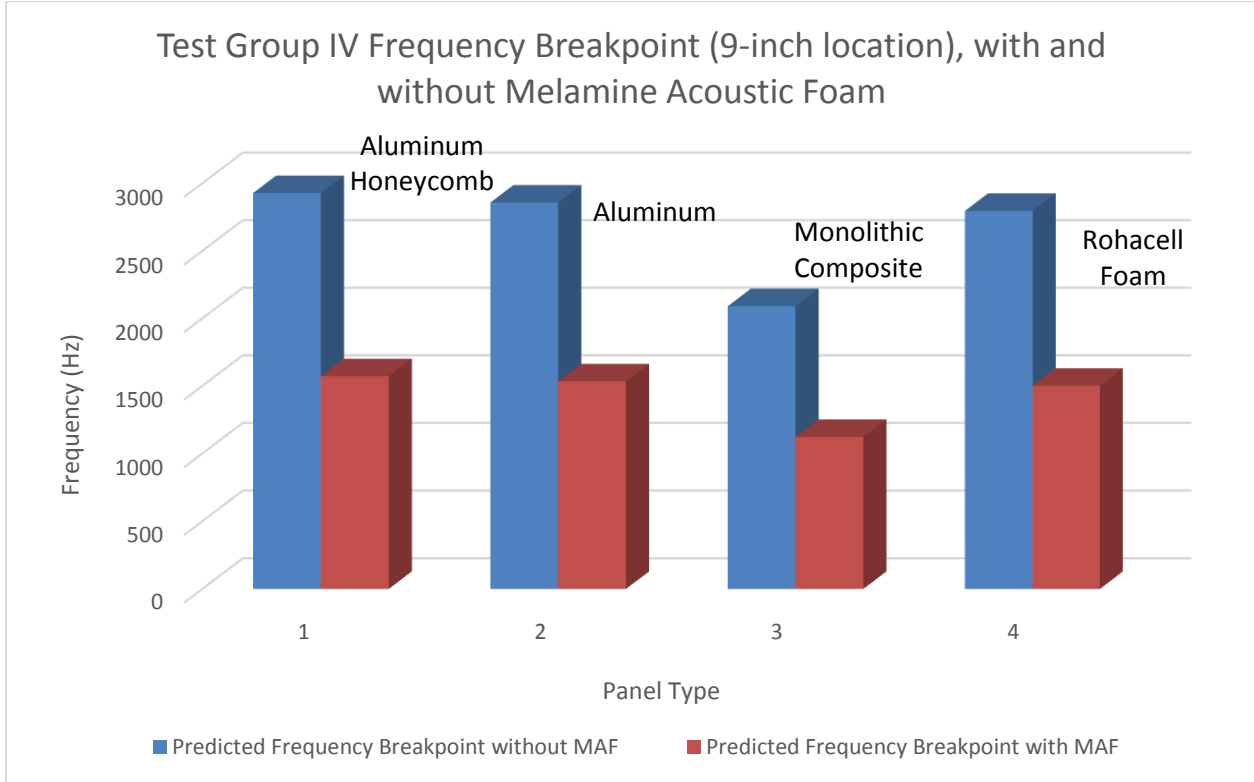


Figure 7.3.12-2. MAF Evaluation, SRS Frequency Breakpoint

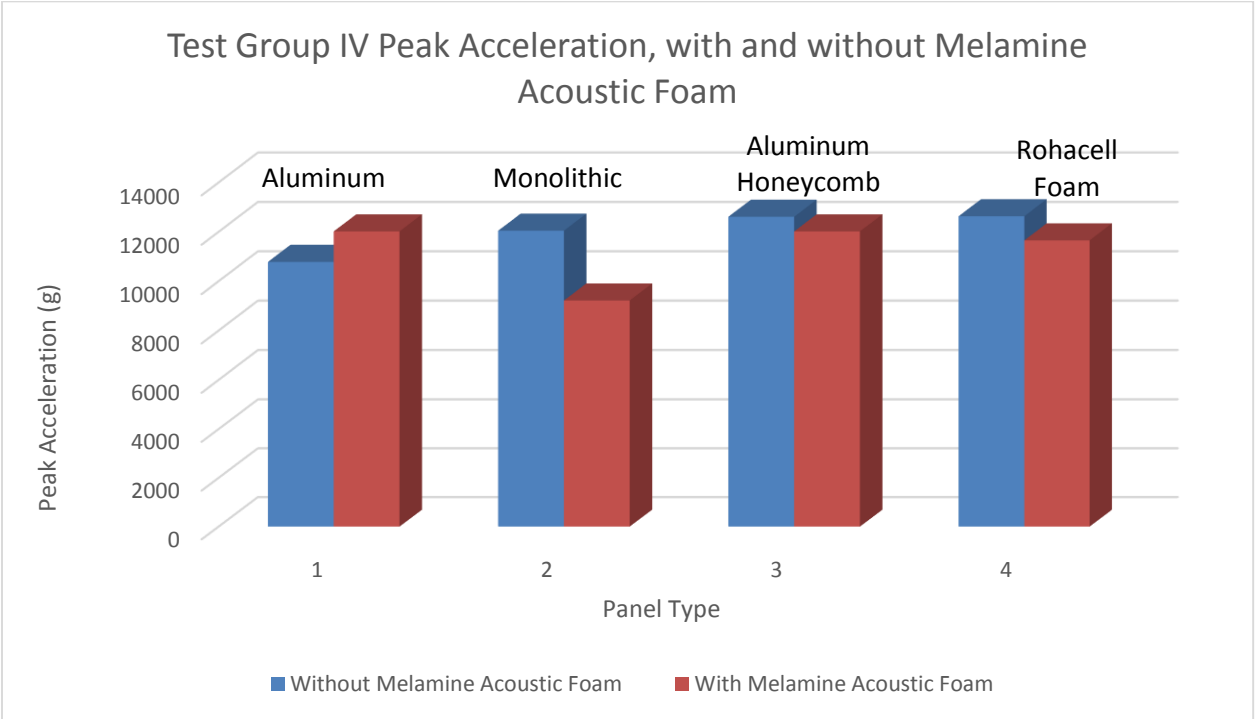



Figure 7.3.12-3. MAF Evaluation, SRS Peak Acceleration

Of the three SRS attributes, only the frequency breakpoint indicated a significant difference for the pyroshock response with melamine foam and without melamine foam. Figure 7.3.12-2 illustrates approximately a 30 to 40% decrease in the frequency breakpoint with the melamine foam adhered to the test panels in comparison to the test panels without the melamine foam. The reduction in the frequency breakpoint may be considered a reflection of lowering the natural frequency of the test panel with the addition of the melamine foam.

	NASA Engineering and Safety Center Technical Assessment Report	Document #: NESC-RP-12-00783	Version: 1.0
Title: Empirical Model Development for Predicting Shock Response on Composite Materials Subjected to Pyroshock Loading		Page #: 118 of 123	

8.0 Findings, Observations, and NESC Recommendations

8.1 Findings

The following findings were identified:

Composite Panel Fabrication and NDE

- F-1.** Phased array, or pulse echo, ultrasound was determined to be an acceptable NDE method for monolithic composite panels up to 0.3 inches thick and the composite skin and bond line for composite sandwich panels.
- F-2.** For the monolithic composite panels used in this study, infrared thermography NDE gave false indications for panels 0.2 inches thick and greater.
- F-3.** Computed radiography was the only nondestructive test method capable of detecting flaws in the composite sandwich fill material.

Pyroshock Test Articles

- F-4.** Subscale flat panels of at least 5 feet in length appear to be sufficient for at least preliminary pyroshock testing on composite panels.

Pyroshock Test Conduct


- F-5.** The response between the PCB350-C02 and PCB350-D02 accelerometers was not discernable.

Pyroshock Acceleration Time History Post-Test Data Processing

- F-6.** The “suitability” or quality of the acquired acceleration data was evaluated and determined to be acceptable.
- F-7.** Initial MATLAB[®] algorithms eliminating human subjectivity used to process the post-test acceleration data did not yield acceptable results. These algorithms required modification to include a level of human subjectivity for determination of the acceptability of the post-test processed data. (Algorithm data output unsubstantiated, without human oversight for acceptability, was evaluated and determined undesirable).

SRS Post-Test Processed Data Evaluation

- F-8.** There was little change in SRS slope from 20 inches to 60 inches from the shock source on the 72-inch panels except for a relatively small-reflected shock end-effect region.
- F-9.** After an initial increase the SRS frequency breakpoint decreases with distance from the shock source.

	NASA Engineering and Safety Center Technical Assessment Report	Document #: NESC-RP-12-00783	Version: 1.0
Title: Empirical Model Development for Predicting Shock Response on Composite Materials Subjected to Pyroshock Loading		Page #: 119 of 123	

- F-10.** The peak acceleration generated from the 10-gpf LSC and the 22-gpf LSC was similar.
- F-11.** Ply orientation (unidirectional versus quasi-isotropic) was not a significant factor for monolithic composite pyroshock response.
- F-12.** The type of ply (fabric versus tape) was not a significant factor for monolithic composite shock response.
- F-13.** The rate at which the shock attenuated with distance for the 0.2-inch-thick and the 0.3-inch-thick monolithic composite panel was equivalent.
- F-14.** The shock attenuation of the sandwich composite panels, either Al honeycomb or ROHACELL[®] foam, was greater than the monolithic composite panel.
- F-15.** The shock attenuation of the ROHACELL[®] fill sandwich panel was greater than the Al honeycomb fill composite sandwich panel.

PVRS Post-Test Processed Data Evaluation


- F-16.** The shock induced into the test panels was moderate-to-severe; reference H. Gaberson, *Shock Severity Estimation*, Sound & Vibration, January 2012, with the overall velocity quantified to be 264 ips.
- F-17.** The skin-stiffened composite layup, which have both monolithic and sandwich-filled characteristics, may respond differently from either the singular monolithic or sandwich composite layups used herein.
- F-18.** Based on the accelerometer(s) response at the 66-inch location, there appeared to be a reflected shock wave from the end of the panel artificially elevating the peak acceleration.

Statistical Analysis of Post-Test Processed Data

- F-19.** The following responses were found to have statistically significant differences depending on panel design: peak acceleration and frequency breakpoint.
- F-20.** In evaluating SRS traces exhibiting multiple frequency break points, it appears that the maximum frequency break, maximum plateau, and maximum slopes have similar quality to response values reduced from single-frequency-break traces.

Pyroshock Response Evaluation of Composites with Melamine Foam

- F-21.** Acoustic damping reduced maximum frequency break point value by 30 to 40% over the un-damped value, with the percent of decrease decreasing with increasing distance from shock source.

	NASA Engineering and Safety Center Technical Assessment Report	Document #: NESC-RP-12-00783	Version: 1.0
Title: Empirical Model Development for Predicting Shock Response on Composite Materials Subjected to Pyroshock Loading		Page #: 120 of 123	

8.2 Observations

Pyroshock Test Conduct

- O-1.** Since the United States Army Redstone Arsenal stores explosives for MSFC, logistical pre-coordination was required to ensure the LSC was available at the test facility for test.

SRS Post-Test Processed Data Evaluation


8.3 NESC Recommendations

The following NESC recommendations were identified and directed towards the SLS Stages Project, specifically the Composites for EUS Technology Development Project:

- R-1.** Conduct additional testing to include a skin-stiffened composite layup as a variable to evaluate its dynamic response. *(F-5, F-6, F-10, F-11, F-12, F-14, O-6)*
- R-2.** Since composite panel design and construction, influences shock response, evaluate and correlate acoustic modal response with pyroshock response for each composites type. *(F-2, F-5, F-6, F-10, F-11, F-12, F-14, O-7)*
- R-3.** Conduct higher-fidelity (more flight-like) pyroshock testing on composite ring structures, of sufficient size to minimize edge effects, to corroborate post-test data processing and MEFÉ predictive evaluation. *(F-2, F-3, F-5, F-6, F-10, F-11, F-12, F-14, O-7)*
- R-4.** Request accelerometer time history data used for qualification or acceptance of flight hardware to evaluate the data quality. *(F-3)*
- R-5.** Process pyroshock acceleration time history data for both SRS and PVRS to correlate severity of the induced shock. *(F-5, F-6, F-7, F-8, F-9, F-10, F-11, F-12, F-13)*
- R-6.** For system designs, utilizing composite materials, where shock response is important to vehicle reliability and risks, uncharacterized designs should be characterized through test. *(F-2, F-14, F-15)*
- R-7.** If attenuation of shock is important to system performance and reliability than weight, consider using ROHACELL[®]-filled construction in lieu of Al honeycomb. *(F-12)*
- R-8.** For NDE to find panel flaws, consider phased array ultrasound for monolithic composite panels and skins on sandwich panels. For sandwich panels, consider computed radiography. Do not use IR thermography for composite materials greater than 3/16-inch in thickness. *(F-1, O-1, O-2)*

9.0 Alternate Viewpoint

There were no alternate viewpoints identified during the course of this assessment by the NESC team or the NRB quorum.

	NASA Engineering and Safety Center Technical Assessment Report	Document #: NESC-RP-12-00783	Version: 1.0
Title: Empirical Model Development for Predicting Shock Response on Composite Materials Subjected to Pyroshock Loading		Page #: 121 of 123	

10.0 Other Deliverables

Deliverables include all data collected during the pyroshock testing, the final report documenting the outcome of the testing and development of the analytical tool, and the empirical analytical tool for prediction of the pyroshock MEFE.

No unique hardware, software, or data packages, outside those contained in this report, were disseminated to other parties outside this assessment.

11.0 Lessons Learned


No applicable lessons learned were identified for entry into the NASA Lessons Learned Information System (LLIS) as a result of this assessment.

12.0 Recommendations for NASA Standards and Specifications

No recommendations for NASA standards and specifications were identified as a result of this assessment.

13.0 Definition of Terms

Corrective Actions	Changes to design processes, work instructions, workmanship practices, training, inspections, tests, procedures, specifications, drawings, tools, equipment, facilities, resources, or material that result in preventing, minimizing, or limiting the potential for recurrence of a problem.
Finding	A relevant factual conclusion and/or issue that is within the assessment scope and that the team has rigorously based on data from their independent analyses, tests, inspections, and/or reviews of technical documentation.
Lessons Learned	Knowledge, understanding, or conclusive insight gained by experience that may benefit other current or future NASA programs and projects. The experience may be positive, as in a successful test or mission, or negative, as in a mishap or failure.
Observation	A noteworthy fact, issue, and/or risk, which may not be directly within the assessment scope, but could generate a separate issue or concern if not addressed. Alternatively, an observation can be a positive acknowledgement of a Center/Program/Project/Organization's operational structure, tools, and/or support provided.
Problem	The subject of the independent technical assessment.
Proximate Cause	The event(s) that occurred, including any condition(s) that existed immediately before the undesired outcome, directly resulted in its

	NASA Engineering and Safety Center Technical Assessment Report	Document #:	Version:
		NESC-RP-12-00783	1.0
Title:		Page #:	
Empirical Model Development for Predicting Shock Response on Composite Materials Subjected to Pyroshock Loading		122 of 123	

occurrence and, if eliminated or modified, would have prevented the undesired outcome.


Recommendation A proposed measurable stakeholder action directly supported by specific Finding(s) and/or Observation(s) that will correct or mitigate an identified issue or risk.

Root Cause One of multiple factors (events, conditions, or organizational factors) that contributed to or created the proximate cause and subsequent undesired outcome and, if eliminated or modified, would have prevented the undesired outcome. Typically, multiple root causes contribute to an undesired outcome.

Supporting Narrative A paragraph, or section, in an NESC final report that provides the detailed explanation of a succinctly worded finding or observation. For example, the logical deduction that led to a finding or observation; descriptions of assumptions, exceptions, clarifications, and boundary conditions. Avoid squeezing all of this information into a finding or observation

14.0 Acronyms List

4CP	Four-Coordinate Paper
Al	Aluminum
AMA	Analytical Mechanics Associates
CAD	Computer Aided Design
CEUS	Composites for Exploration Upper Stage
CT	Computed Tomography
DAS	Data Acquisition System
DOE	Design of Experiments
DR	Digital Radiography
EM42	Nonmetallic Materials and Manufacturing Branch
EMR	Electromagnetic Radiation
ES22	Mechanical, Thermal and Life Support Analysis Branch
ESD	Energy Spectral Density
ET40	Structural Dynamics Test Branch
EUS	Exploration Upper Stage
gpf	Grains Per Foot
IIR	Infinite-Impulse-Response
ips	Inches per Second
IR	Infrared
JSC	Johnson Space Center
LaRC	Langley Research Center
LSC	Linear-Shaped Charge

	NASA Engineering and Safety Center Technical Assessment Report	Document #:	Version:
		NESC-RP-12-00783	1.0
Title:		Page #:	
Empirical Model Development for Predicting Shock Response on Composite Materials Subjected to Pyroshock Loading		123 of 123	

MAF	Melamine Acoustic Foam
MEFE	Maximum Expected Flight Environment
MSFC	Marshall Space Flight Center
MTSO	Management and Technical Support Office
NDE	Nondestructive Evaluation
NESC	NASA Engineering and Safety Center
PAUT	Phased Array Ultrasonic Testing
pcf	Pounds Per Cubic Feet
PV	Pseudo-Velocity
PVRS	Pseudo-Velocity Response Spectrum
RELM	Restricted Maximum Likelihood
RMS	Root Mean Square
SLS	Space Launch System
SME	Subject Matter Experts
SRS	Shock Response Spectrum
SVI	Single Value Inputs
TCP	Test Checkout Procedure
TE	Temporal Energy

15.0 References

1. NASA CR-114606, *Pyrotechnic Shock Design Guidelines Manual*
2. IEST-RP-DTE012.1, *Handbook for Dynamic Data Acquisition and Analysis*
3. Fisher, R. A., (1925). *Statistical Methods for Research Workers*. Edinburgh: Oliver and Boyd
4. Box, G. E. P. and Cox, D. R. (1964). An analysis of transformations, *Journal of the Royal Statistical Society, Series B*, 26, 211-252
5. NASA-HDBK-7005, *Dynamic Environmental Criteria*, Figure 5.7 (*Shock Response Spectrum versus Distance from the Pyroshock Source*)
6. NASA-STD-7003, Figure 1
7. ANSI/ASA S2.62-20098, *Shock Test Requirements for Equipment in a Rugged Shock Environment*
8. *Shock and Vibration*, Vol 1, No 6, pp 507-527 (1994) © 1994 John Wiley and Son, *Characterization and Simulation of Transient Vibrations Using Band Limited Temporal Moments*
9. *Smallwood: A Methodology for Defining Shock Tests Based on Shock Response Spectra and Temporal Moments*, Jerome S. Cap and David O. Smallwood, Sandia National Laboratories, *Mechanical and Thermal Environments Department*
10. NESC TI-12-00811, *NESC Enhanced Melamine Foam Acoustic Tests*

REPORT DOCUMENTATION PAGE			Form Approved OMB No. 0704-0188		
<p>The public reporting burden for this collection of information is estimated to average 1 hour per response, including the time for reviewing instructions, searching existing data sources, gathering and maintaining the data needed, and completing and reviewing the collection of information. Send comments regarding this burden estimate or any other aspect of this collection of information, including suggestions for reducing this burden, to Department of Defense, Washington Headquarters Services, Directorate for Information Operations and Reports (0704-0188), 1215 Jefferson Davis Highway, Suite 1204, Arlington, VA 22202-4302. Respondents should be aware that notwithstanding any other provision of law, no person shall be subject to any penalty for failing to comply with a collection of information if it does not display a currently valid OMB control number.</p> <p>PLEASE DO NOT RETURN YOUR FORM TO THE ABOVE ADDRESS.</p>					
1. REPORT DATE (DD-MM-YYYY) 01-07 - 2015		2. REPORT TYPE Technical Memorandum		3. DATES COVERED (From - To) April 2012 - April 2015	
4. TITLE AND SUBTITLE Empirical Model Development for Predicting Shock Response on Composite Materials Subjected to Pyroshock Loading			5a. CONTRACT NUMBER		
			5b. GRANT NUMBER		
			5c. PROGRAM ELEMENT NUMBER		
6. AUTHOR(S) Gentz, Steven J.; Ordway, David O.; Parsons, David S.; Garrison, Craig M.; Rodgers, C. Steven; Collins, Brian W.			5d. PROJECT NUMBER		
			5e. TASK NUMBER		
			5f. WORK UNIT NUMBER 869021.05.05.09.13		
7. PERFORMING ORGANIZATION NAME(S) AND ADDRESS(ES) NASA Langley Research Center Hampton, VA 23681-2199			8. PERFORMING ORGANIZATION REPORT NUMBER L-20590 NESC-RP-12-00783		
9. SPONSORING/MONITORING AGENCY NAME(S) AND ADDRESS(ES) National Aeronautics and Space Administration Washington, DC 20546-0001			10. SPONSOR/MONITOR'S ACRONYM(S) NASA		
			11. SPONSOR/MONITOR'S REPORT NUMBER(S) NASA/TM-2015-218781/Volume I		
12. DISTRIBUTION/AVAILABILITY STATEMENT Unclassified - Unlimited Subject Category 24 Composite Materials Availability: NASA STI Program (757) 864-9658					
13. SUPPLEMENTARY NOTES					
14. ABSTRACT The NASA Engineering and Safety Center (NESC) received a request to develop an analysis model based on both frequency response and wave propagation analyses for predicting shock response spectrum (SRS) on composite materials subjected to pyroshock loading. The model would account for near-field environment (~9 inches from the source) dominated by direct wave propagation, mid-field environment (~2 feet from the source) characterized by wave propagation and structural resonances, and far-field environment dominated by lower frequency bending waves in the structure. This report documents the outcome of the assessment.					
15. SUBJECT TERMS NASA Engineering and Safety Center; Shock response spectrum; Pyroshock loading; Model development					
16. SECURITY CLASSIFICATION OF:			17. LIMITATION OF ABSTRACT	18. NUMBER OF PAGES	19a. NAME OF RESPONSIBLE PERSON
a. REPORT	b. ABSTRACT	c. THIS PAGE			STI Help Desk (email: help@sti.nasa.gov)
U	U	U	UU	128	19b. TELEPHONE NUMBER (Include area code) (443) 757-5802